The Role of Adrenergic Receptor Signaling in Embryonic Ventricular Cell Proliferation and Differentiation

by

Brittney Allen

Submitted in partial fulfillment of the requirements
for the degree of Master of Science

at

Dalhousie University
Halifax, Nova Scotia
July 2018

Dedicated to my family and loved ones. Thank you for your support, guidance, and continuous encouragement.

Table of Contents

List of Tables

List of Figures

Abstract

In the adult heart, cardiomyocytes (CM) that die in response to aging or pathological insults are replaced by scar tissue. Transplantation of embryonic cardiac progenitor cells (CPC) was shown to increase the contractile function of a failing heart. Previous studies demonstrated that a non-selective beta-adrenergic receptor (β-AR) agonist isoproterenol (ISO) can decrease proliferation of CPCs in vitro and reduce graft size after intracardiac cell transplantation. A β1-AR antagonist (Metoprolol) abrogated the anti-proliferative effects of ISO and increased graft size. Carvedilol, a commonly used heart failure medication is known to block both alpha-adrenergic receptor (α-AR) and β-AR subtypes. There is no information available on the expression profiles of different α1-AR subtypes during cardiac ontogeny and whether these receptors play any role in proliferation and differentiation of embryonic ventricular cells. It is hypothesized that expression of α1-AR subtypes is differentially regulated during embryonic heart development and α1-AR signaling plays an important role in ventricular cell proliferation and differentiation. Total RNA samples isolated from different developmental stages of embryonic ventricles were processed for quantitative RT-PCR analysis using α1-AR subtype specific primers. These experiments revealed that α1B or α1D gene expression levels were significantly higher than that of α1A at several stages of cardiac development. Subcellular localization of α1-AR subtypes in embryonic ventricular cells revealed the presence of α1A, α1B, and α1D subtypes in the nucleus as well as the cytoplasm. Embryonic ventricular cultures treated with carvedilol in the presence or absence of ISO did not show any changes in cell size compared to control cultures. Additionally, cells treated with carvedilol and prazosin, resulted in no change in proliferation and cell size parameters in embryonic ventricular cells. However, treatment of embryonic ventricular cells with isoproterenol and carvedilol led to a significant decrease in the relative gene expression of a cardiac transcription factor, Hand2. However, these drug treatments did not affect the relative percentages of CPCs and differentiated cardiomyocytes in embryonic ventricular cell cultures. Therefore, these results suggest that it may be safe to use non-selective adrenergic receptor blockers with cell transplantation studies.

List of Abbreviations and Symbols Used

~	Approximately
°	Degree
µg	Micro gram
µl	Micro liter
µM	Micro molar
#	Number
%	Percent
α	Alpha
α-AR	Alpha adrenergic receptor
AC	Adenylyl cyclase
ACE	Angiotensin converting enzyme
ANS	Autonomic nervous system
AT1R	Angiotensin II type 1 receptor
β	Beta
β-gal	β-galactosidase
Bp	Base pairs
β-AR	Beta adrenergic receptor
Ca^{2+}	Calcium
cAMP	Cyclic adenosine monophosphate
CDK	Cyclin dependent kinase
cDNA	Complimentary DNA
CEC	Chloroethylclonidine
CHO	Chinese hamster ovary
CM	Cardiomyocyte
CPC	Cardiac progenitor cell
cPLA2	Cytosolic phospholipase A2
C_T	Cycle threshold
CVD	Cardiovascular disease
Da	Dalton
DAG	Diacylglycerol
DMEM	Dulbecco's Modified Eagles Medium
DMSO	Dimethyl sulfoxide
E	Embryonic day
EGFR	Epidermal growth factor
ERK	Extracellular signaling regulated kinase
Epi	Epinephrine
ESC	Embryonic stem cell
FBM	Filamin binding motif
FBS	Fetal bovine serum
FGF	Fibroblast growth factor
FLNa	Filamin A
FLNc	Filamin C
FRET	Fluorescence resonance energy transfer

GAPDH	Glyceraldehyde 3-phosphate dehydrogenase
G-protein	Guanine nucleotide binding protein
GPCR	G-protein coupled receptor
GDP	Guanosine diphosphate
GTP	Guanosine triphosphate
HA	Hyaluronan
HF	Heart failure
IBMX	3-isobutyl-1-methylxanthine
IL	Interleukin
IP1	Inositol monophosphate
IP2	Inositol biphosphate
IP3	Inositol triphosphate
iPSC	Induced pluripotent stem cell
IRES	Internal ribosomal entry sequence
ISO	Isoproterenol
JNK	c-Jun-NH_2-terminal kinase
K^+	Potassium
kD	KiloDalton
Meto	Metoprolol
MAPK	Mitogen activated protein kinase
MF20	Sarcomeric myosin
miPSC	Murine induced pluripotent stem cell
ml	Millilitre
NC	Nkx2.5-Cre
NCRL	Nkx2.5-Cre / Rosa lacZ
NE	Norepinephrine
Neo	Neonatal
NIS	Nonimmune serum
PBS	Phosphate buffered saline
PCR	Polymerase chain reaction
PDE	Phosphodiesterase
PE	Phenylephrine
PI	Phosphatidylinositol
PKA	Protein kinase A
PKC	Protein kinase C
PLB	Phospholamban
PLC	Phospholipase C
PNS	Parasympathetic nervous system
qPCR	Quantitative polymerase chain reaction
RAS	Renin angiotensin system
RL	Rosa-lacZ
RT-qPCR	Real Time Quantitative Polymerase Chain Reaction
SNS	Sympathetic nervous system
WT	Wild type

Acknowledgements

I would like to thank my supervisor, Dr. Kishore Pasumarthi, who offered continuous support and guidance throughout my graduate research. As my mentor, he provided me with direction and encouragement, and patiently answered endless amounts of questions. I am beyond grateful to have had not only the opportunity to complete my research in his lab, but to learn from someone with such an exceptional level of knowledge and expertise.

To past and present members of the Pasumarthi lab, I also extend my sincere thanks. I would like to thank Dr. Arun Govindapillai for his support and for being a great friend. I thankfully acknowledge Dr. Mark Baguma-Nibasheka for teaching me new lab techniques, and Sarita Chinni whose assistance over the past 2 years has been invaluable.

I would also like to acknowledge my advisory committee Dr. Chris Sinal and Dr. Keith Brunt for providing valuable insights and advice during the course of my research. Additionally, thanks are extended to staff members in the Department of Pharmacology, Luisa Vaughan, Sandi Leaf, and Cheryl Bailey for their administrative assistance. I am also grateful to my thesis examining committee, Dr. Keith Brunt, and Dr. Roger Croll for reviewing my work.

Lastly, I would like to extend thanks to my family and loved ones for their support and encouragement.

Chapter 1: Introduction

1.1 Cardiovascular Disease and Sympathetic Regulation

Cardiovascular diseases (CVD) include disorders comprised of the heart and blood vessels and are the leading cause of death worldwide. CVD is a hypernym for conditions such as coronary artery disease, myocardial infarction, cardiomyopathy, congenital heart disease, and heart failure, all of which result from poor lifestyle choices or genetic predisposition. Physical inactivity, poor diet, and substance abuse are common behavioural risk factors of CVD, whereas lifestyle changes have been shown to reduce this risk. CVD can also be attributed to other underlying determinants such as ageing population, urbanization, globalization, as well as hereditary factors, stress, and poverty (WHO, 2017).

Heart function is regulated by the autonomic nervous system (ANS), which is divided into two branches, the sympathetic nervous system (SNS) and the parasympathetic nervous system (PNS). These branches work in opposing fashion to regulate the heart via neurotransmitters that exert excitatory and inhibitory effects through adrenergic and muscarinic receptors at their target tissues (Florea & Cohn, 2014). Catecholamines mediating the SNS responses, epinephrine (Epi) and norepinephrine (NE), activate cardiac alpha and beta adrenergic receptors (Florea & Cohn, 2014) and exert effects on cardiac physiology (Santulli, 2015). These effects mediate positive inotropic and chronotropic responses, atrioventricular conduction and cardiac relaxation. While both autonomic branches are responsible for the control of heart rate, the SNS branch is practically the sole regulator of cardiac

contraction and relaxation (Lymperopoulos et al., 2013). The SNS also regulates vascular tone through control of peripheral resistance and cardiac output (Santulli, 2015).

Pathological insults to the heart, both direct and indirect that can lead to heart failure, including atherosclerosis, hypertension, renal and CNS disorders, and substance abuse. After an insult, the heart may experience a decline in pumping capacity and damage to the myocardium results in decreased cardiac output, a common biological marker used for the diagnosis of heart failure (HF). Following loss of cell contractility as a result of strain on cardiomyocytes (CMs), there is a decrease in cardiac output. This is a result of systolic or diastolic dysfunction, or a combination of both (Capote et al., 2015). HF is characterized by autonomic imbalance with increased sympathetic activity, withdrawal of vagal activity, and neurohormonal activation (Tina Shah, 2015). During HF, activity of the adrenergic (sympathetic) nervous system is greatly elevated due to catecholamine signaling leading to augmented heart rate and ventricular contractility, which helps to maintain cardiac output (Lymperopoulos et al., 2013; Tina Shah, 2015). Blood pressure is also maintained through systemic vasoconstriction and enhanced venous tone by increased SNS activity. Acutely, these compensatory responses will restore cardiac function, however if the insult persists, the elevated activity of the adrenergic nervous system will push the heart to work beyond its capabilities causing toxicity and increasing morbidity and mortality (Lymperopoulos et al., 2013). Increased sympathetic stimulation can result in ventricular remodelling along with increased myocardial mass. Chronic SNS and catecholamine activity in HF results in elevated

stimulation of the cardiac beta-adrenergic receptor system, which responds through desensitization and downregulation of receptors. Consequently, the heart will experience chronic inotropic reserve depletion (Tina Shah, 2015).

1.2 Adrenergic Receptor Classification

Adrenergic receptors are G-protein coupled receptors (GPCR), which are activated by endogenous catecholamine signaling hormones, epinephrine and norepinephrine. There are two types of adrenergic receptors, alpha adrenergic receptors (α-ARs) and beta adrenergic receptors (β-ARs), which are further classified into subtypes. There are two types of α-ARs, α1 and α2, and there are three types of β-ARs, β1, β2, and β3 adrenergic receptors (Lymperopoulos et al., 2013; Santulli & Iaccarino, 2016).

The postnatal heart contains two main ARs, β1-ARs, which account for 90% of ARs in the heart, and α1-ARs, accounting for 10% of ARs. β1-ARs mediate inotropic and chronotropic responses, however during heart failure, they are down regulated or dysfunctional due to increased levels of catecholamines. β1-ARs are also thought to exacerbate pathologic remodelling following long-term activation. α1-ARs are responsible for smooth muscle contraction. During long-term activation cardiac α1-ARs initiate trophic effects, which may counteract β1-AR over stimulation, and this is thought to be cardioprotective (O'Connell et al., 2014). β2-ARs are also expressed in the heart comprising 20-25% of cardiac β-ARs. Additionally, β2-ARs are located in the kidneys, lungs, and blood vessels. β3-ARs are found in minimal amounts within the heart with their primary location being adipose tissue (Madamanchi, 2007). β3-ARs

induce relaxation of smooth muscles in the airway, inhibit ileum and colon contractile activity, reduce the force of contraction in human ventricular muscle, stimulate L-type calcium current in human atrial myocytes, and produce peripheral vasodilation (Skeberdis, 2004). The α1-ARs are present in the heart and are further divided into 3 subtypes, α1A, α1B, and α1D, with all three subtypes expressed in a cell type specific manner within the heart (Santulli & Iaccarino, 2016). The α2-AR subfamily also consists of three subtypes α2A, α2B and α2C-ARs, while some species express an additional subtype, α2D (Ruuskanen et al., 2005; Santulli & Iaccarino, 2016). α2-ARs are located in neurons in the peripheral and CNS along with renal and intestinal epithelial cells (Saunders & Limbird, 1999).

α1-AR subtypes, each encoded by three separate genes, which have been pharmacologically defined and cloned, possess unique tissue distribution and drug specificity. The information available on pharmacologically defined subtypes of α1-ARs has been controversial for many years. Originally it was thought that there were four α1-AR subtypes, α1A, α1B, α1C and α1D, however evidence reveals that clones for α1C encode the α1A subtype (Zhong & Minneman, 1999).

The gene encoding the α1A subtype (ADRA1A) can generate four transcript variants from alternative gene splicing. Each variant encodes a different isoform differing in sequence and length of C-terminal domains, although they share similar properties for ligand binding (Chang et al., 1998). In humans, the α1A subtype canonical sequence has a molecular mass of 51, 487 daltons (Da) (UniProt, 1995b). The gene encoding the α1B subtype (ADRA1B), is identified as a protooncogene, owing to its ability to induce neoplastic transformation following transfection into

NIH 3T3 fibroblasts and other cell lines (Allen et al., 1991). In humans, the α1B subtype has a molecular mass of 56, 836 Da (UniProt, 2006). The human gene encoding the α1D subtype (ADRA1D), consists of a single intron interrupting the coding region along with 2 exons, which is also seen with the α1B gene (Hawrylyshyn et al., 2004). In humans, the α1D subtype has a molecular mass of 60, 463 Da (UniProt, 1995a).

1.3 Adrenergic Receptor Signaling

Adrenergic receptors belong to the class of guanine nucleotide binding protein (G-protein) coupled receptors. GPCRs contain seven transmembrane domains with one external N-terminal domain, three extracellular loops, three intracellular loops, and one intracellular C-terminal tail (Prazeres & Martins, 2015). GPCR transduce intracellular signals, which are initiated by ligand binding of neurotransmitters or hormones. The initial binding of a ligand induces a conformational change in the GPCR, leading to coupling of heterotrimeric G protein subunits, α, β, and γ. Coupling results in the exchange of guanosine diphosphate (GDP), which is bound to the G protein, with guanosine triphosphate (GTP). As a result of GTP binding, the G protein dissociates into Gα and Gβγ subunits, mediating downstream signaling (Madamanchi, 2007).

G proteins are divided into four subfamilies based on functionality: G_s, which stimulates the enzyme adenylyl cyclase (AC) activity and increases the formation of cyclic adenosine monophosphate (cAMP), G_i, which inhibits AC and decreases the formation of cAMP, G_q, is responsible for an increase in intracellular calcium levels,

and G_{12} which regulates RhoGEF (Madamanchi, 2007; Siehler, 2009; Xiao, 2001). GPCR subunits modulate several effector molecules differentiating cellular signals. In turn, these effector molecules regulate second messenger concentrations leading to the activation of several downstream signaling molecules (Madamanchi, 2007).

Alpha-1 adrenergic receptor subtypes are $G_q/11$ ($G\alpha_q$) coupled GPCRs, however they possess different characteristics that vary from typical Gq-coupled receptors in that α1-AR expression is limited to cardiomyocytes in the heart and they are localized to, and signal at the nucleus. In general, when α1-ARs are stimulated, this signaling mechanism occurs at the plasma membrane and results in the activation of phospholipase C (PLC). Following its activation, PLC cleaves phosphatidylinositol (PI) leading to an increase in inositol triphosphate (IP3) and diacylglycerol (DAG). As a result, IP3 releases calcium from intracellular stores by binding to an IP3 receptor, and DAG leads to the activation of protein kinase C (PKC) (O'Connell et al., 2014). PKC phosphorylates calcium channels leading to an increase of calcium within cells, causing smooth muscle contraction**.** IP3 is rapidly degraded to inositol biphosphate (IP2), and then inositol monophosphate (IP1) (Arkin et al., 2004). Through activation of G_q-coupled receptors in the heart, α1-ARs are cardioprotective as they prevent cardiomyocyte death, activate physiologic hypertrophy, induce preconditioning, and increase contractile function during heart failure (O'Connell et al., 2014).

Alpha-2 adrenergic receptors are coupled to the G_i protein, resulting in an inhibitory effect on adenylyl cyclase activity. α2-AR stimulation leads to the activation of potassium (K^+) channels and the inhibition of voltage-gated Ca^{2+} channels

(Saunders, 1999). By inhibiting adenylyl cyclase, cAMP levels are reduced resulting in hyperpolarization of noradrenergic neurons located in the locus ceruleus. cAMP inhibition causes potassium efflux through calcium channels, which prevents the entry of calcium ions into the nerve terminal. This suppresses neural firing leading to hypnosis and sedation. This negative feedback loop can also result in attenuation of the sympathetic stress response, along with reductions in blood pressure and heart rate (Giovannitti et al., 2015). Activation of α2-ARs also results in reduction of voltage gated Ca^{2+} currents and reduced release of NE (Boehm & Huck, 1995).

Beta-1 adrenergic receptors in cardiomyocytes bind to the G_s subunit when stimulated, leading to the activation of AC. Second messenger cAMP is generated in response, and increased levels of cAMP result in the activation of cAMP-dependent protein kinase A (PKA). Once activated, PKA increases contractility by phosphorylating troponin I, phospholamban (PLB), and the L-type Ca^{2+} channel (Madamanchi, 2007). Phosphodiesterase (PDE) is an enzyme that mediates signal termination by catalyzing the conversion of cAMP to 5′AMP (Moorthy et al., 2011).

Beta-2 adrenergic receptors are coupled to the G inhibitory (G_i) protein. Activation of G_i inhibits AC activity and activates mitogen-activated protein kinases (MAPK) downstream. Additionally, $G_i\alpha$ coupling leads to the activation of cytosolic effector molecule phospholipase AC (cPLA2), which results in calcium signaling and cardiac contraction, independent of cAMP. The effect of β2-ARs on the heart varies based on the pathophysiological state of the heart and on the species (Madamanchi, 2007). Additionally, there is evidence that α1A GPCRs can activate MAPK pathways. Briefly, MAPK signaling is subdivided into three pathways including extracellular

signaling regulated kinases 1 and 2 (ERKs), c-Jun-NH2-terminal kinase (JNK), and p38 MAPK. MAPK pathways are activated by various intracellular and extracellular stimuli such as growth factors, hormones, cytokines, and cellular stressors including endoplasmic reticulum stress and oxidative stress. Activation of MAPK signaling plays a prominent role in the regulation of cell survival and death, cell proliferation, and cell differentiation (Kim & Choi, 2010). Studies have shown that the α1A-AR subtype coupled to G_q can activate MAPK signaling pathways, including EKR, JNK, and p38 MAPK, promoting differentiation (Williams et al., 1998).

1.4 Relative Expression of α1-ARs in Postnatal Tissues

α1-AR mRNA levels in different species (human, rat, mouse, guinea pig, rabbit) are widely distributed in several areas of the brain and extracerebral tissues, however there is heterogeneity among species and subtypes. The distribution of mRNA is tissue selective creating differences seen among species. In humans, α1-ARs are expressed in brain, heart, liver, spleen, kidney, adrenal, and pancreas. For all three α1-AR subtypes, mRNA can be seen in varying degrees among the aorta, kidney and liver along with α1B expression in the retina (Price et al., 1994).

Alpha-1 adrenergic receptor mRNA expression is widely distributed in mouse tissues with expression in several areas of the brain including the striatum, brainstem, and hippocampus. The receptors are also present in other tissues including the heart, lung, kidney, spleen, and liver (Alonso-Llamazares et al., 1995). α1-AR expression is also widely distributed in rat tissue, and experiences heterogeneity among subtypes; α1A and α1D receptor mRNA has significant

expression in the vas deferens, while the highest level of α1B mRNA expression is in the heart (Scofield et al., 1995).

1.5 Ontogeny of Adrenergic Receptors

There is limited information on the ontogeny of α1-AR subtypes, however several studies characterized the total α1-AR content using various methodologies. A study conducted by Schaffer and Williams on rat ventricular myocardium membranes using [^{125}I] 2-(β hydroxy phenyl) ethylaminomethyl tetralone binding isotherms found that a high concentration of α1-ARs is maintained from the late fetal stage through to weaning specified as 25 days post birth (Schaffer & Williams, 1986). Their study also found that the concentration of α1-ARs in rat myocardium is maintained at a lower level from early adult life (42 days) through to senescence (24 months). The presence of α1-ARs during early development suggests that the receptors play a role in the promotion of growth within the heart (Schaffer & Williams, 1986). Studies using knockout mice also suggest that α1-ARs are required during postnatal cardiac development for hypertrophic growth as this is a time for physiologic heart growth (O'Connell et al., 2014).

There is evidence that the concentrations of α1-ARs and β-ARs shift with age. Noguchi, Whitsett, and Dickman used radioligands [^{3}H]-prazosin for α-AR binding sites and (-)-[3H]-dihydroalprenolol [(-)-[^{3}H]-DHA] for β-AR binding sites were used to measure adrenergic receptors in rat myocardium (Noguchi et al., 1981). Radioligand activity revealed that α1-AR binding sites increased rapidly during the

first 15 days of age while (-)-[^{3}H]-DHA binding sites for β-AR revealed a gradual decrease with advancing age (Noguchi et al., 1981).

A study conducted by Buchthal, Bilezikian, and Danilo (1987) using radioligand binding in canine cardiac membranes found that the density of α1-ARs decreases during maturation. Experiments using canine ventricular myocardium isolated from fetal, neonatal, and adult stages suggested that there were 2 classes of α1-AR receptors. The first class had high affinity and limited capacity, while the second class had lower affinity but a higher capacity. All age groups (fetal, neonatal, adult) showed similar affinities and capacities for the higher affinity receptor, while the second class of receptor with a lower affinity site resulted in greater capacity for fetal and neonatal compared to adult canine myocardium (Buchthal et al., 1987). Similar results were also reported by Felder, Calcagno, Eisner, & Jose, which found that during maturation, the density of α-AR decreases in canine cardiac membranes (Felder et al., 1982). Currently, there is no mRNA or expression data available for α1-AR subtypes during cardiac ontogeny particularly during embryonic development.

In rodents, β-ARs are present as early as embryonic day E10.5. It is known that stimulation of -ARs can decrease embryonic ventricular cell proliferation in vitro and result in reduced graft size following intracardiac cell transplantation. Additionally, it is known that β1-AR antagonists can abrogate the antiproliferative effects resulting from stimulation of β-ARs and can also increase graft size (Feridooni et al., 2017). Studies conducted by Feridooni et al. found that treatment of cultured embryonic ventricular cells with isoproterenol (ISO) resulted in decreased cell proliferation of cardiac progenitor cells (CPCs) and cardiomyocytes (CMs) (Feridooni et al., 2017).

Their results indicated that cotreatment with metoprolol abrogated the antiproliferative effects of ISO. In comparison to control groups, the study also found that treatment with ISO resulted in an increased percentage of differentiated CMs. Furthermore, their results indicated that ISO stimulation of recipient mice following intracardiac cell transplantation resulted in decreased graft size, whereas metoprolol treated mice exhibited protection from the inhibitory effects (Feridooni et al., 2017). Although there is information regarding the role of β-AR signaling during embryonic cell proliferation and differentiation, the role of α1-AR signaling in cardiac ontogeny and cell proliferation or differentiation is not clear.

1.6 Cardiac Context of α1-ARs

As mentioned, α1-ARs constitute the minority of ARs in the heart, accounting for 10% of ARs. Cardiac expression is consistent across all species, however rat α1-AR levels are approximately 10-fold higher in comparison to all other species. Another difference found in α1-AR cardiac expression is that CMs of all species contain mRNA for all three subtypes, however only receptor proteins for α1A and α1B are detected (O'Connell et al., 2014).

Although cardiomyocytes contain mRNA for α1-AR subtypes, previous knockout studies in mice revealed that only α1A and α1B subtype receptor proteins are expressed in adult CM and that α1B is predominant (O'Connell et al., 2014). Additionally, rodent studies suggest that the α1D subtype may only be expressed in coronary vasculature (O'Connell et al., 2014). α1-AR expression levels in humans are similar to that of mice and other species. Humans possess mRNA for all α1-AR

subtypes with α1A and α1B expression in the myocardium, while coronary smooth muscle contains the α1D subtype (O'Connell et al., 2014).

1.7 α1-AR Signaling in Cardiomyocytes

Conventional models for GPCR signaling are referred to as “outside-in” where the receptor is activated at the plasma membrane initiating downstream signaling within the cell. New models for GPCR signaling are described as “novel signaling” (nuclear to cytoplasmic) where signaling occurs at the nucleus. This type of signaling has been seen in several cell types including hepatocytes, neurons, and cardiomyocytes (O'Connell et al., 2014).

The prevalent view is that GPCRs are primarily localized to the plasma membrane. Recent studies have shown that α1-AR GPCRs localize to binucleated CMs in adults, and they may regulate important physiologic functions. Knowledge of subcellular localization of α1-AR in CMs is important as the location of signaling molecules determines function. In adult mouse CMs, approximately 80% of α1-AR localize to the nucleus (O'Connell et al., 2014).

Functional nuclear localization sequences have been identified for α1-ARs. Proteins containing nuclear localization sequences are recognized and these sequences facilitate the transport of proteins targeting the nucleoplasm and inner nuclear membrane. Studies conducted by Wright et al. in adult cardiomyocytes identified α1A and α1B subtype nuclear localization sequences. Additionally, this study found that mutation of the nuclear localization sequence resulted in loss of nuclear localization of α1A and α1B subtypes (Wright et al., 2012). The study also

found that the α1A subtype has a putative bi-partite nuclear localization sequence, while the α1B subtype has a nuclear localization sequence with an arginine rich glycine-arginine repeat (Wright et al., 2012).

There are a couple of suggestions surrounding the localization of α1-AR GPCRs in the nucleus. If the ligand binding domain is oriented facing inside the nucleus, the ligand would be required to enter the nucleus. The ligand would then initiate signaling on the cytoplasmic side between the inner and outer nuclear membrane space. Alternatively, if the ligand binding domain of the GPCR were oriented between the outer and inner nuclear membrane, the ligand would initiate signaling inside the nucleus (**Figure 1.1**) (O'Connell et al., 2014). Nuclear signaling involving the α1-AR GPCR would require ligands to traverse the plasma membrane and transit to the nucleus. In adult cardiomyocytes, an organic cation transporter 3 (OCT3) is expressed at the plasma membrane and nuclear membrane. OCT3 actively transports α1-AR agonists (NE/PE) across membranes. The α1-AR antagonist, prazosin, is capable of crossing the plasma membrane to inhibit the α1-AR (O'Connell et al., 2014).

α1-ARs are known to be cardioprotective contrary to β1-ARs, which exacerbate pathologic remodelling. As a result, differences in receptor localization may potentiate differences between pathologic and physiologic signaling. This suggests that it may be possible that different signaling pathway activation occurs at the nucleus (Wu et al., 2014). Variations in receptor localization of different GPCRs could potentially provide therapeutic targets for heart disease (O'Connell et al., 2014). A recently published study confirmed that ligand binding of nuclear α1-ARs can induce cardiomyocyte hypertrophy via PLCβ1 activation at the nuclear

membrane, IP3 production and influx of nuclear calcium followed by activation of calcium-calmodulin dependent protein kinase II (CaMKII) and export of histone deacetylase 5 (HDAC5) into the cytoplasm, which in turn facilitates the hypertrophic gene expression program (Dahl et al., 2018).

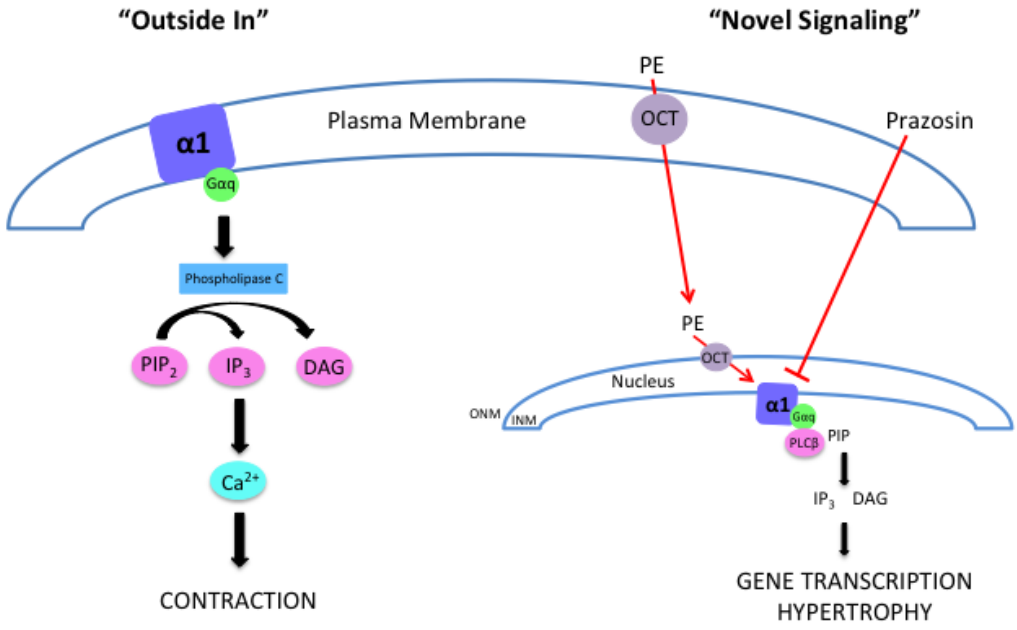

Figure 1.1: Conventional model Vs. suggested novel model for α1-AR signaling in cardiomyocytes. The "**Outside In**" signaling model for α1-ARs positions the receptor at the plasma membrane with the ligand binding domain facing outward. Catecholamines bind to the α1-AR and initiate second messenger signaling downstream inside the cell. The "**Novel Signaling**" model suggests that the ligand binding domain for the α1-AR is oriented facing inside the nucleus or between the outer and inner nuclear membrane. On the basis of the orientation in the figure above, the α1-AR is localized to the inner nuclear membrane. This orientation positions the receptor with the ligand binding domain facing the space between the inner nuclear membrane (INM) and outer nuclear membrane (ONM). This suggests that agonist stimulation of the α1-AR induces signaling inside the nucleus. Following stimulation of the α1-AR, activated PLCβ cleaves PIP_2 into IP_3 and DAG. IP3 and DAG activate further downstream signaling involved in gene transcription and cardiomyocyte hypertrophy. The organic cation transporter 3 (OCT) actively transports α1-AR agonists (PE) across membranes. The α1-AR antagonist, prazosin, is capable of crossing the plasma membrane and inhibits the α1-AR. Modified from (Dahl et al., 2018; O'Connell et al., 2014).

In cardiomyocytes, it is proposed that following GPCR activation in the nucleus, the signal transduces to targets in the cytosol (sarcomere) or membrane to regulate survival signaling and contractile functions. In adult mouse CMs, an ERK survival signaling pathway has been identified for the α1A subtype. This pathway is thought to be important in the response to pathologic stress induced by pressure overload, whereas absence of this pathway may result in a maladaptive response. The resulting stress has been known to induce heart failure resulting from fibrosis, contractile dysfunction, CM cell death, and cardiac specific gene transcription failure (Wu et al., 2014).

1.8 Adrenergic Receptor Agonists and Antagonists

Carvedilol, a drug that is prescribed extensively for the treatment of heart failure and hypertension, is a third-generation beta-blocker due to its additional vasodilating effects. Carvedilol is a non-selective β1 and β2-AR antagonist with α1-AR blocking activity and is thought to have additional benefits over selective β1-AR blockers such as metoprolol (Wisler et al., 2007). Carvedilol also possesses antiproliferative effects and is known to inhibit oxygen-free radicals (Thomas C. Malig, 2017).

Carvedilol, administered orally, is a basic, lipophilic compound, which primarily binds to the plasma protein albumin. Carvedilol has substantial distribution into extravascular tissues and is metabolized extensively with less than 2% of the original dose excreted in urine in unchanged form. Metabolism of carvedilol produces three active metabolites, with beta blocking activity that is more potent compared to

the parent drug, however metabolites possess weak vasodilating capabilities (FDA, 2005).

The antioxidant activity of carvedilol is thought to be attributed to the drug's phenolic metabolites (Thomas C. Malig, 2017). The mechanism of carvedilol's antioxidant activity is linked to its inhibition of lipid oxidation via scavenging free radicals. This novel property differs from other beta-blockers and is thought to account for its cardioprotective activity (Yue et al., 1992). In addition to its antioxidant activity against oxygen-free radicals, carvedilol prevents infiltration of ischemic myocardium by inflammatory cells and blocks calcium channels at higher concentrations (Ruffolo & Feuerstein, 1997; Ruffolo et al., 1990).

During heart failure, pressure and volume overload impair myocardial contractility, leading to myocardial ischemia, which generate free radicals. Reactive oxygen species are attributed to cytotoxic effects following cardiac ischemic injury. Induced oxygen radicals are known to activate genes and transcription factors that are associated with cardiac remodelling and inflammation (Ruffolo & Feuerstein, 1997).

Treatment with carvedilol decreases morbidity and mortality in patients with hypertension and congestive heart failure. Through the beta blockade, carvedilol decreases myocardial work by reducing myocardial oxygen demand. As a result, carvedilol decreases contractility, heart rate, and wall tension. Through the α blockade, carvedilol decreases afterload through vasodilation, offsetting lusitropic effects that typically result from the beta blockade, stemming from impedance to left

ventricular ejection. As a result, cardiac output and stroke volume is maintained and possibly increased with carvedilol treatment (Ruffolo & Feuerstein, 1997).

Metoprolol is a selective β1-AR antagonist that is administered orally and used to treat angina, hypertension, and heart failure (FDA, 2006). Treatment with metoprolol has also been shown to reduce mortality and morbidity in patients with heart failure. Metoprolol reduces blood pressure and the rate and force of myocardial contraction, while increasing femoral and systemic artery resistance. Treatment with metoprolol also increases left ventricular volume and end diastolic pressure while consequently decreasing cardiac output. Decreased cardiac output is undesirable as it leads to enhanced constriction of systemic arteriolar resistance vessels (Weber et al., 1998).

Prazosin is a non-selective α1-AR ligand antagonist with vasodilating activity used for the treatment of hypertension (Schirger & Sheps, 1977). Previous experiments conducted by Zhang et al. (2002) revealed prazosin binding sites in five rat tissues including heart, kidney, spleen, liver, and submaxillary gland. Binding studies showed prazosin binding to α1A and α1B subtypes in the heart while α1D subtype binding was undetectable (Zhang et al., 2002).

At low doses in vitro, prazosin is an inhibitor of phosphodiesterase and is capable of binding with a moiety of cAMP and a moiety of papaverine, which is a known PDE inhibitor (Koch-Weser et al., 1979). cAMP is a mediator of smooth muscle relaxation and prazosin inhibition of cAMP hydrolysis via PDE inhibition contributes to vasodilation effects. However, when prazosin is administered at therapeutic doses, it is unlikely that concentrations required for prazosin inhibition of PDE can be

achieved (Koch-Weser et al., 1979). Through the α blockade, prazosin reduces peripheral vascular resistance. Prazosin has been shown to exert alpha blocking action by reversing the epinephrine pressor response (increase in arterial blood pressure) along with inhibiting norepinephrine's vasoconstrictor action (Koch-Weser et al., 1979).

Phenylephrine (PE) is an α1-AR agonist used for arterial pressure control during anaesthesia. PE causes an increase in arterial pressure, systemic vascular resistance, and left ventricular afterload, however the effect on cardiac output is not clear. It is expected that the PE induced rise in afterload results in lowered cardiac output. One study suggested that the effects of PE on cardiac output are dependent on the position of the heart (preload dependency). Researchers found that PE decreases cardiac output when the heart is preload independent (when the heart is operating on the flat part of the ventricular function curve), and induces an increase in cardiac output when the heart is preload dependent (when the heart is operating on the steep part of the ventricular function curve) (Cannesson et al., 2012).

There are limited selective α1-AR subtype specific agonists and antagonists available. A61603 is a highly selective and potent α1A agonist. This agonist is known to activate ERK in 62% of wildtype (WT) cardiomyocytes. There are no selective agonists for α1B. Additionally, 5-methylurapidil is a selective α1A antagonist (Myagmar et al., 2017). Chloroethylclonidine (CEC) is a selective α1B antagonist and BMY7378 is a selective α1D antagonist (Liu et al., 2014).

Isoproterenol (ISO) is a non-selective β-AR agonist, which can induce chronotropy. ISO increases contractility and heart rate (through β1 and β2

stimulation) and also causes vasodilation in skeletal muscle, renal, and mesenteric tissue (β2). Stimulation of β2-ARs in vascular smooth muscle results in vasodilation following an increase in cAMP. The increase in cAMP inhibits myosin light chain kinase, which is responsible for smooth muscle myosin light chain phosphorylation. Use of ISO also results in vasodilation of the pulmonary circulation, usually accompanied by tachycardia. Together, tachycardia and increased contractility lead to increased myocardial oxygen consumption. Additionally, ISO is an effective bronchodilator via β2-AR stimulation (Shukla AC et al., 2009). Following stimulation of the β2-AR, cAMP formation and PKA activation results in phosphorylation of proteins inducing airway smooth muscle relaxation (Shore & Drazen, 2003).

1.9 Interacting Partners for α1-ARs

Novel proteins have been identified that bind with α1-ARs. In yeast cells, filamin C protein (a cytoskeletal protein) was identified to interact with α1-AR subtypes. Zhang et al. performed a yeast two-hybrid assay to screen a library of human brain cDNA using the α1A-AR C terminus as a bait to determine proteins that bind and interact with α1-ARs (Zhang et al., 2004). Filamin C (FLNc) exists only in myocardiac muscles and cytoskeleton of muscle cells, a characteristic different from the tissue distribution of filamin A and filamin B. It was determined that FLNc interacted with the C-terminal domain of α1-AR subtypes, suggesting that FLNc plays a role in cellular signaling and localization of α1-ARs, however interaction of FLNc with α1-AR subtypes in mammalian cells requires additional studies (Zhang et al., 2004).

Typical consideration of GPCRs focused on activation of signaling cascades (involving GTPases, adenylyl cyclases, protein kinases, phospholipases, ion channels), leading to indirect interaction with cytoskeletal proteins. Filamin is an actin cross-linking cytoskeletal protein known to interact with GPCRs. Tirupula et al. suggested that GPCRs involved in cardiac physiology may contain a filamin A binding motif, which binds and activates filamin A (Tirupula et al., 2015). Binding of the α1D subtype specific filamin binding motif by a filamin A surrogate (filamin A Ig16-24) was shown to trigger the phosphorylation of filamin by cellular protein kinases. Phosphorylation of filamin A is important for the regulation of the structure and dynamics of the cytoskeleton. In the human genome, less than 20% of GPCRs contain a filamin binding motif (FBM) in the cytoplasmic domain (Tirupula et al., 2015).

α1-ARs regulate multiple signaling pathways including protein kinase C, phospholipase C, MAPK pathways, and they are known to mediate gene expression. α1-AR have been shown to play a role in novel signaling pathways that induce the secretion of factors including interleukin (IL)-6, fibroblast growth factor (FGF7), and hyaluronan (HA). These factors regulate cell motility, adhesion, and proinflammatory responses by interacting with the extracellular matrix (Shi et al., 2006).

Additionally, it has been reported that there is a cross talk between α1-ARs and AT1R. It has been suggested that cross talk is bidirectional and counterregulatory. Studies conducted using NE stimulation of α1-ARs induced down regulation of AT1R gene expression in hamsters. There is an important balance between the sympathetic nervous system and the renin-angiotensin system (RAS), which is crucial for the maintenance of cardiovascular homeostasis, and it is

suggested that alterations to signaling pathways and cross talk could be linked to heart failure (Crespo, 2000).

1.10 Role of Adrenergic Receptors in Cell Proliferation and Cell Size

α1-ARs mediate several physiological actions including their prominent role in the regulation of cell growth and proliferation. However, there is a debate regarding the role of α1-ARs in regulating cell proliferation. It is known that α1-AR stimulation results in anti-proliferative and hypertrophic effects, while some studies suggest that α1-AR stimulation increases proliferation. Lei, Schwinn, and Morris conducted experiments using rat-1 fibroblasts expressing human α1A-AR tagged with hemagglutinin and found that stimulation with PE resulted in antiproliferative hypertrophy or cell proliferation depending on the concentration of PE (Lei et al., 2013). Cells treated with a high dose of PE ($>10^{-7}$ M) resulted in an antiproliferative hypertrophic response, while stimulation with a low dose of PE ($>10^{-8}$ M) induced an increase in cell proliferation dependent on ERK signaling (Lei et al., 2013).

Evidence supports the involvement of α1-ARs in enhancing gene expression related to cell growth within cells including hepatocytes, adipocytes, vascular smooth muscle cells, and cardiomyocytes (Shibata K et al., 2003). It is also suggested that the physiological roles of α1-ARs may be subtype specific with distinct coupling properties related to signal transduction and regulation of cell growth at the cellular level (Shibata et al., 2003; Williams et al., 1998).

α1-ARs have been shown to regulate novel signaling pathways including pathways that promote growth. Studies conducted by Shi et al. have indicated that

following prolonged stimulation of α1-ARs, alterations in gene expression pathways were notable, with a dramatic down-regulation in cell cycle and mitotic cycle gene expression (Shi et al., 2006). Previous studies have shown that α1-ARs play a role in the regulation of genes that control the cell cycle. Activation of α1-ARs results in arrest of the G1-S cell cycle of different cell types including rat-1 fibroblasts, however the effects are dependent on the receptor subtype (Gonzalez-Cabrera et al., 2004; Shi et al., 2006). The phenotypic response of α1-ARs is unclear as subtypes have expressed antiproliferative as well as proliferative phenotypes (Lei et al., 2013).

Recent studies conducted using Chinese hamster ovary (CHO) cells found that α1-ARs may play different roles in the regulation of cell growth and proliferation. Research conducted by Shibata et al. found that subtypes α1A and α1B are involved in stimulation of the cAMP signaling pathway, which blocks depletion of $p27^{Kip1}$, a cell cycle-dependent kinase inhibitor, whereas α1D did not play a role (Shibata et al., 2003). As a result, α1A and α1B inhibit serum-promoted cell proliferation, as $p27^{Kip1}$ is a mediator of G1 phase arrest, which is induced by cAMP. The anti-proliferative differences (α1A and α1B vs. α1D) may be attributed to differences in ERK isoforms in the MAPK signal transduction pathway (Shibata et al., 2003).

Studies conducted by Gonzalez-Cabrera et al. showed that subtypes α1A and α1D exerted control on the cell cycle by decreasing cell cycle progressive cyclin transcription and through down-regulation of cyclin dependent kinases (CDK-1 and CDK-2) (Gonzalez-Cabrera et al., 2004). As a result, stimulation of α1A and α1D subtypes can lead to G1-S cell cycle arrest. However, α1B-AR stimulation in Rat-1 fibroblasts did not result in cell cycle arrest, but rather lead to cell cycle progression.

Some studies found that stimulation of the α1 receptors resulted in up-regulation of genes CCND1/cyclin D1. These genes are known to be involved in unchecked cell cycle progression (Gonzalez-Cabrera et al., 2004).

It was recently demonstrated that a non-selective β-AR agonist, ISO, decreased proliferation of CPCs in vitro and reduce graft size after intracardiac cell transplantation. A β1-AR antagonist (Metoprolol) abrogated the anti-proliferative effects of ISO and increased graft size. Overexpression of β1-ARs in cardiac cells results in hypertrophy of cardiomyocytes (Feridooni et al., 2017; Madamanchi, 2007).

Cardiac hypertrophy results in remodelling of the heart due to increased myocardial mass and CM size induced by physiological or pathological stimuli (Cotecchia et al., 2015). Physiological hypertrophy is characterized as an adaptive response resulting from exercise or pregnancy. Pathological hypertrophy is commonly seen following stress or injury to the heart (myocardial infarction, hypertension), with the potential to decompensate to heart failure (Fu et al., 2013).

Excessive stress can result in the initiation of myocardial hypertrophy in an attempt to preserve cardiac function, however prolonged hypertrophy can result in heart failure (Cotecchia et al., 2015). In an attempt to maintain efficiency of the hypertrophic heart, prolonged activation of the SNS, attempting to maintain blood pressure and cardiac output, becomes maladaptive (Madamanchi, 2007).

The hypertrophic response activates multiple signaling pathways. Simultaneously, consistent elevation of catecholamine initiates overstimulation of β-ARs signaling pathways. Over time, β-AR function will be diminished along with loss of contractility as a result of sustained activation of hypertrophic processes and the β-

AR system (Madamanchi, 2007). Treatments with β-AR antagonists have been shown to restore levels of β-ARs and cardiac function, which may result from inhibition of β-AR activity and hypertrophic effects. It has also been suggested that antagonists may reverse abnormalities in signaling and re-sensitize the receptor system, and also reverse consequences due to prolonged stimulation by catecholamines (Madamanchi, 2007).

Studies have demonstrated that α1-ARs can induce cardiac hypertrophy leading to improvements in cardiac output. Following birth, α1-ARs play an important role in physiological heart growth and can also exert protective effects on the heart, demonstrated by α1A and α1B knock out studies. In the absence of α1-ARs, the heart may experience pathological hypertrophy and cardiomyopathy (Cotecchia et al., 2015).

Other α1A and α1B knock out studies have shown that cells lacking receptor subtypes exhibited necrosis following exposure to toxic stimuli, whereas re-expression of the α1A (and not α1B) subtype rescued CMs, which were experiencing increased susceptibility to death. This suggests that α1-ARs play a prominent role in survival of heart cells. Altogether, this suggests that α1-ARs exhibit cytoprotective tendencies during heart failure by inducing adaptive hypertrophy and preventing death of CMs (Cotecchia et al., 2015).

1.11 Role of Adrenergic Receptors in Cell Differentiation

α1-ARs have been implicated in cell differentiation in several different cell types. As mentioned, α1-ARs affect cell growth through activation of MAPK signaling

pathways. α1-AR subtypes can activate pathways including EKR, JNK, and p38 MAPK, which results in the promotion of cell differentiation. Treatment of a stable clone of PC12 cell expressing α1A-ARs with NE has been shown to increase the levels of inositol phosphate and promote differentiation of PC12 cells into a neuronal-like phenotype (Williams et al., 1998).

Another study demonstrated how murine-induced pluripotent stem cells (miPSC) differentiated into functional cardiomyocytes in vitro following activation of α1-ARs (Li et al., 2017). In this study, stimulation of stem cell cultures with Epi as an agonist resulted in enhanced CM differentiation via MEK/ERK1/2 signaling pathway. Alternatively, blocking α1-ARs with phentolamine resulted in a significant reduction in CM differentiation (Li et al., 2017). In addition, stimulation of day 7 $Nkx2.5^{+}$ CPCs in miPSC cultures with PE led to a significant increase in BrdU incorporation compared to control cultures, whereas, stimulation of day 15 CMs with PE did not have any effect on cell proliferation. Interestingly, α1-AR stimulation with PE in undifferentiated miPSC cultures led to a significant decrease in the proportion of cells undergoing S-phase compared to the controls (Li et al., 2017). Collectively, these results suggest that α1-ARs can play a role in the proliferation and differentiation of miPSC cultures using a MEK-ERK1/2 dependent mechanism.

Regulation of heart formation during embryogenesis is marked by the expression of key transcription factors such as homeobox gene Nkx2.5 (NK2 transcription-factor related, locus 5), ANP (Govindapillai et al., 2018), connexion 40 (Cx40) (Delorme et al., 1995), GATA4, 5 and 6 (Molkentin, 2000), Hand1/2 (heart and neural crest derivatives expressed transcript 1/2) (Srivastava et al., 1995),

hyperpolarization-activated cyclic nucleotide-gated cation channel (HCN4) (Garcia-Frigola et al., 2003), Mef2b/c (myocyte enhancer factor) (Desjardins & Naya, 2016), and Tbx5 and 20 (Meins et al., 2000). Knockout of particular factors such as mice homozygous for a null mutation of Mef2c inhibited looping morphogenesis of the heart tube, right ventricle formation, and resulted in a lack of expression of a subset of cardiac muscle genes (Lin et al., 1997). In embryonic day 10.5 mouse embryos, Srivastava et al. (1997) showed that targeted gene deletion of dHAND resulted in embryonic lethality as a result of heart failure (Srivastava et al., 1997).

Studies conduced by Ieda et al. showed that a combination of transcription factors including Mef2c, Tbx5, and GATA4 reprogrammed fibroblasts into differentiated cardiomyocyte-like cells (Ieda et al., 2010). Another showed that four transcription factors including GATA4, Hand, Mef2c, and TBX5 are required for cardiomyogenic conversion of non-cardiomyocytes (Song et al., 2012). Based on these studies, it is known that several transcription factors are important for the differentiation of CPCs and CMs however the effect of carvedilol on these transcription factors during embryonic development is unknown.

1.12 Rationale

There has been a progression in the standard treatments for HF including beta adrenergic receptor blockers, angiotensin-converting enzyme (ACE) inhibitors, aldosterone antagonists, and resynchronization therapy, however there still remains poor prognosis with approximately half of those diagnosed dying within five years. Pharmacological blockade of the SNS with β blockers have proven to reduce mortality and reverse ventricular remodelling (Florea & Cohn, 2014). Metoprolol, a selective

β1-AR antagonist, is a drug commonly used to treat hypertension, cardiac arrhythmias, and angina. Carvedilol, which is a non-selective and β-AR and α1-AR blocker, is thought to have additional benefits over selective β1-AR blockers such as metoprolol. The exact mechanism behind carvedilol is unclear, although it is thought to block α1-AR vasoconstriction. **However, the effects of carvedilol blockade on embryonic ventricular cell proliferation and differentiation are unknown.**

Since carvedilol has α1-AR, β1 and β2-AR blocking activity we used α1-AR and β-AR agonists and antagonists to investigate their effects on embryonic ventricular cell proliferation and differentiation. The non-selective β-AR agonist ISO was used to investigate β-AR activity, and PE and prazosin were used to investigate α1-AR activity in association with cell proliferation and differentiation.

Induced pluripotent stem cells (iPSC) and embryonic stem cells (ESC) derived CPCs and CMs are important cell based therapies for studying heart disease. These regenerative cell based therapies are capable of differentiating into CMs in vitro. Research surrounding CMs derived from iPSC and ESC focus on transplantation of these cells as a regenerative hearth therapy (Li et al., 2017). Embryonic E11.5 ventricular cultures represent a good model system to study the mechanisms regulating proliferation and differentiation of CPCs and CMs and results obtained from such studies are directly applicable to stem cell based interventions.

It is important to study any potential drug interactions with cell based therapies in terms of graft size, proliferation and differentiation potential of transplanted cells. It is known that β-blockers have a positive effect on transplanted cells based on previous studies conducted by Feridooni et al. (2017). Feridooni and

colleagues found that treatment with metoprolol protected graft cells following injection of the E11.5 ventricular cells into adult mice (Feridooni et al., 2017). Additionally, it is known that administration of calcium channel blockers have negative effects on transplanted cells. Hotchkiss et al. found that E11.5 ventricular cells transplanted into adult mice resulted in smaller graft sizes following treatment with Ca^{2+} channel blocker, nifedipine (Hotchkiss et al., 2014).

It is also important to study drug interactions with the developing heart as results from these findings can better inform physicians about potential cardiac developmental risks associated with using AR blockers during pregnancy. Meidahl Peterson et al. conducted a population based retrospective cohort study focused on pregnant women who redeemed β-blockers during their pregnancy (Meidahl Petersen et al., 2012). Based on their survey, they discovered that exposure to β-blockers during pregnancy was associated with an increased risk of preterm birth, being born small-for-gestational-age (SGA), and perinatal mortality (Meidahl Petersen et al., 2012).

Thus, the following questions were developed for my masters work: What are the expression profiles of different α1-AR subtypes during cardiac ontogeny?; do these receptors play any role in cell size regulation?; and do they play any role in cell proliferation and differentiation of embryonic ventricular cells? **It is hypothesized that expression of α1-AR subtypes are differentially regulated during embryonic heart development and α1-AR signaling plays an important role in ventricular cell proliferation and differentiation.**

My first research aim was to examine the gene expression profiles of different α1-AR subtypes (α1A, α1B, α1D) during cardiac development. This was accomplished though RT-qPCR analysis of total RNA samples extracted from embryonic ventricular cells at different developmental stages. My second research aim focused on examining the subcellular localization of α1-AR subtypes in embryonic ventricular cells using specific antibodies for α1A, α1B, and α1D subtypes. My third research aim was to examine the second messenger responses in embryonic ventricular cells in the presence or absence of adrenergic receptor agonists and antagonists including ISO, and PE (agonists), carvedilol, and prazosin (antagonists). The fourth research aim examined the effects of adrenergic receptor agonists and antagonists on embryonic ventricular cell proliferation. Using immunostaining methods, cell counts were conducted to determine differences in the percentage of CMs and CPCs and cell proliferation was studied using Click iT EdU methods. The fifth and final research aim was to examine the effects of adrenergic receptor agonists and antagonists on embryonic ventricular cell differentiation through cell size measurements of CMs and gene expression analysis.

Chapter 2: Materials and Methods

2.1 Animal Maintenance and Mouse Strains

All animal procedures were performed according to the Canadian Council on Animal Care guidelines and were approved by the Dalhousie University Committee on Laboratory Animal Care (CCAC, Ottawa, ON: Vol 1.1.2, 2nd edition, 1993; Vol 2, 1984, Protocol No. 16-048). The Nkx2.5-Cre (NC) mouse strain (Cre recombinase inserted into the Nkx2.5 allele) was initially characterized by (Stanley et al., 2002) and was provided by Dr. Richard Harvey (Victor Chang Cardiac Research Institute, University of South Wales, Australia). At the 3' untranslated region of the Nkx2.5 gene, an internal ribosomal entry sequence (IRES) and a Cre-recombinase (Cre) coding sequence were inserted into the gene. The R26R reporter strain (designated as Rosa-lacZ) was obtained from Jackson Laboratories (Bar Harbor, Maine, USA) with the Lac Z gene inserted into the Rosa locus (**Figure 2.1**). Both, Nkx2.5-Cre and Rosa-lacZ strains were maintained in C57BL6/J background. CD1 mice were utilized for all experimental procedures unless otherwise stated.

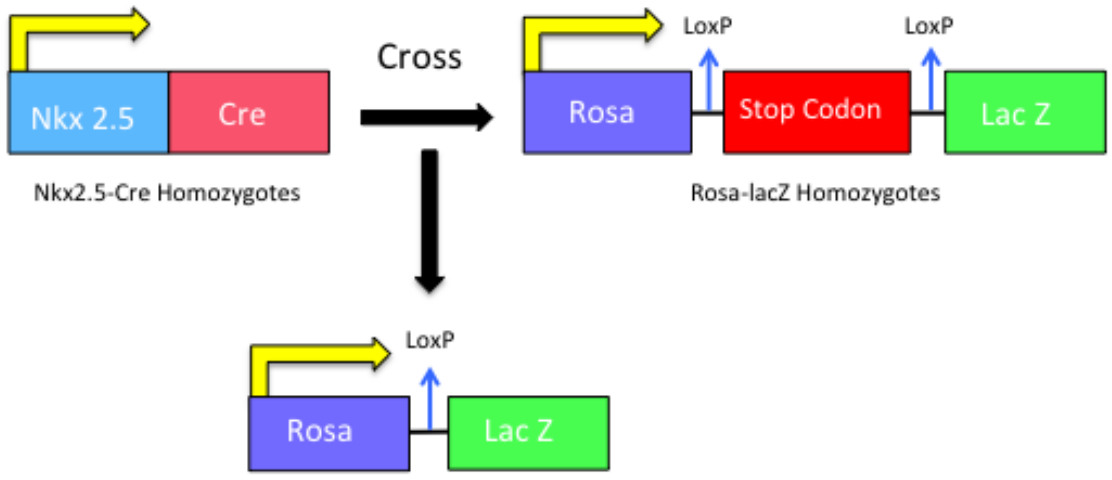

Figure 2.1: Nkx2.5-Cre (NC) mouse strain. Nkx2.5-Cre mice contain an internal ribosomal entry sequence followed by a cre recombinase coding sequence, which are inserted into the 3' untranslated region of the Nkx2.5 locus, therefore wherever Nkx2.5 is expressed Cre is also expressed. For the Rosa-LacZ strain, the β-galactosidase (LacZ) gene is inserted into the Rosa locus, however the LacZ gene is preceded by a transcriptional termination sequence. When Nkx2.5-Cre mice are crossed with Rosa-LacZ mice, the stop codon is eliminated, and expression of the LacZ gene is linked to Nkx2.5-Cre expression.

2.2 Genomic DNA Extraction

The genotype of knock-in mouse strains was determined by extracting genomic DNA from ear punch biopsies. The REDExtract-N-AMP tissue PCR kit (Sigma, Oakville, Ontario, Canada) was used for DNA extraction according to instructions from the manufacturer. Ear punch biopsies were placed in a 50µl DNA extraction solution consisting of 40µl of extraction solution and 10µl of tissue prep solution. Samples were manually crushed and incubated for 10 minutes at room temperature followed by a 3 minute incubation at 95°C. 40µl of neutralization solution was added and samples were vortexed. Samples were then stored at -20°C for future use or used immediately for polymerase chain reaction (PCR).

2.3 Genotyping by polymerase chain reaction (PCR)

PCR was performed using the REDExtract N-AMP kit (Sigma) according to the manufacturer's instructions. The PCR cocktail mixture contained 5µl of PCR RedExtract-n-Amp reaction mix, 0.5µl of each primer, 1.5µl of RNAse free water (Ambion, USA) and 2µl of tissue extract per sample (total reaction volume of 10µl). Primers were obtained form (ThermoFisher Scientific, Burlington, Ontario, Canada) and primer sequences are listed in **Table 2.1**. The PCR reaction for **Rosa-LacZ genotyping** consisted of 30 cycles and was performed as follows: 30 sec at 94°C, 30 sec at 60°C, and 60 sec at 72°C. Expected PCR product size for the knock-in allele was 320 base pairs (bp) and 650 bp for wild-type allele (**Figure 2.2**). The PCR reaction for **Nkx2.5-Cre genotyping** consisted of 30 cycles and was performed as follows: 30 sec

at 94°C, 20 sec at 60°C, and 60 sec at 72°C.Expected PCR product size for the knock-in allele was 583 bp and 264 bp for the wild-type allele (**Figure 2.2**).

Name of Primer	Primer Sequence (5'→3')	Expected Band Sizes (bp)	
		Wild-type allele	Knock-in allele
Nkx2.5-S	GCCCTGTCCCTCGGATTTCACACC	264	583
Nkx2.5-AS	ACGCACTCACTTTAATGGGAAGAG		
Cre-S	GATGACTCTGGTCAGAGATACCTG		
Rosa 1	AAAGTCGCTCTGAGTTGTTAT	650	320
Rosa 2	GCGAAGAGTTTGTCCTCAACC		
Rosa 3	GGAGCGGGAGAAATGGATATG		

Table 2.1: List of primers, primer sequences and expected band sizes required for genotyping Nkx2.5Cre and Rosa-LacZ mouse strains. PCR was performed to confirm wild-type or knock-in genotypes of Nkx2.5Cre and Rosa-LacZ mice according to expected band sizes listed in the table.

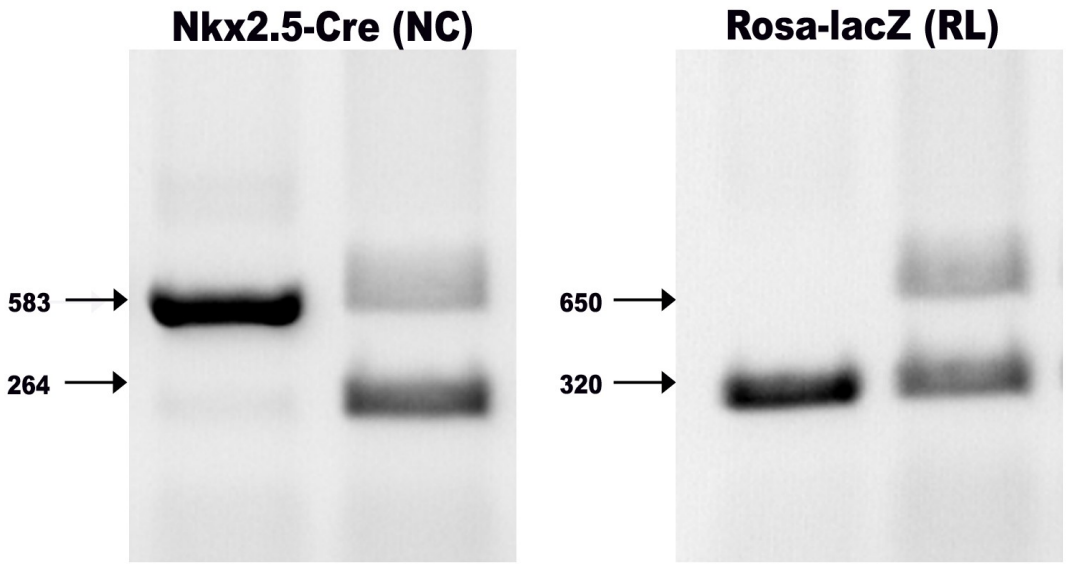

Figure 2.2: Expected band sizes (bp) for Nkx2.5-Cre (NC) and Rosa-lacZ (RL) genotypes.

2.4 Timed Pregnancies

Timed pregnant CD1 mice were purchased from Charles River, Sherbrooke, Canada. Breeding pairs consisting of **Nkx2.5-Cre** and **Rosa-lacZ** mice were placed in the same cage for varying amounts of time depending on the desired developmental stage. Following mating of Nkx2.5-Cre and Rosa-lacZ mice, timed pregnant females at each developmental stage were anaesthetized using 4% isoflurane and were sacrificed by cervical dislocation. Embryos were extracted from pregnant females and embryonic heart ventricles were isolated using Leica MZ16SF stereomicroscope (Leica Microsystems, Richmond Hill, Ontario, Canada). Embryonic hearts were isolated from different developmental stages including embryonic day E11.5, E14.5, and E16.5. Neonatal hearts were harvested from embryos 1 day after birth and adult hearts were harvested from mice 3-5 months of age. Ventricles were isolated following the removal of the atria. Hearts from older developmental stages, neonates, and adults, were used only for RNA or protein extractions.

2.5 Embryonic Ventricular Cell Cultures

After harvesting heart tissue from E11.5 embryos, the atria and outflow tracts were removed and both left and right ventricles from multiple hearts were pooled. Subsequently, pooled ventricles were placed in 0.2% collagenase solution (Worthington Biochemical Corp, Lakewood, NJ, USA) and incubated for 30 minutes at 37°C to digest ventricular tissues. Following incubation and digestion at 37°C, cells were mixed using a pipette set to 200µl to mechanically dissociate cells. Cells were centrifuged at 1,500 rcf for 4 minutes and the supernatant was discarded. The

remaining pellet was washed with 10% DMEM (Dulbecco's Modified Eagles Medium; Wisent, Saint Bruno, Quebec, Canada) containing 10% fetal bovine serum (FBS; Wisent, Saint Bruno, Quebec, Canada) and 1% Ab/Am. Cells were re-suspended in 10% FBS-DMEM and a hemocytometer was used to determine cell number. Cells were plated on 4-well slides previously coated with fibronectin (Sigma) with 250,000 cells/well (Nunc, Rochester, New York, USA) or on 35 mm dishes with 500,000 cells/well (Corning, Corning, New York, USA). Slides were placed in the CO_2 incubator at 37°C for 20 hours.

2.6 Drug Treatment

α1-AR agonists and antagonists as well as non-selective β-AR agonists and antagonists were used to examine the effects on proliferation and differentiation of embryonic ventricular cells. Carvedilol (Sigma; Cat#: C3993) was diluted in dimethyl sulfoxide (DMSO;Acros; Cat#: AC348440010) to make a 33.3mM stock. Carvedilol was prepared by diluting 1µl of 33.3mM stock into 33.3µl of H_2O (Ambion, USA) to make a 1mM solution. 10µl of the 1mM solution was then added to 1ml of 10% FBS-DMEM to get a 10µM dose. Isoproterenol (ISO; Sigma, Cat#: I6504) was prepared by diluting 0.0123g of ISO into 0.5ml of H_2O. 1µl was added to 99µl of H2O to make a 1mM solution. To obtain a 1µM dose of ISO, 1µl of 1mM solution was added to 1ml of 10% FBS-DMEM. Control treatments received 1ml 10% FBS-DMEM with or without DMSO at a final concentration of 0.03%. DMSO was prepared (3µl of DMSO + 97 ul of H2O) to make 3% DMSO, and 10µl of 3% DMSO was added to 1ml of ISO and control treatment groups. A combination treatment of ISO and carvedilol was prepared by

adding 1µl of 1mM ISO and 10µl of 1mM carvedilol to 1ml of 10% FBS-DMEM. Following the 20-hour incubation for cell growth, slides were removed from the incubator and 1ml of media supplement with drug treatment was added to each well. Slides were placed in the CO_2 incubator at 37°C for 18 hours.

Prazosin HCL (Sigma; Cat#: P7791-50mg) was weighed and 0.01g was diluted in 10ml of H2O to make a 2.38mM stock. The stock solution was aliquoted and stored at -20°C. To achieve a 1µM solution of prazosin, 2.1µl of the 2.38mM stock was diluted in 5ml of 10% FBS-DMEM. (R)-(-)-Phenylephrine hydrochloride (PE; Sigma; Cat#: P6126-5g) was prepared by diluting 0.02g of PE in 1ml of H2O to achieve a 100mM solution. 2.5µl of the 100mM stock of PE was mixed with 5ml of 10% FBS-DMEM. 1ml of media supplemented with PE was added to each well and slides were placed in the CO_2 incubator at 37°C for 18 hours.

2.7 Click-iT EdU Cell Proliferation Assay

For cell proliferation experiments, Click-iT Plus EdU Alexa Fluor 647 Imaging Kit (ThermoFisher Scientific; Cat#: 10640) was used and solutions were prepared according to instructions from the manufacturer. 12µl of the EdU (Ref#: C10640) stock solution was added to 12ml 10% FBS-DMEM (10µm working solution). For each well, 1ml of the 10% FBS-DMEM EdU solution was added and slides were incubated at 37°C for 6 hours.

2.8 Fixation

Following drug treatments or Click-iT EdU probing, slides with primary NCRL cultures were fixed with ice-cold methanol (Fisher Scientific; A412P-4) for 15 minutes at 4°C. For α1-AR antibody immunostaining experiments, slides with embryonic CD1 ventricular cell cultures were fixed with 4% paraformaldehyde (1g paraformaldehyde in 100ml PBS, pH adjusted to 7.4, using NaOH) for 5 minutes at 4°C. Following fixation, slides were washed with 1X phosphate-buffered saline (PBS) and stored with 1ml of PBS/well at 4°C until further use.

2.9 Immunostaining for EdU Labelled Slides

Slides containing primary NCRL cultures (E11.5 and E14.5) previously fixed and stored at 4°C were permeabilized with 0.1% v/v Triton X-100 (Sigma) for 10 minutes and washed with 1ml PBS twice for 2 minutes each. The box covering around each well was removed and the border was traced with hydrophobic wax.

For EdU cell proliferation experiments, a click-iT reaction cocktail was prepared using solutions from Click-iT Plus EdU Alexa Fluor 647 Imaging Kit (Invitrogen; Cat#: 10640) that were previously prepared according to the manufacturer's instructions. The cocktail was prepared to a total volume of 1ml for one 4-well slide. The cocktail contained 880µl of 1X Click-iT® reaction buffer, 20µl of copper protectant, 2.5µl of Alexa Fluor® picolyl azide, and 100µl of reaction buffer additive. Following permeabilization, 200µl was pipetted onto each well and

incubated in the dark at room temperature for 30 minutes. Slides were washed with PBS 2 times for 3 minutes.

Following EdU incubation, slides were covered with 200µl of blocking buffer solution [10% v/v goat serum (Gibo), and 1% w/v bovine serum albumin (BSA; ThermoFisher Scientific) in PBS] for 1 hour. Following the 1-hour block, the solution was replaced by blocking buffer mixed with primary antibodies for β-galactosidase and sarcomeric myosin. Primary antibody details and concentrations are listed in **Table 2.2**. Slides were incubated in the dark at room temperature for 1 hour and then washed with PBS 3 times for 5 minutes. Next, slides were incubated with chosen secondary antibodies for 1 hour at room temperature. Secondary antibody concentrations are listed in **Table 2.3**. Secondary antibodies used were Alexa Flour 488 goat anti-chicken IgG (H+L) and Alexa fluor 555 F(ab')2 fragment of goat anti-mouse IgG (H+L) ThermoFisher Scientific.

Following secondary incubation, slides were counterstained for cell nuclei by washing with 200µl of solution containing 1 µg/ml Hoechst 33258 (Sigma) and washed with PBS 3 times for 5 minutes. All washes were done in the dark at room temperature. Slides were mounted with 0.1% propyl gallate (Sigma) solution [(0.1% w/v propyl gallate, 50% v/v glycerol (ThermoFisher Scientific), 50% v/v PBS] and examined using a Leica DM2500 fluorescence microscope. Leica DFC 500 digital acquisition system was used to capture images.

Primary Antibody	Dilution	Source/Catalogue #
ß-galactosidase	1:75	Aves Lab Catalogue # BGL-1040
Sarcomeric Myosin (MF20)	1:50	Developmental Studies Hybridoma Catalogue #: MF-20

Table 2.2: List of primary antibodies and corresponding dilutions used for immunostaining of NCRL cells

Secondary Antibody	Dilution	Source/Ref #
α-chick 488	1:75	ThermoFisher Scientific Cat # A11039
α-mouse 555	1:150	ThermoFisher Scientific Cat # A21425
α-Rabbit 488	1:150	ThermoFisher Scientific Cat # A21206

Table 2.3: List of secondary antibodies and corresponding dilutions used for immunostaining of NCRL cells

2.10 Immunostaining with α-1 AR Subtype Specific Antibodies

Embryonic CD1 ventricular cell cultures (E11.5) fixed with 4% w/v paraformaldehyde were permeabilized with 0.1% Triton X-100 for 5 minutes followed by 2 washes with PBS for 2 minutes. Blocking buffer (200µl) was added to each well for 1.5 hours. α1-AR subtype specific antibodies and associated peptides were reconstituted according to the manufacturer's instructions. 3µl of nonimmune serum (NIS) stock (Sigma, **Table 2.4**) was added to 123µl of PBS and frozen at -20°C until future use.

α1-AR subtype specific antibodies are from Alomone Labs and are highly specific antibodies that are directed against extracellular epitopes of the human α1-Adrenoceptors. The α1-AR antibodies are designed to recognize α1-Adrenoceptors from human, rat, and mouse samples. The α1A-AR antibody contains peptide EDETI*SQINEEPG(C), corresponding to amino acid residues 171-183 of human α1A adrenoceptor with replacement of cysteine 176 (C176) with serine (*S) (Accession P35348) located at the 2nd extracellular loop. The α1B-AR antibody contains peptide (C)KNANFTGPNQTSSNS, corresponding to amino acid residues 21-35 of human α1B-adrenoceptor (Accession P35368) located at the extracellular, N-terminus. The α1D-AR antibody contains peptide (C)EPVPPDERF*SGITEE, corresponding to amino acid residues 231-245 of rat α1D-Adrenoceptor with replacement of cysteine 240 (C240) with serine (*S) (Accession P23944) located at the 3rd extracellular loop.

Following the 1.5 hour block, wells received primary α1A-AR antibodies, NIS working solution, α1-AR antibodies-1:1 block with respective peptides, or α1-AR antibodies-1:5 block with respective peptides. Primary antibodies were used at 1:50 dilution (150µl /well): Anti- α1A adrenoceptor (Alomone Labs, Cat#: AAR-015), Anti- α1B adrenoceptor (Alomone Labs, Cat#: AAR-018), Anti- α1D adrenoceptor (Alomone Labs / Cat #: AAR-019). Primary α1-AR antibodies are listed in **Table 2.4**.

Each α1-AR subtype specific peptide (40 µg) was reconstituted in 50µl of Ambion water and aliquoted into separate tubes (25µl each) to avoid multiple thawing / freezing cycles. For the 1:1 block, 3µl α1-AR antibody and 3µl of peptide were mixed and incubated at room temperature for 1 hour with gentle agitation. For the 1:5 block 3µl of the α1-AR antibody and 15µl of peptide were mixed and incubated at room temperature for 1 hour with gentle agitation. Peptide blocking information is listed in **Table 2.5**. Following the 1 hour incubation, the peptide and antibody mixture was diluted in blocking buffer with a final volume of 150µl. All preparations contained MF20 antibody (1:50 dilution, listed in **Table 2.2**). Each well received 150µl of solution and slides were incubated in the dark at room temperature for 1 hour. For wells receiving NIS, 3µl of NIS working solution and 3µl of MF20 antibody (1:50 dilution) were mixed in blocking buffer and each well received 150µl of solution. Samples were incubated in the dark at room temperature for 1 hour.

Following primary incubation, slides were washed with PBS 3 times for 5 minutes. Secondary antibodies including Alexa Fluor 488 donkey anti-rabbit IgG (H+L) (ThermoFisher Scientific, Cat #: A21206) and Alexa fluor 555 F(ab')2 fragment of goat anti-mouse IgG (H+L) (ThermoFisher Scientific, Cat #: A21425) were

prepared in blocking buffer (each 1:150 dilution). Secondary antibody information is listed in **Table 2.3.** Wells received 150µl of secondary antibody and were incubated in the dark at room temperature for 1 hour. Slides were washed with PBS containing 1 µg/ml Hoechst 33258 (Sigma) and PBS 3 times for 5 minutes. All washes were done in the dark at room temperature. The box covering around the slide was removed and slides were mounted with 0.1% propyl gallate. Slides were examined using a Leica DM2500 fluorescence microscope and Leica DFC 500 digital acquisition system was used to capture images.

Antibody	Dilution	Source/Cat#
Anti- α1A adrenoceptor	1:50	Alomone Labs / Cat# AAR-015
Anti- α1B adrenoceptor	1:50	Alomone Labs / Cat# AAR-018
Anti- α1D adrenoceptor	1:50	Alomone Labs / Cat # AAR-019
Rabbit nonimmune serum	1:50	Sigma / Cat# R9133

Table 2.4: List of α1-AR subtype specific antibodies and corresponding dilutions used for immunostaining

Peptide	Block	Source / Cat#
α1A-AR Peptide	1:1 Block (3µl antibody, 3µl peptide) 1:5 Block (3µl antibody, 15µl peptide)	Alomone Labs For # AAR-015
α1B-AR Peptide	1:1 Block (3µl antibody, 3µl peptide) 1:5 Block (3µl antibody, 15µl peptide)	Alomone Labs For # AAR-018
α1D-AR Peptide	1:1 Block (3µl antibody, 3µl peptide) 1:5 Block (3µl antibody, 15µl peptide)	Alomone Labs For # AAR-019

Table 2.5: List of α1-AR subtype specific peptides and corresponding dilutions used for immunostaining

2.11 Cell Size Measurements

Primary NCRL cultures were prepared as previously described and treated with different agonists and antagonists. Cells subjected to immunostaining were stained with MF20 primary antibody for detection of CMs, β-gal for detection of CPCs, and nuclei were counterstained with Hoechst 33258 (Sigma) in PBS. Slides were examined using a Leica DM2500 fluorescence microscope and Leica DFC 500 digital acquisition system was used to capture images. CM cell sizes were measured using a colour subtractive image analysis method previously described by (Gaspard & Pasumarthi, 2008). Cell size was determined using Adobe Photoshop 7.0 software and the Image Processing Tool Kit 5.0 (Reindeer Graphics, Ashville, NC). The lasso tool was used to mark contours of the cell periphery and the filled areas were assessed in 40X magnification images using the IP* measure feature.

2.12 Cell Counts

Primary NCRL cultures were prepared as previously described and treated with different agonists and antagonists. Cells subjected to immunostaining, were stained for MF20 primary antibody for detection of CMs, β-gal for detection of CPCs, and nuclei were counterstained with Hoechst 33258 (Sigma) in PBS. Cells were also prepared using a Click-iT EdU proliferation assay. Slides were examined using a Leica DM2500 fluorescence microscope and Leica DFC 500 digital acquisition system was used to capture images.

Images were captured in 40X magnification and 8 separate images were taken for each stain (nuclei, CMs, CPCs, EdU) for each well. The total number of cells was

determined by counting the nuclei in each field. The total number of nuclei was used to determine the percentage of CMs, CPCs, and non-CMs in reference to the number of nuclei present in each field. The percentage of proliferating CMs, CPCs, and non-CMs was also determined in reference to the amount of nuclei positive for EdU.

2.13 Total RNA Extraction from Ventricular Tissue and Cell Cultures

Ventricles (both left and right) from different developmental stages (E11.5, E14.5, E16.5, Neo, Adult) were harvested and total RNA was extracted using Trizol method (ThermoFisher Scientific). Approximately 50-100mg of tissue obtained from each developmental stage was minced into smaller pieces and homogenized in 1ml TRIzol using a homogenizer. Subsequently, tissue lysates were incubated at room temperature for 5 minutes and 0.2ml chloroform was added to each sample followed by incubation at room temperature for 3 minutes. Samples were centrifuged at 16,612 rcf for 15 minutes at 4ºC and supernatant was transferred to a fresh tube. Next, 0.5ml of isopropyl alcohol was added to the sample to precipitate the RNA from the aqueous supernatant. The sample was then incubated for 10 minutes at room temperature followed by centrifugation at 16,612 rcf rpm for 10 minutes at 4ºC. The RNA pellet was washed with 75% ethanol and then solubilized in nuclease free H_2O (Ambion). The RNA concentrations and purity were determined by measuring absorbance of all samples at 260nm and 280nm using a spectrometer (SmartSpec™ Plus, Bio-Rad, Mississauga, Ontario, Canada).

For extraction of total RNA from the primary cultures, E11.5 ventricular cells were plated on 35 mm dishes with 500,000 cells/well (Corning, Corning, New York, USA) and incubated at 37°C for 20 hours. Following drug treatments as described in the "drug treatment" section, cells were prepared for RNA extraction with Aurum Total RNA Mini Kit (Bio-Rad; Cat#: 732-6820). Cells were washed twice with PBS and 350µI of the beta-mercaptolated Lysis Solution (Bio-Rad; Cat#: 732-6802) was added to each 35mm dish. Cells were further homogenized by pipetting cell lysates through an 18 gauge needle multiple times. The homogenized cells were scraped and transferred to a 2ml capped vial. Cell lysates were then stored at -80°C or used immediately by adding 350µI of 70% ethanol (total sample 700ul).

An RNA binding column was inserted into a 2ml capless wash tube and the 700µl sample was pipetted into the binding column (provided by the kit). The sample was spun for 60 sec at 12,000 rcf, RT, the binding column was removed, and the flow-through was discarded from the wash tube. This step was repeated. To remove genomic DNA, 700µl of total RNA low stringency wash solution (Bio-Rad; Cat#: 732-6804) supplemented with ethanol was added to the column and spun for 30 sec at 12,000 rcf and the flow-through was discarded. DNase mix was prepared (5µl of DNase-in-Tris Stock solution with 75µl of DNase dilution solution per sample) and 80µl was pipetted to the centre of the membrane stack at the bottom of each column. Samples were incubated for 25 minutes at room temperature.

Following incubation, 700µl of total RNA high stringency wash solution (Bio-Rad; Cat#: 732-6803) was pipetted to the column. Columns were spun for 30 sec at 12,000 rcf and the flow-through was discarded. 700µl of low stringency wash solution

was added to the column, spun for 60 sec at 12,000 rcf and the flow through was discarded. The solution was spun 2 more times and the column was transferred to a 1.5ml capped microcentrifuge tube provided by the kit.

To the centre of the column, 40µl of Elution Solution (Bio-Rad; Cat#: 732-6801) was pipetted and samples were incubated for 1 minute. Columns were spun for 2min at 12,000 rcf to elute the purified RNA. For purity checks, 8µl of sample was removed and the rest of the samples were stored at -80°C.

RNA purity checks were conducted to ensure high level of RNA purity. Samples meeting quality control standards of 260:280 ratio > 1.8 were used for gene expression analysis experiments. Samples were converted to complementary DNA (cDNA) sequences and stored at -80°C until real time quantitative PCR (RT-qPCR) gene expression analysis experiments were conducted.

2.14 Real Time Quantitative Polymerase Chain Reaction (RT-qPCR)

To generate cDNA sequences, samples from RNA extraction were reverse transcribed into cDNA using SuperScript VILO MasterMix reverse transcriptase kit (ThermoFisher Scientific). A reaction mixture was prepared containing 1µg of RNA with 2µl of SuperScript VILO MasterMix, and RNAse/DNAase-free H2O (Ambion, USA) to a total of 20µl. Eppendorf tubes were incubated at 25°C for 10 min, 42°C for 90 min, and heat inactivated at 85°C for 5 min. cDNA samples were amplified by real time quantitative polymerase chain reaction (qPCR) using α1-AR primers or cell differentiation primers listed in **Table 2.6**. Primers for α1-AR subtypes, GAPDH, ANP, Cx40, GATA4, HAND2, HCN4, MEF2C, and Tbx5 were generated using the NIH primer

design tool (https://mouseprimerdepot.nci.nih.gov/) developed by (Cui et al., 2007). All primers used for gene expression analysis were designed to span exon-exon boundaries to ensure that genomic DNA is not amplified in the final PCR reactions.

qPCR reaction mixtures contained 2µl of 5X EVOlution EvaGreen® qPCR mix (Montreal Biotech Inc., Quebec City, Canada), 2.0µl RNAse/DNAse free H2O (Ambion, USA), and 1.0µl of the forward and reverse primers (2µM), and 1.0µl of cDNA product. Samples were spun at 700rpm for 2 min, and the sample plate was inserted into the ECO thermocycler (Illumina, San Diego, California, USA). ECO thermocycler ran at 50°C for 2 min; 95°C – 10 min; Amplification cycles ran for 40 cycles at 95°C – 15sec and 60°C – 1min for each cycle. Melt curves were generated with a cycle of 95°C, 60°C, 95°C, for 15sec each. Melt curve analysis was used to confirm amplification of a single band. In addition, samples were also run on agarose gels along with size markers to confirm the presence of a single band of expected size for each primer set.

qPCR reactions were performed in duplicate wells for each sample. Results from gene expression were normalized to the control housekeeping gene glyceraldehyde 3-phosphate dehydrogenase (GAPDH) and the cycle threshold (C_T) value was set to 0.1. The C_T value represents the number of cycles required for the particular gene to cross the threshold (exceeding the background level). The following calculations were performed in order to compare the relative expression of a gene of interest between groups and the $2^{-\Delta\Delta CT}$ value was determined for each group according to the method described earlier (Livak & Schmittgen, 2001). The C_T value of the control (GAPDH) gene was subtracted from the C_T value of the

corresponding experimental gene to determine the ΔC_T value for each sample. The ΔC_T values of all samples were then averaged and the resulting average was then subtracted from the ΔC_T values for each sample to create $-\Delta\Delta C_T$ values.

In order to express the qPCR sample data as the relative expression of each group compared to the control group, the $2^{-\Delta\Delta CT}$ values were determined for each sample. The relative expression for each gene was then determined by dividing the $2^{-\Delta\Delta CT}$ obtained for each sample by the average $2^{-\Delta\Delta CT}$ value of the control group. The control group was set to a value of 1.0, and the data could then be expressed as the relative expression of each group. This method represents the data as fold changes in gene expression, which is normalized to GAPDH gene expression, and relative to controls.

Name of Primer	Primer Sequence (5'→3')	Expected Amplicon Size (bp)
GAPDH-F GAPDH-R	TCGTCCCGTAGACAAAATGG TTGAGGTCAATGAAGGGGTC	132
α1A-R α1A-L	TTTCTTGAACTCCTGGCTGG CTGCCATTCTTCCTCGTGAT	150
α1B-R α1B-L	AGCTGTTGAAGTAGCCCAGC AACCTTGGGCATTGTAGTCG	143
α1D-R α1D-L	GATGGTTTCAGCTGAGGGAA TCCGTAAGGCTGCTCAAGTT	140
ANP-F ANP-R	GGACTAGGCTGCAACAGCTTCCG CCAAGCTGCGTGACACACCAC	119
Cx40-F Cx40-R	CAGAGCCTGAAGAAGCCAAC GACTGTGGAGTGCTTGTGGA	137
GATA4-F GATA4-R	CTGGAAGACACCCCAATCTC CCATCTCGCCTCCAGAGT	100
HAND2-F HAND2-R	CGGAGATCAAGAAGACCGAC TGGTTTTCTTGTCGTTGCTG	96
HCN4-F HCN4-R	CCTCCTGCGCCTCTTGAGGCTTT TGCCAATGAGGTTCACGATGCGT	119
MEF2C-F MEF2C-R	TGGAGAGATGAAGTGAAGCG GCACAGCTCAGTTCCCAAAT	93
TBX5-F TBX5-R	TGGTTGGAGGTGACTTTGTG GGCAGTGATGACCTGGAGTT	101

Table 2.6: List of primers, primer sequences and expected amplicon sizes for real time quantitative PCR (RT-qPCR)

2.15 Primer Efficiencies

Primer efficiency tests were conducted to determine the efficiency of α1-AR subtype (α1A, α1B, α1D) specific primers prior to completing RT-qPCR result comparisons between subtypes. To determine the efficiency of a primer set, a known concentration of a cDNA template was serially diluted to generate a standard curve. The slope of the curve is related to the efficiency with an ideal slope of -3.32, which correlates with an amplification efficiency of 100%. Generally, amplification efficiencies between 90% and 110% are acceptable. RT-qPCR was conducted using E11.5 ventricular cDNA (**Section 2.14**) treated with α1A, α1B, and α1D subtype specific primers along with GAPDH for normalization. Results from primer efficiency tests revealed that the efficiencies for all primer pairs were in the 90-110% range (**Figure 2.3**).

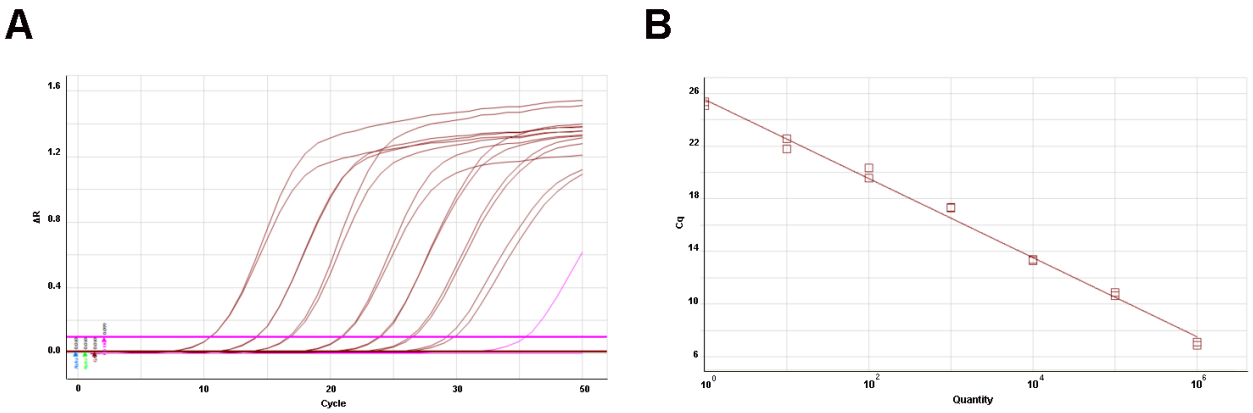

Figure 2.3: Primer efficiency test to determine the efficiency of α1-AR subtype specific primers. Primer efficiency tests were conducted for α1A, α1B, and α1D subtype specific primers. A known concentration of a cDNA template was serially diluted to generate a standard curve. The slope of the curve is related to the efficiency. qPCR was conducted using E11.5 ventricular cDNA treated with α1A, α1B, and α1D subtype specific primers along with GAPDH for normalization. **A)** An example of amplification plots generated using different dilutions of cDNA samples with GAPDH primers. ΔR = fluorescence without a reporter dye. **B)** A standard curve is plotted with the copy number from each cDNA dilution on the X-axis and quantitation cycle value (Cq) on the Y-axis. All primer efficiencies were between 90-110% for α1A, α1B, and α1D subtypes primers as well as for GAPDH primers.

2.16 Protein Extraction

Mem-Per Plus protein extraction kit (ThermoFisher Scientific, Cat#: 89842) was used to separate cytosolic and membrane proteins from ventricles using a reagent-based procedure recommended by the supplier with some modifications. Ventricles from various stages were transferred into eppendorf tubes and ~20-30 mg of tissue from each developmental stage were washed in 1ml of cell wash solution (E11.5 ventricles were washed in PBS). Samples were vortexed and the wash was discarded. Ventricular tissues were cut into smaller pieces and 250µl of permeabilization buffer was added. Next, tissues were ground with a pestle and vortexed to obtain a homogenous suspension. Samples were topped with 250µl of permeabilization buffer and incubated for 30 minutes at 4°C with agitation. Permeabilized cells were centrifuged at 4°C for 15 minutes at 16,000 rcf. Supernatant containing the cytosolic proteins was transferred to a new eppendorf tube and kept on ice (or stored at -80°C). For membrane protein extraction, 250µl of solubilisation buffer was added to the pellet, which was resuspended by pipetting. Samples were incubated at 4°C for 30 minutes with constant agitation. Membrane protein samples were then centrifuged at 16,000 rcf for 15 minutes at 4°C. The supernatant containing the solubilized membrane and proteins was transferred to a new eppendorf tube and kept on ice (or stored at -80°C).

Protein concentrations were estimated against a BSA standard curve and were generated using Bradford Assay. The Bradford Assay utilizes a colour shift method, which is based on shift in the absorbance maximum of Coomassie Blue (Pierce, Rockford, Illinois, USA) from 465 mm to 595 mm when bound to protein. The

resulting colour shift from brown to blue can be measured using a spectrophotometer.

A total of 23µg of protein was separated on 7.5% SDS-PAGE polyacrylamide gels [0.375 M Tris/HCl pH 8.8, 0.08% w/v SDS, 7.5% w/v acrylamide, 0.2% v/v ammonium persulphate (APS), 40µl TEMED] using a 1x Tris-glycine migration buffer (25mM Tris base, 190 mM glycine and 0.1% SDS at 8.3 pH) at 100 volts in a Mini-PROTEAN 3 gel electrophoresis unit (Bio-Rad, Mississauga, Ontario, Canada). Subsequently, separated proteins were transferred to a nitrocellulose membrane (BioTrace NT, PALL Life Sciences) using a Bio-Rad transfer apparatus at a constant current of 100 volts for 1 hour (Transfer buffer: 25mM Tris base, 190 mM glycine and 20% methanol at pH 8.3). After the transfer, nitrocellulose membranes were stained with napthol blue (1% w/v napthol blue black, 45% v/v methanol, 45% v/v water, 10% v/v acetic acid) for 2 minutes to enable protein visualization and determine protein loading. Prior to Western blot analysis, nitrocellulose membranes were then rinsed in ddH_20 and air-dried.

2.17 Western Blot Analysis

The first step to detecting a protein of interest involves incubating the nitrocellulose membrane with two changes of fresh blocking buffer (3% w/v BSA in PBS with 0.1% w/v Tween) for 1.5 hours each. Next, membranes were incubated with primary antibodies diluted in blocking buffer overnight at 4°C. Primary antibodies used for Western blot analysis: Anti- α1A adrenoceptor (Alomone Labs, Cat#: AAR-015), Anti- α1B adrenoceptor (Alomone Labs, Cat#: AAR-018), Anti- α1D adrenoceptor (Alomone Labs, Cat #: AAR-019) (all 1:200 dilution).

Following incubation, primary antibodies were removed and the membranes were washed 3 times in PBS containing 0.1% Tween (0.1% PBST) for 15 minutes with agitation. The membranes were then incubated for 1 hour with secondary antibodies (Goat anti-rabbit IgG (H+L) Horseradish Peroxidase Conjugate; Biorad, Cat#: 170-6515) diluted in blocking buffer (1:3000 dilution) at room temperature. After secondary antibodies were removed, membranes were washed 3 times in PBST for 15 minutes each with agitation. Protein bands were detected by enhanced chemiluminescence method using ECL Plus Western Blotting Detection System (Cell Signaling, SignalFire Cat#: 6883S) according to instructions from the manufacturer.

Following the detection of the proteins, Restore Western Blot Stripping Buffer (ThermoFIsher Scientific, Cat#: 21059) was used to strip the antibodies from the nitrocellulose membrane. Each membrane was covered with stripping buffer for 5 minutes at room temperature and then washed with PBS 3 times for 10 minutes.

The nitrocellulose membranes were then incubated with two changes of fresh blocking buffer for 1.5 hours each. Next, membranes were incubated with GAPDH diluted in blocking buffer overnight (α1A and α1B membranes 1:3000 dilution; α1D membrane 1:2000 dilution). Following incubation, GAPDH was removed and the membranes were washed 3 times in PBS containing 0.1% Tween (0.1% PBST) for 15 minutes with agitation. The membranes were then incubated for 1 hour with secondary antibody diluted in blocking buffer. Secondary antibody: Goat anti-rabbit IgG (H+L) (Human IgG Absorbed, Horseradish Peroxidase Conjugate (Bio-Rad, Cat#: 170-6515), 1:3000 dilution**.** After secondary antibodies were removed, membranes were washed 3 times in PBST for 15 minutes each with agitation. Protein bands were detected by enhanced chemiluminescence method using ECL Plus Western Blotting Detection System (Cell Signaling, SignalFire Cat#: 6883S) according to instructions from the manufacturer.

2.18 Second Messenger Assay: cAMP

Embryonic CD1 ventricular cells were cultured and a cAMP competitive immunoassay was performed using a two-step protocol of the cAMP dynamic 2 *htrf* assay kit (Cisbio, Cat#: 62AM4PEB) to determine the amount of endogenous cAMP. The assay was performed according to the manufacturer's instructions. The cAMP kit contained d2-dye labelled cAMP analogue (d2-cAMP) and anti-cAMP monoclonal antibodies that have been labelled with Cryptate (mAb-Cryptate). Calculated delta F values obtained from multiple standards were used to generate a standard curve for

cAMP. Values covered several concentrations ranging from a concentration of 0.01 to 712nm of cAMP per well.

Cells were plated with 5µl of cells diluted in 10% FBS-DMEM with 5000 cells/well. Cells were treated with ISO [1µm], carvedilol [0.1µm, 1µm, 10µm], or a combination of ISO and carvedilol (1µm of ISO + 0.1µm, 1µm, or 10µm of carvedilol) for 30 minutes before the assay was measured.

The mechanism of this assay was based on competition between endogenous cAMP and a d2-dye labelled cAMP analogue (d2-cAMP) for binding sites on anti-cAMP monoclonal antibodies labelled with Cryptate (mAb-Cryptate). A fluorescence resonance energy transfer (FRET) signal, designated as delta F, is detected when energy is transferred between d2-cAMP and Cryptate. This signal was inversely proportional to the concentration of the endogenous cAMP in the sample (**Figure 2.4**).

In the first step of the protocol for the cAMP competitive immunoassay, a volume of 5µl of cells (5000 cells) in 10% FBS-DMEM was added to wells of 384-well plates (Greiner Bio-One, Cat#: 784075). Additionally, 5µl of dilution buffer consisting of drug compounds (ISO, carv, etc.) were diluted in 10% FBS-DMEM and added to the experimental wells totalling a final volume of 10µl/well. The broad substrate phosphodiesterase inhibitor 3-isobutyl-1-methylxanthine (IBMX; Sigma) at a concentration of 500µM was also added to the dilution buffer to prevent the degradation of cAMP. The plate was then sealed and incubated at room temperature for 30 minutes.

Following incubation, a volume of 5µl of d2-cAMP analogue was diluted in lysis buffer and added to each experimental well, however d2-cAMP was omitted from negative control wells in order to determine if non-specific signal was present. Additionally, a volume of 5µl mAb-Cryptate was added to all wells totalling a volume of 20µl/well. The plate was then sealed and stored at room temperature for one hour. Following incubation, the plate was read on a POLARstar Omega plate reader (BMG Labtech). The d2-cAMP fluorophore was excited at a wavelength of 337nm and emission was detected at 665nm and 620nm. To minimize the photophysical interference (which may have occurred due to medium conditions such as the presence of serum) the fluorescent ratio 665 nm/620 nm was calculated. Results expressed as delta F values were calculated using the 665nm/620nm ratio according to instructions from the supplier as described below. First the 665nm/620nm ratio for each well was multiplied by 10^4, which was followed by calculating the average values from replicate wells. Next, the delta F values were obtained by subtracting the negative control 665/620 ratio value from the sample 665/620 ratio value, followed by dividing that value by the negative control 665/620 ratio and multiplying by 100. Delta F values were plotted from standards with known cAMP concentrations in order to generate a standard curve for cAMP. The standard values covered an average range from 0.01-712nM final concentration of cAMP/well. The concentrations of cAMP in experimental samples were determined by extrapolating respective delta F values from the standard curve.

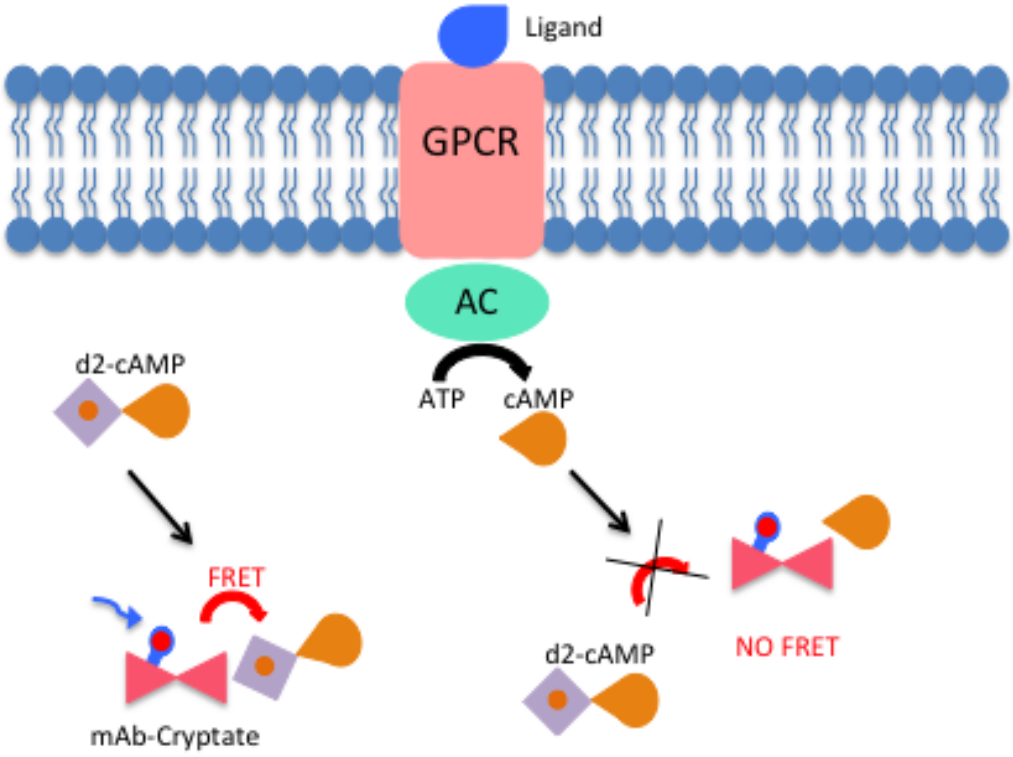

Figure 2.4: Diagram depicting the concept for homogenous time resolved fluorescence (HTRF) second messenger immunoassay for cAMP. Second messenger immunoassays were performed for cAMP and IP1, which rely on the same HTRF concept. This description only focuses on the cAMP assay for simplicity. In step 1 of the assay, cells are incubated with chosen drugs (carvedilol, isoproterenol, phenylephrine, etc.). Next, the competition assay is initiated between endogenous cAMP and the artificial d2-dye labelled cAMP analogue (d2-cAMP) for binding sites on anti-cAMP monoclonal antibodies labelled with the energy acceptor Cryptate (mAb-Cryptate). A fluorescence resonance energy transfer (FRET) signal is detected when a donor and acceptor are in close proximity. The FRET signal, designated as delta F, is detected when energy is transferred between d2-cAMP and Cryptate. If the drug of choice stimulates the production of cAMP, the endogenous cAMP will outcompete the artificial d2-cAMP for binding sites on Cryptate, decreasing the energy transfer and minimizing FRET. Drug inhibition of endogenous cAMP would allow d2-cAMP to outcompete for binding sites on Cryptate and the energy transfer would increase. Delta F values are inversely proportional to endogenous cAMP concentrations. A cAMP standard curve is used to extrapolate delta F values to determine the concentrations of cAMP for each sample.

2.19 Second Messenger Assay: IP1

Embryonic CD1 ventricular cells were cultured and a IP1 competitive immunoassay was performed using a two-step protocol of the IP1 dynamic 2 *htrf* assay kit (Cisbio, Cat#: 62IPAPEB) to determine the amount of endogenous IP1. The assay was performed according to the manufacturer's instructions. The IP1 kit contained d2-dye labelled cAMP analogue (d2-cAMP) and anti-cAMP monoclonal antibodies that have been labelled with Cryptate (mAb-Cryptate). Calculated delta F values obtained from multiple standards were used to generate a standard curve for IP1. Values covered several concentrations ranging from a concentration of 0.01 to 7700nM of IP1 per well.

Cells were plated with 7µl of cells diluted in 10% FBS-DMEM with 10,000-80,000 cells/well to measure dose response. Cells were treated with PE 10µm and incubated for 45 minutes at room temperature before the assay was measured.

To determine the level of IP1 in E11.5 cells, IP1 competitive immunoassays were performed using the protocol of the cAMP dynamic 2 *htrf* assay kit (Cisbio, Cat#: 62AM4PEB) according to the supplier's instructions. The mechanism and the protocol of the IP1 competitive immunoassays were identical to those described above for the cAMP assay, with a few important exceptions: 40,000-80,000 cells were added to each well (diluted in 7µl of 10% DMEM). Drugs were added in 7µl of 10% DMEM and 50mM lithium chloride (LiCl) was added for prevention of IP1 degradation. Plates were incubated with drugs for 45 minutes. Additionally, d2-IP1 and anti-IP1 monoclonal antibodies that have been labelled with Cryptate (mAb-Cryptate) solutions were used in steps 3 and 4. The IP1 standard curve was generated by

plotting the delta F values obtained from multiple standards of known IP1 concentrations and covered an average range of 0.01-7700nM (final concentration of IP1/well).

Chapter 3: Results

3.1 Subtype specific α1-AR mRNAs are expressed at different levels during mouse cardiac development

RT-qPCR analysis was used to determine the relative mRNA abundance of α1-AR subtypes in mouse ventricles during various stages of cardiac development. α1-AR expression was normalized to the housekeeping gene, GAPDH, as mRNA levels remain consistent throughout development (Hotchkiss et al., 2014). Results revealed that α1-ARs are present in embryonic mice as early as E11.5 days old while mRNA expression levels increase as development progresses. Relative to the α1A-AR subtype at E11.5, mRNA expression increased by 4-6-fold at E14.6 and E16.5, and significantly increased by 36-fold at neonatal, and 295-fold at the adult stage (**Figure 3.1A**).

Relative to the α1B-AR subtype at E11.5, mRNA expression increased by 25-fold at neonatal stages. Contrary to the significant increase observed with the α1A-AR subtype, the α1B-AR subtype only increased by 6–fold at the adult stage compared to the levels at E11.5 stage (**Figure 3.1B**). Relative to the α1D-AR subtype at E11.5, the mRNA expression increased by 5-6-fold at E16.5 and neonatal stages and by 3-fold at adult stages (**Figure 3.1C**).

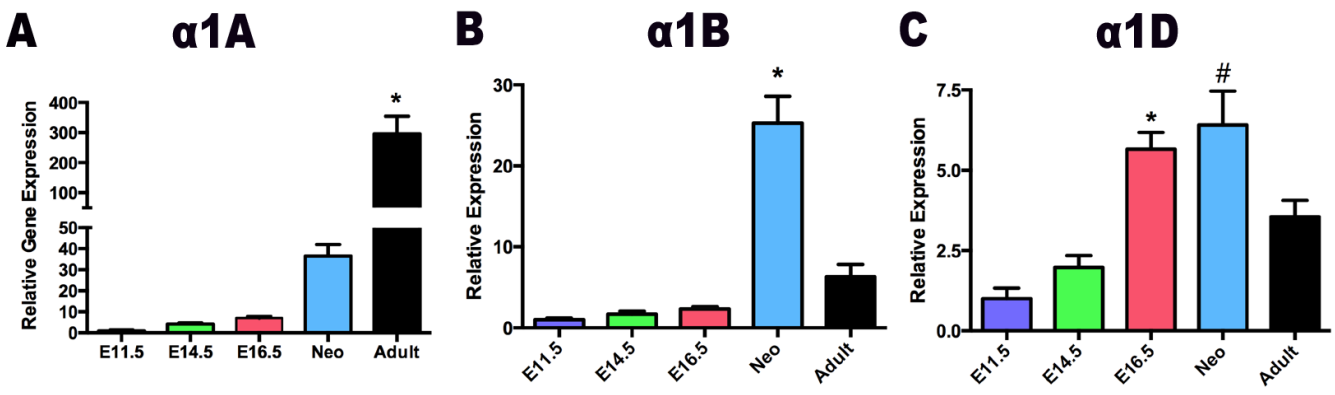

Figure 3.1: RT-qPCR analysis of total RNA samples extracted from cardiac ventricles at different developmental stages. (A-C) The relative expression of α1A, α1B, and α1D ARs from different developmental stages was determined in relation to the E11.5 stage. Levels of E11.5 were set as 1.0 in all panels. GAPDH was used as the house keeping gene for normalization of gene expression. **A)** * $P < 0.005$, Adult Vs. all other stages. **B)** * $P < 0.005$, Neonatal day 1 (Neo) Vs. all other stages. **C)** * $P < 0.005$, E16.5 Vs. E11.5 or E14.5; # $P < 0.005$, Neo Vs. E11.5 or E14.5; $P < 0.05$ Neo Vs. Adult. Each bar represents mean ± SEM, N=3-4 independent RNA extractions/developmental stage, analyzed in duplicates for each extraction. One-way ANOVA with Tukey's multiple comparison test.

Given the primer efficiencies for all primer pairs were in the range 90-110%, RT-qPCR analysis was subsequently used to compare normalized gene expression levels of α1-AR subtypes at each stage of ventricular development. The analysis revealed that the α1B subtype is predominant among the three subtypes, while the α1D subtype also shows higher levels of expression compared to α1A at all developmental stages examined (**Figure 3.2**).

Comparisons between mRNA expression levels of α1-AR subtypes were expressed relative to the α1A levels. At E11.5, the α1B subtype mRNA was more abundant (67-fold Vs. α1A**; Figure 3.2A**), than at E14.5 and E16.5 developmental stages (20-30 fold Vs. α1A**; Figure 3.2B and 3.2C**). However, the level of α1B expression spiked again by 46-fold at neonatal stages (**Figure 3.2D**), while remaining at similar levels in the adult ventricles relative to the α1A subtype (**Figure 3.2E**).

For the α1D-AR subtype, mRNA expression was more abundant when compared to that of α1A at all developmental stages examined with the exception of adult ventricles (5-32-fold Vs. α1A; **Figure 3.2A-3.2C**). Interestingly, mRNA expression of α1D was less abundant than that of α1A subtype in the adult ventricles (2-fold Vs. α1A**; Figure 3.2E**).

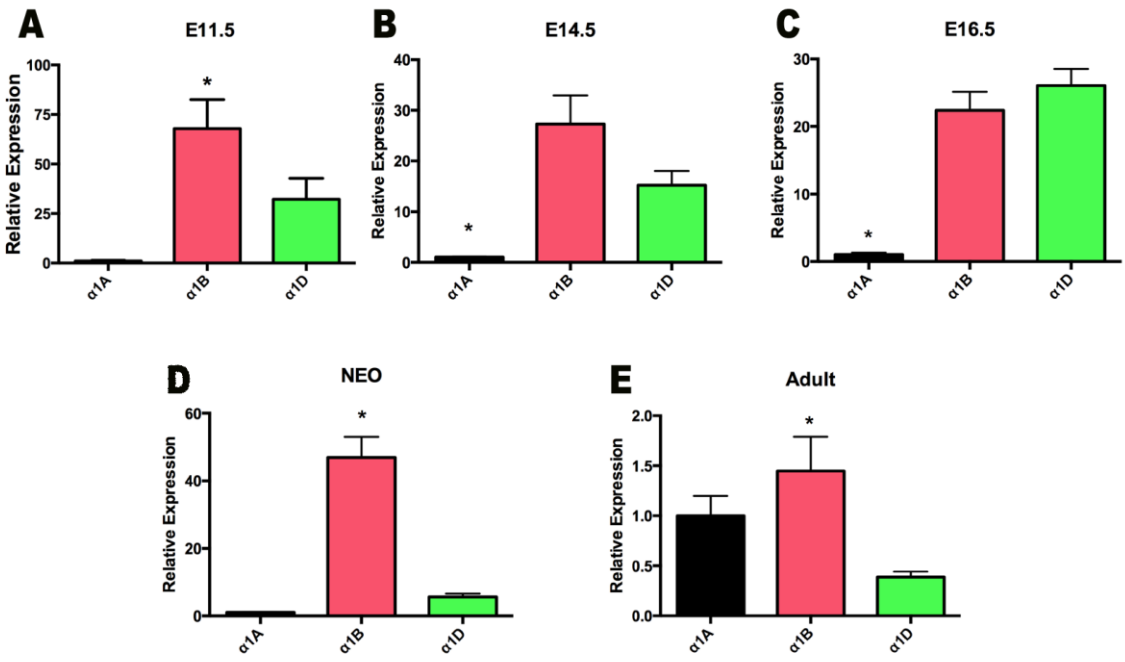

Figure 3.2: Quantification of mRNA levels of α1-AR subtypes during ontogeny of cardiac ventricles. (A-E) Relative expression levels of α1A, α1B, and α1D ARs in different developmental stages of cardiac ventricles by RT-qPCR analysis. α1-ARs are present in embryonic mice as early as E11.5 days old and the α1B mRNA appears to be the predominant one among all three subtypes. Expression levels of α1A were set as 1.0 in all panels. GAPDH was used as the house keeping gene for normalization of gene expression. **A)** E11.5 developmental stage. * $P < 0.005$, α1A Vs. α1B. **B)** 14.5 developmental stage. * $P < 0.005$, α1A Vs. α1B; $P < 0.05$ α1A vs. α1D. **C)** E16.5 developmetnal stage. * $P < 0.005$, α1A Vs. α1B or α1D. **D)** Neonatal day 1 (Neo) developmental stage. * $P < 0.005$ α1B Vs. α1A or α1D. **E)** Adult developmental stage. * $P < 0.05$, α1B Vs. α1D. Each bar represents mean ± SEM, N=3-4 independent RNA extractions/developmental stage, analyzed in duplicates for each extraction. One-way ANOVA with Tukey's multiple compasison test.

3.2 Immunodetection of α1-ARs in cytosolic and membrane fractions of ventricular lysates using subtype specific antibodies

Western blot analysis was conducted using tissue extracts from multiple developmental stages (E11.5 – adult) to detect the presence of α1-AR subtype proteins. Although sufficient quantities of cytosolic proteins were obtained from the ventricular lysates at all developmental stages (23 μg per each lane; **Figure 3.3.1C, 3.3.2C, 3.3.3C)**, Mem-Per Plus extraction procedure did not yield sufficient membrane protein quantities from E11.5 and E16.5 ventricular lysates. As a result, 50μg of membrane fractions were loaded per lane for these early developmental stages. 23μg of membrane lysate per lane was loaded for neonatal and adult samples. Thus, the protein loading for membrane fractions for all developmental stages could not be maintained at similar levels **(Figure 3.3.1C, 3.3.2C, 3.3.3C).** Protein loading in each lane was confirmed by both napthol blue staining **(Figure 3.3.1C, 3.3.2C, 3.3.3C)** as well as via GAPDH levels **(Figure 3.3.1B, 3.3.2B, 3.3.3B)** for cytosolic fractions. Protein loading for membrane fraction was only confirmed with napthol blue staining since GAPDH is not expected to be present in the membrane. Based on the western results, all three α1-AR subtype proteins were readily detectable in the cytosol **(Figure 3.3.1A, 3.3.2A, 3.3.3A).** The α1A and α1B subtype proteins were also present in the membrane fractions of E16.5, neo and adult stages whereas α1D was not detected in any of the membrane fractions **(Figure 3.3.1A, 3.3.2A, 3.3.3A).** Additionally, multiple protein isoforms ranging from 55-90 kilodaltons (kD) were observed with α1A specific antibodies **(Figure 3.3.1A).** Notably, some α1A isoforms apart from 55 kD and 90 kD proteins were absent in the cytosolic lysates from adult

ventricles. In contrast, 90 kD or 63 kD protein bands were detected with α1B and α1D antibodies respectively in many ventricular samples **(Figure 3.3.2A, 3.3.3A).** While there was a progressive increase in the α1B protein levels from E11.5 to adult stage, the levels of α1D remained relatively constant in all stages of ventricular development **(Figure 3.3.2A, 3.3.3A).**

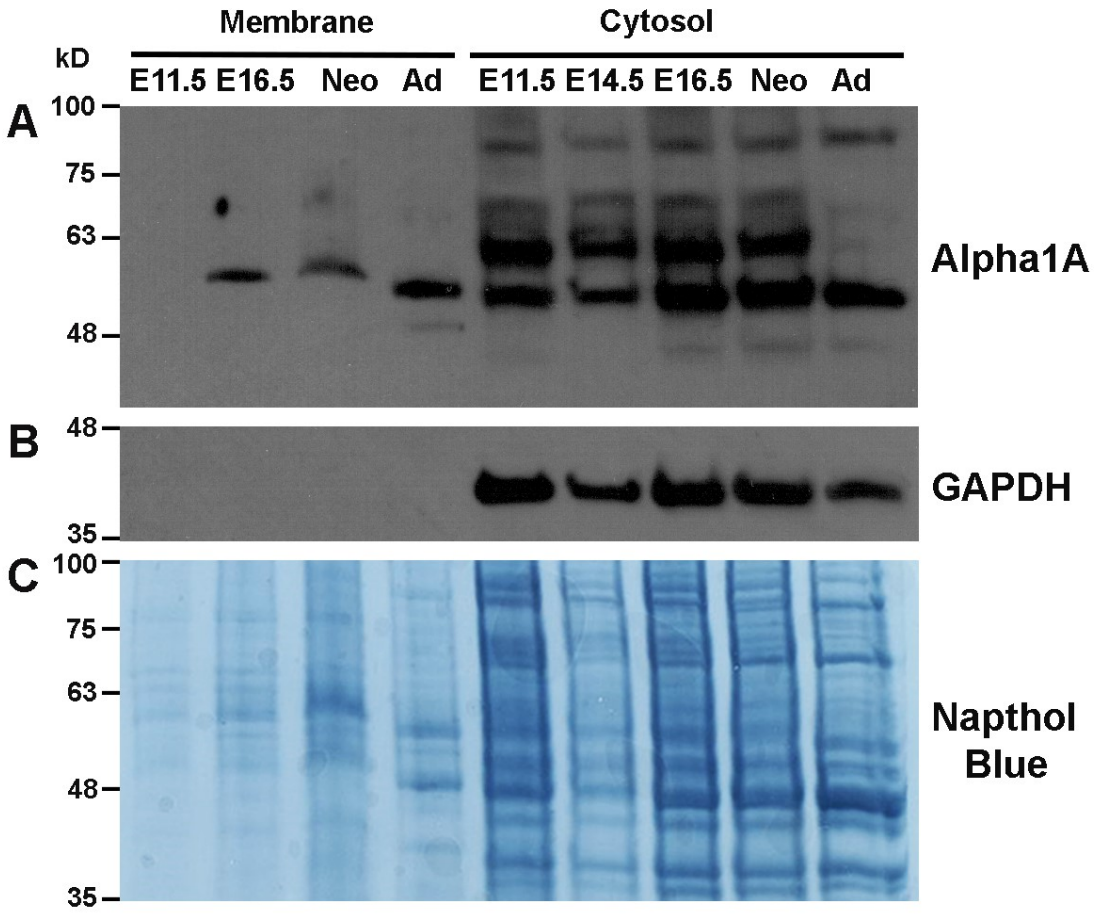

Figure 3.3.1: Western blot analysis of α1A-AR subtype proteins in the cytosol and membrane fractions following extraction from cardiac ventricles at different developmental stages. Cytosolic and membrane proteins were extracted from ventricles at different developmental stages [E11.5, E14.5 E16.5, neonatal (neo), and adult (Ad)] were separated by electrophoresis on 7.5% polyacrylamide gels. 23μg of protein lysate per lane was loaded for all samples except for E11.5 and E16.5 membrane samples where 50μg of lysate per lane was loaded due to low sample yields. **A)** α1A proteins were present in membrane fractions of E16.5, neo and adult stages and multiple protein isoforms were observed in the cytosol. **B)** GAPDH housekeeping protein used for loading control. **C)** Napthol blue staining for detecting of all proteins transferred to the membrane. N = 2 independent protein extractions/developmental stage.

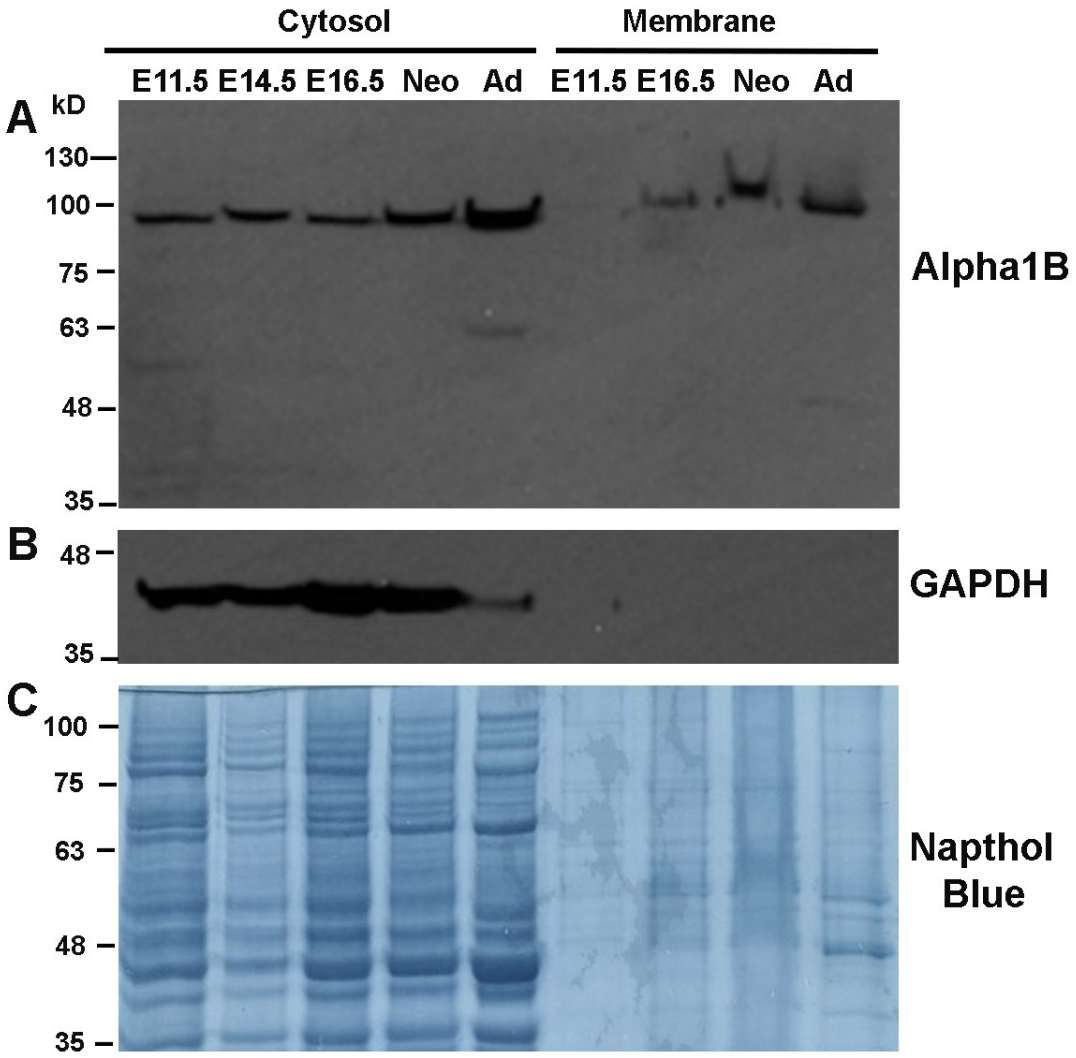

Figure 3.3.2: Western blot analysis of α1B-AR subtype proteins in the cytosol and membrane fractions following extraction from cardiac ventricles at different developmental stages. Cytosolic and membrane proteins were extracted from ventricles at different developmental stages [E11.5, E14.5 E16.5, neonatal (neo), and adult (Ad)] were separated by electrophoresis on 7.5% polyacrylamide gels. 23μg of protein lysate per lane was loaded for all samples except for E11.5 and E16.5 membrane samples where 50μg of lysate per lane was loaded due to low sample yields. **A)** α1B proteins were present in the cytosol and membrane fractions of E16.5, neo, and adult stages. **B)** GAPDH housekeeping protein used for loading control. **C)** Napthol blue staining for detecting of all proteins transferred to the membrane. N = 2 independent protein extractions/developmental stage.

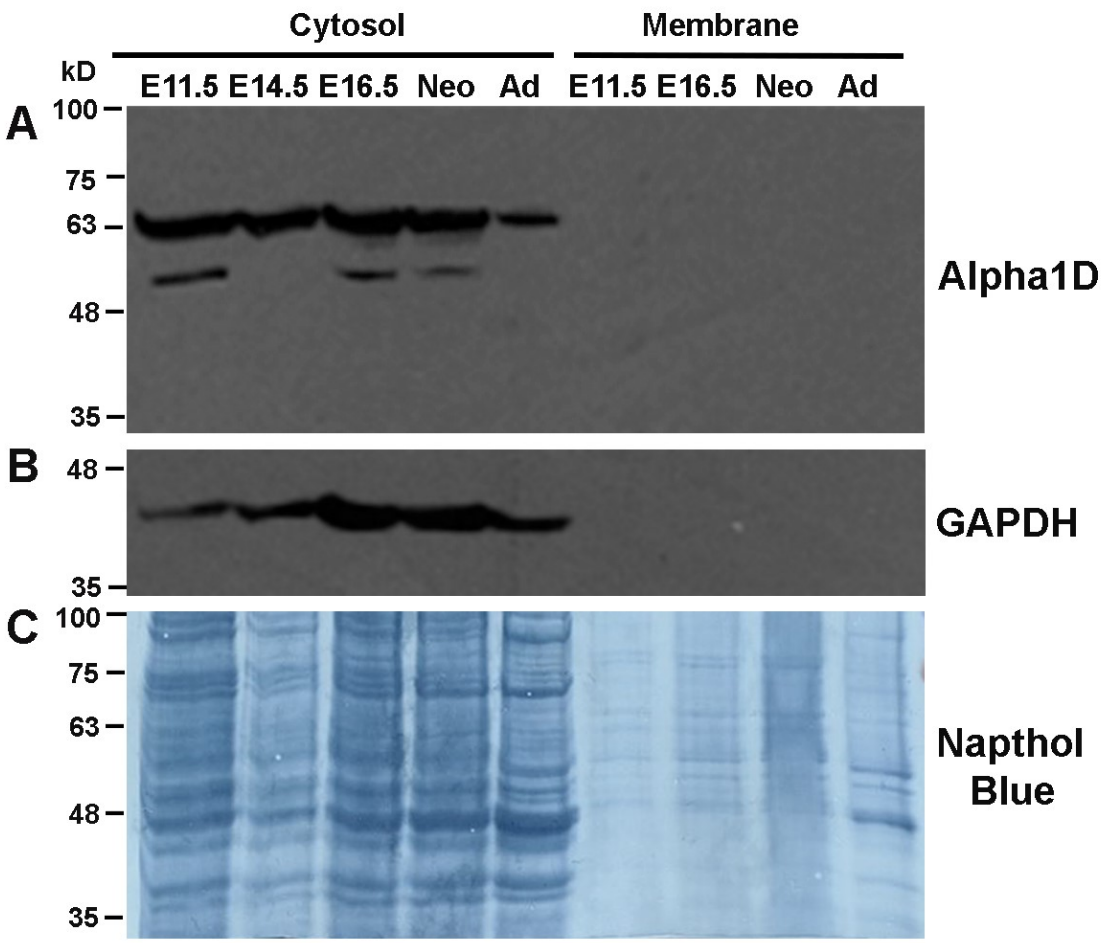

Figure 3.3.3: Western blot analysis of α1D-AR subtype proteins in the cytosol and membrane fractions following extraction from cardiac ventricles at different developmental stages. Cytosolic and membrane proteins were extracted from ventricles at different developmental stages [E11.5, E14.5 E16.5, neonatal (neo), and adult (Ad)] were separated by electrophoresis on 7.5% polyacrylamide gels. 23μg of protein lysate per lane was loaded for all samples except for E11.5 and E16.5 membrane samples where 50μg of lysate per lane was loaded due to low sample yields. **A)** α1D proteins were present in the cytosol but were not detected in membrane fractions. **B)** GAPDH housekeeping protein used for loading control. **C)** Napthol blue staining for detecting of all proteins transferred to the membrane. N = 2 independent protein extractions/ developmental stage.

3.3 Subcellular localization of α1-AR subtypes in embryonic ventricular cells

α1-AR subtype specific antibody immunostaining methods were used to determine subcellular localization of α1-ARs in embryonic ventricular cell cultures derived from E11.5 CD1 embryos. Cells cultured on 4-well chamber slides were incubated with polyclonal α1-AR subtype specific antibodies that were pre-incubated with or without receptor specific antigen peptides along with monoclonal MF20 antibodies, which stained for sarcomeric myosin, and Hoechst's stain, which counterstained for nuclei. Samples were examined using a Leica DM2500 fluorescence microscope. Cells staining positive with MF20 antibodies were designated as cardiomyocytes (CMs) and cells negative for MF20 were considered non-cardiomyocytes (NMCs). Immunostaining revealed the presence of α1-AR subtypes (α1A, α1B, α1D) in both CMs and NMCs (**Figure 3.5-3.7).**

Rabbit nonimmune serum (NIS) and peptide blocking experiments were conducted to ensure the signal specificity after staining with α1-AR subtype specific antibodies. Results from NIS immunostaining revealed minimal background level of fluorescence (**Figure 3.4A**). Peptide blocking with three different antigen specific peptides (1:5 dilution) also revealed minimal background level of fluorescence for α1A, α1B, and α1D subtype specific antibodies (**Figure 3.4C, 3.4E, 3.4G**).

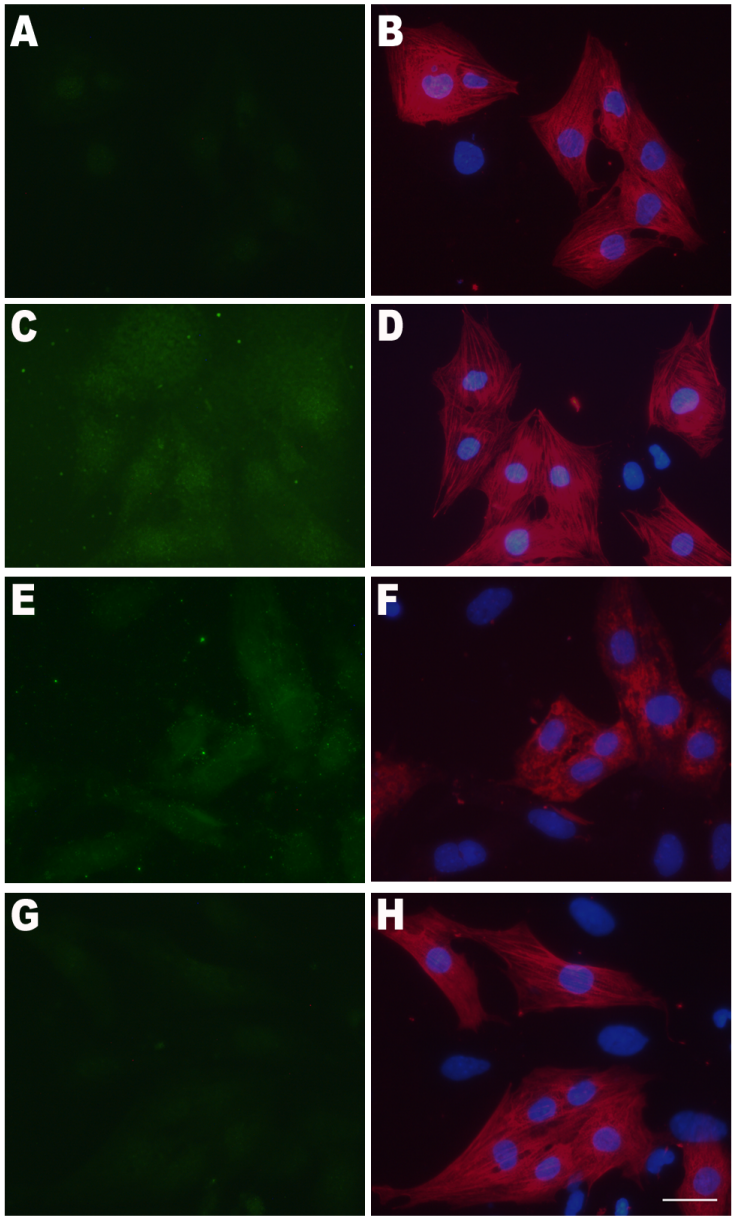

Figure 3.4: Immunostaining with nonimmune serum (NIS) stain and peptide blocking experiments with α1-AR antibodies on embryonic ventricles extracted from E11.5 CD1 mice. Immunostaining methods using nonimmune serum (NIS), α1-AR peptide, and α1-AR antibodies. Pictures were taken at 40X magnification. **A)** NIS stained cells incubated with antirabbit Alexa 488 antibodies. **B)** Overlay of MF20 staining with Hoechst's stain. **C)** α1A-AR antibody preincubated with α1A peptide (1:5 Block). **D)** Overlay of MF20 staining with Hoechst's stain. **E)** α1B-AR antibody preincubated with α1B peptide (1:5 Block). **F)** Overlay of MF20 staining with Hoechst's stain. **G)** α1D-AR antibody preincubated with α1D peptide (1:5 Block). **H)** Overlay of MF20 staining with Hoechst's stain. Scale Bar = 25μM for all panels.

In parallel wells of the same chamber slides, cells were processed for α1-AR subtype specific antibody immunostaining in the absence of control antigen peptides. The α1A-AR subtype was readily detectable in nuclear and cytoplasmic compartments of both CMs and non-cardiomyocytes (NMCs)(**Figure 3.5A**). Although α1A staining was visible in the cell membrane region of some cells, it was predominantly localized in the nuclear compartment. In a small number of CMs (<1%), α1A-AR antibody staining also co-localized with the sarcomeric myosin staining (**Figure 3.5B**), as α1A-ARs were visible along the cross-striations of MF20 stained sarcomeric myosin (**Figure 3.5D**).

The α1B-ARs were visible in E11.5 ventricular cells in the nuclear and cytoplasmic compartment of CMs as well as NMCs (**Figure 3.6**) however, the immunoreactivity of α1B-AR antibodies was not as strong as the signal observed with α1A and α1D-AR antibodies. Moreover, α1B-ARs did not show co-localization with MF20 stained sarcomeric myosin. The α1D-ARs were visible in E11.5 ventricular cells predominantly in the nuclear compartment in both CMs and NMCs. Additionally, α1D nuclear staining appeared as small puncta in the nucleus, however the significance of this punctate staining is unknown. Punctate staining could possibly indicate involvement of α1-ARs in nuclear transcription events (**Figure 3.7A**). Similar to α1A staining, α1D-ARs also co-localized with sarcomeric myosin in a small number of cardiomyocytes (<1%) (**Figure 3.7D**).

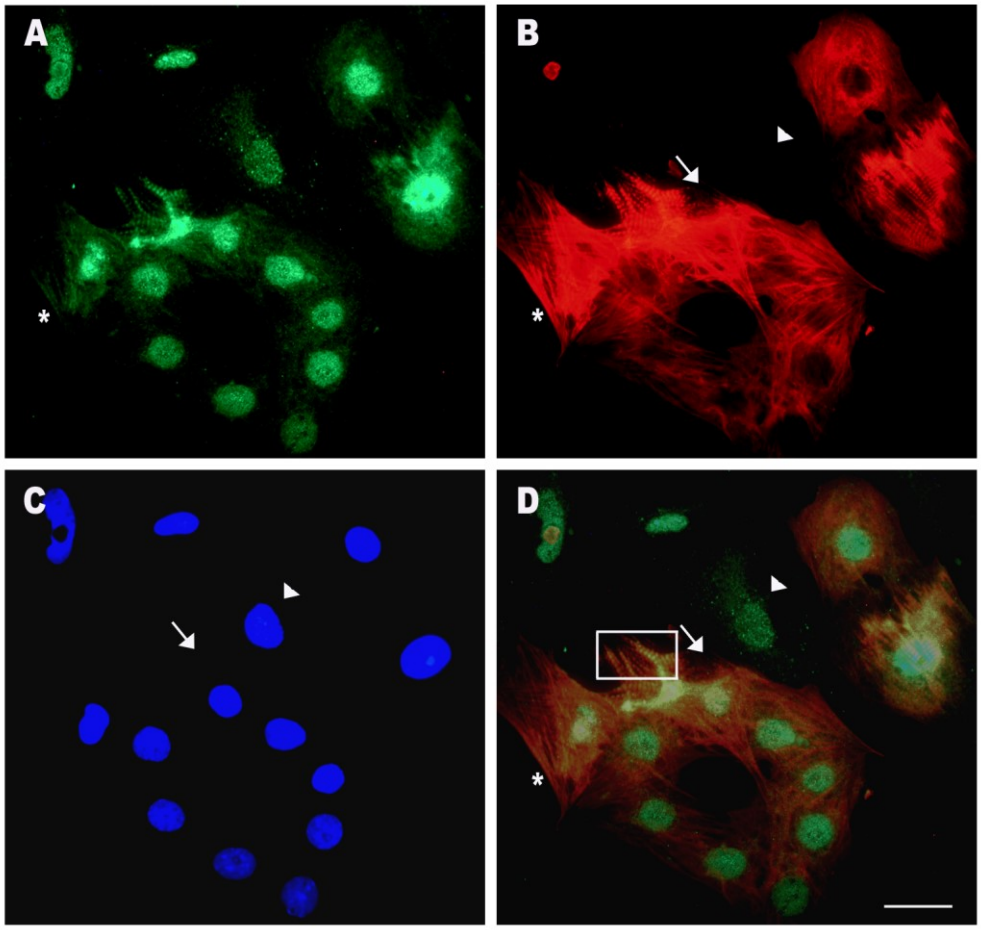

Figure 3.5: Immunostaining of E11.5 ventricular cells with α1A-AR specific antibodies. Representative images of cells co-stained with **A)** α1A-AR and **B)** MF20 sarcomeric myosin specific antibodies along with **C)** Hoechst nuclear stain. **D)** Overlay of cells co-stained with α1A-AR and MF20 antibodies. Arrow indicates a cardiomyocyte with α1A-AR staining in both nuclear and cytoplasmic compartments. Arrowhead indicates a non-cardiomyocyte with α1A-AR staining in both nuclear and cytoplasmic compartments. Membrane staining is denoted by an asterisk (*). Boxed area indicates co-localization of α1A-ARs in MF20 positive sarcomeric regions. Scale bar: 25μm for all panels.

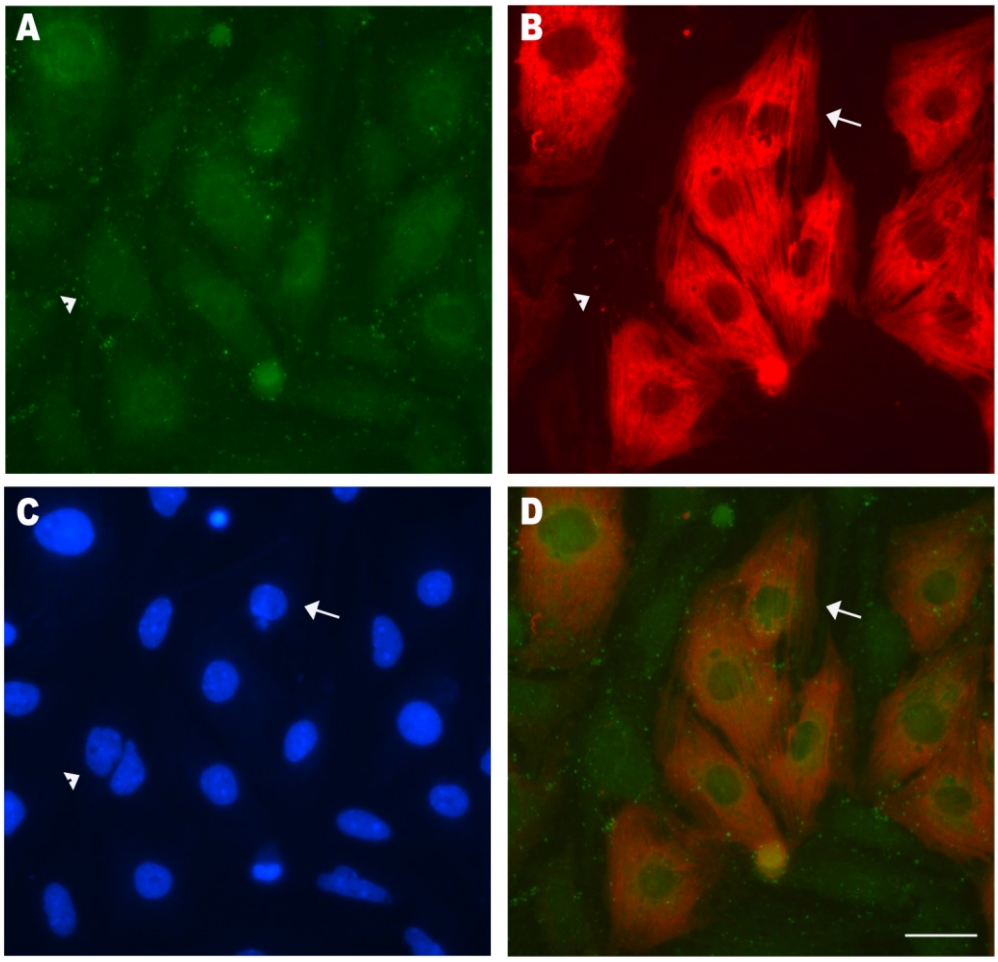

Figure 3.6: Immunostaining of E11.5 ventricular cells with α1B-AR specific antibodies. Representative images of cells co-stained with **A)** α1B-AR and **B)** MF20 sarcomeric myosin specific antibodies along with **C)** Hoechst nuclear stain. **D)** Overlay of cells co-stained with α1B-AR and MF20 antibodies. Arrow indicates a cardiomyocyte with α1B-AR staining in both nuclear and cytoplasmic compartments. Arrowhead indicates a non-cardiomyocyte with α1B-AR staining in both nuclear and cytoplasmic compartments. Scale bar: 25μm for all panels.

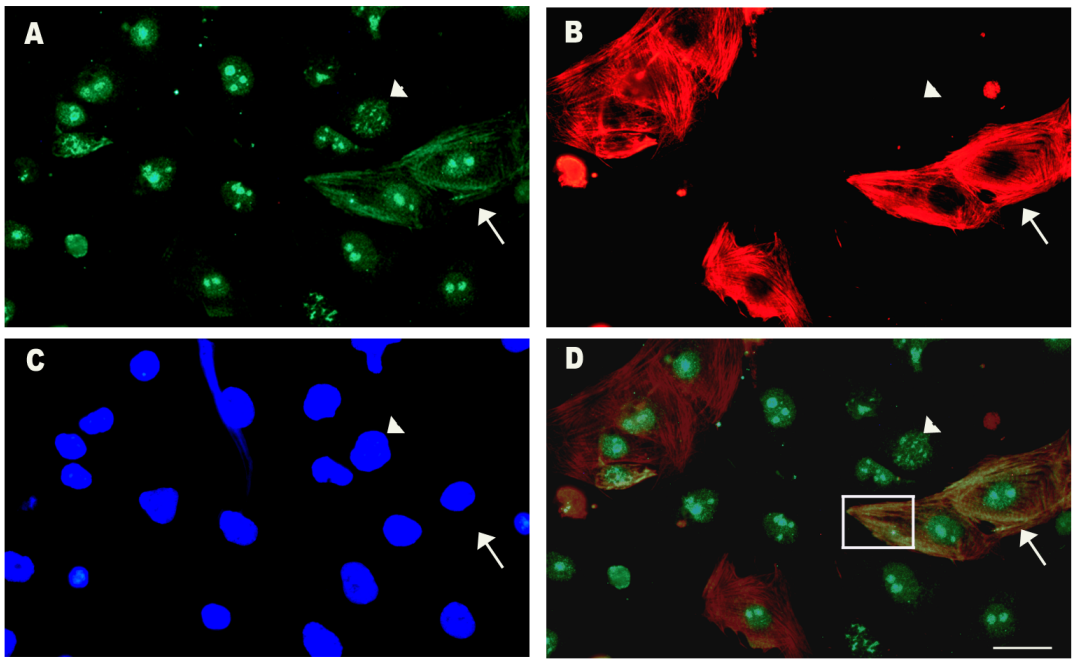

Figure 3.7: Immunostaining of E11.5 ventricular cells with α1D-AR specific antibodies. Representative images of cells co-stained with **A)** α1D-AR and **B)** sarcomeric myosin (MF20) specific antibodies along with **C)** Hoechst nuclear staining. **D)** Overlay of cells co-stained with α1D-AR and MF20 antibodies. Arrow indicates a cardiomyocyte with α1D-AR staining in both nuclear and cytoplasmic compartments. Arrowhead indicates a non-cardiomyocyte with α1D-AR staining of puncta in the nuclear compartment. Boxed area indicates co-localization of α1D-ARs in MF20 positive sarcomeric regions. Scale bar: 25 μm for all panels.

3.4 Characterizing the effects of carvedilol (a non-selective AR blocker) on cAMP levels in E11.5 ventricular cells

Carvedilol is used for the treatment of hypertension and congestive heart failure and is known to decrease patient morbidity and mortality. Carvedilol is a non-selective β1 and β2-AR antagonist with α1-AR blocking activity and was shown to induce PDE3 levels and control β-AR mediated effects in failing human hearts (Molenaar et al., 2014). Due to the β blocking activity of carvedilol, we examined the effects of carvedilol blockade on cAMP levels. In order to determine the effects of carvedilol (Carv) on the second messenger responses associated with β-ARs in embryonic cells, cAMP levels were assessed in E11.5 ventricular cells treated with or without Carv in the presence or absence of a non-selective β-AR agonist (isoproterenol, ISO). Embryonic ventricular cells (5000 cells/well) were treated with ISO [1μM] and different concentrations of carvedilol [0.1, 1 and 10μM] and a competitive HTRF immunoassay was performed to determine the levels of cAMP production. In untreated cell preparations (Control group), the basal cAMP levels were determined to be (0.44 ± 0.16 nM). One-way ANOVA revealed that there was a significant increase in cAMP levels induced by ISO compared to the control or other treatment groups (9-fold Vs, Cont, * $P < 0.005$, **Figure 3.8**). Cells treated with a combination of ISO and 10μM Carv revealed similar levels of cAMP compared to control suggesting that 10μM Carv can effectively block ISO induced changes in second messenger levels in embryonic ventricular cells. Notably, cells treated with Carv alone did not reveal any significant changes in cAMP levels (**Figure 3.8**).

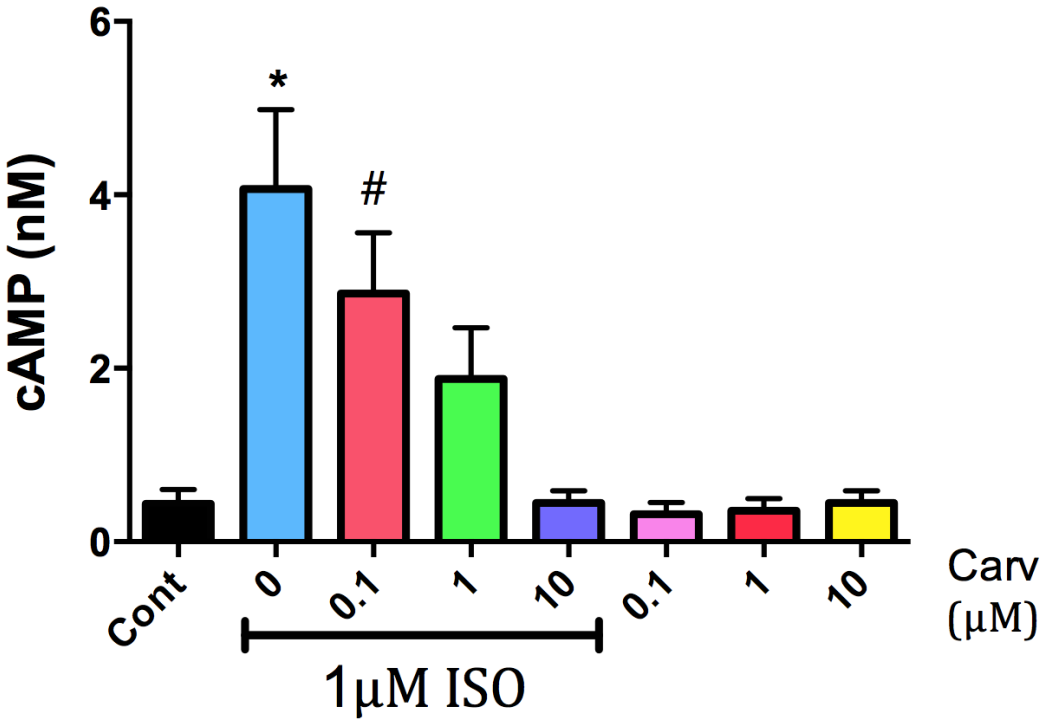

Figure 3.8: Effects of a β-AR stimulant (isoproterenol; ISO) and a non-selective AR blocker (Carvedilol; Carv) on cAMP production in E11.5 ventricular cells. Ventricular cells were treated with ISO [1μM] and/or Carv [0.1, 1 and 10μM] for 30 mins and processed for a HTRF based cAMP assay. Stimulation of cells with ISO resulted in approximately 9-fold increase in cAMP levels compared to the control group (Cont). Cells treated with ISO and 10 μM Carv revealed similar levels of cAMP compared to control groups suggesting that 10 μM Carv can effectively block ISO induced changes in second messenger levels in embryonic ventricular cells. * $P < 0.005$ ISO Vs. all other groups except ISO+0.1μM Carv; # $P < 0.05$. ISO+0.1μM Vs. Cont, ISO+10μM Carv or 0.1, 1 and 10μM Carv treatments alone. Each bar represents mean ± SEM, N=6 experiments per group. One-way ANOVA with Tukey's multiple comparison test.

3.5 α1-AR associated IP1 second messenger responses vary with cell densities

Stimulation of α1-ARs results in the release of second messenger IP3, which is rapidly degraded to IP2, and then IP1 (Garbison et al., 2004). As a result, it is easier to measure levels of IP1 within cells. IP1 assays were conducted to determine α1-AR second messenger responses in embryonic ventricular cells. Embryonic (E11.5) ventricular cells were plated with increasing densities ranging from 40,000 to 80,000 cells. Cells were treated with 10μM phenylephrine (PE) to determine the effects of an α1-AR stimulant on IP1 second messenger levels in untreated cell preparations (Control group). The basal IP1 ranged from (40K = 172 ± 10.6 nM; 50K = 150.2 ± 3.8 nM; 60K = 162.4 ± 9.4 nM; 80K = 212 ± 26.6 nM) depending on the plating densities. Addition of PE did not stimulate any significant increase in IP1 levels when cells were plated at 40,000/well density (**Figure 3.9A**). Whereas, PE treatment of cells plated with 50,000 to 80,000 cells/well resulted in ~1.4-fold increase when compared to untreated control groups (**Figure 3.9B-3.9D**). These results suggest that α1-ARs are functionally active and involved in mediating IP1 second messenger responses in embryonic ventricular cells.

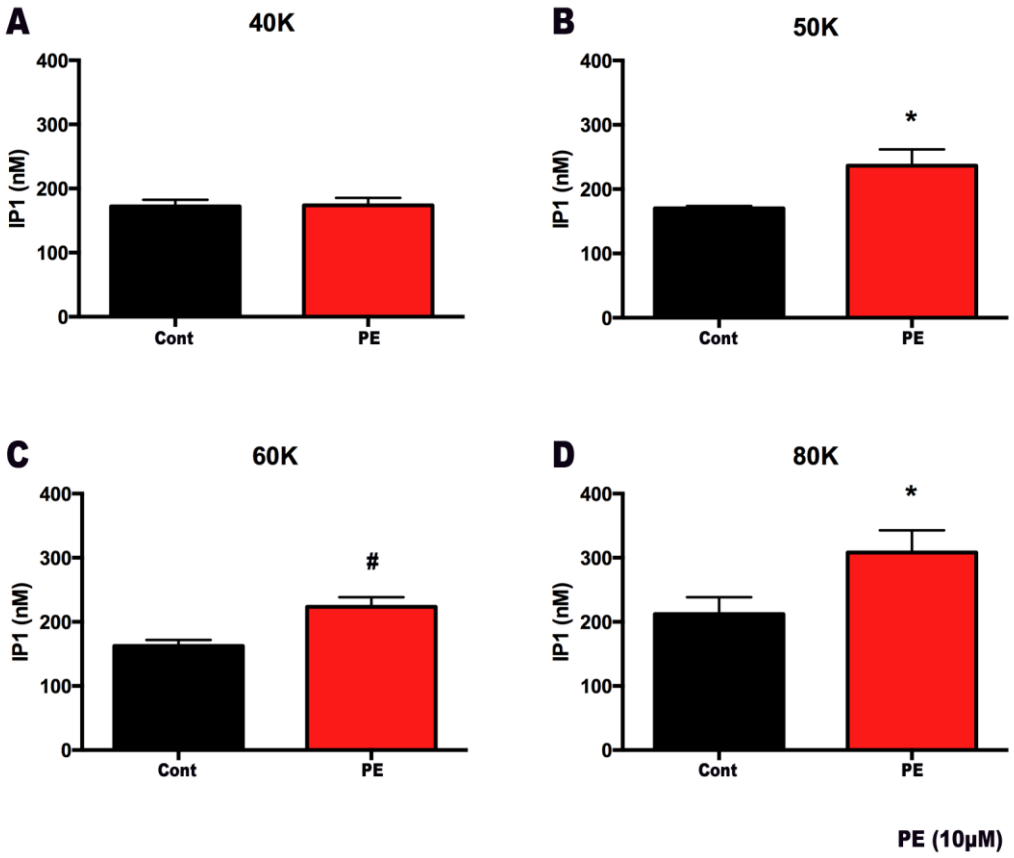

Figure 3.9: Effects of an α1-AR stimulant (phenylephrine, PE) on IP1 levels in E11.5 ventricular cells. E11.5 ventricular cells were plated with densities ranging from 40,000 to 80,000 cells (40K-80K) cells per well, treated with 10µM PE for 45 mins and processed for a HTRF based IP1 assay. Three different cell densities (50K, 60K and 80K) produced significantly higher amounts of IP1 after treatment with 10µM PE compared to the untreated controls. **A)** No significant difference between Cont and PE. **B and D);** * $P < 0.05$, Cont Vs. PE for 50K and 80K panels. **C)** # $P < 0.005$ Cont Vs. PE for 60K panel. Each bar represents mean ± SEM, N=6 experiments. Unpaired Student's t-test.

3.6 Identification of cardiac progenitor cells (CPCs) and cardiomyocytes (CMs) undergoing DNA synthesis using a novel lineage tracking method combined with Click-iT EdU staining

Nkx2.5-Cre and Rosa-lacZ (NCRL) transgenic mouse strains were used to differentiate between CMs and CPCs. The **Nkx2.5-Cre (NC)** mouse strain has a Cre recombinase inserted into the Nkx2.5 allele. The Rosa-lacZ mouse strain contains the **R26R** reporter strain (Rosa-*LacZ*) with the Lac Z gene inserted into the Rosa locus. Primary NCRL embryonic E11.5 ventricular cell cultures were treated with different agonists and antagonists to determine the effect on cell proliferation. Immunostaining methods were used to differentiate between CMs and CPCs. Cells that stained positive for β-Gal and MF20 ($\beta\text{-Gal}^+/\text{MF20}^+$) were designated as CMs and cells that stained positive for β-Gal but were negative for MF20 ($\beta\text{-Gal}^+/\text{MF20}^-$) were designated as CPCs because $\text{Nkx2.5}^+/\text{MF20}^-$ cells were shown to differentiate into CMs (McMullen et al., 2009; Zhang et al., 2015).

Click-iT EdU imaging kit was used to identify cells undergoing DNA synthesis. EdU staining in combination with cre-lox based lineage tracking were used to determine differences in the cell cycle activity and proliferation of CMs and CPCs in E11.5 ventricular cultures. Figure 10 depicts immunostaining experiments with Click-iT EdU^+ (**Figure 3.10**). Immunostaining results suggested that some of the CPCs and CMs were undergoing cell cycle changes based on the presence of EdU^+ cells (**Figure 3.10E and 3.10F)**.

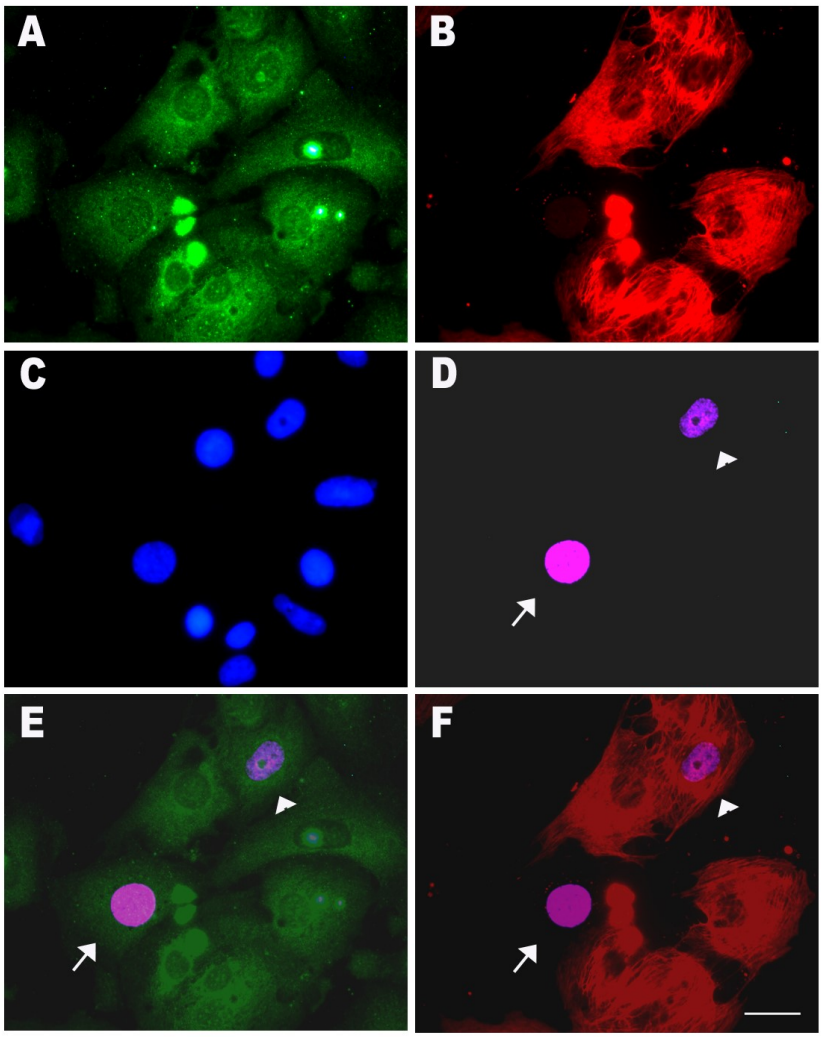

Figure 3.10: Click-iT EdU labeling of E11.5 ventricular cells. E11.5 ventricular cells prepared from NCRL mice were stained with MF20 and β-Gal antibodies followed by Hoechst and Click-iT EdU labeling to identify CMs and CPCs undergoing DNA synthesis. Pictures were taken at 40X magnification. Representative images of cells co-stained with **A)** β-Gal antibodies. **B)** MF20 antibodies. **C)** Hoechst's stain for nuclei. **D)** Click-iT EdU. **E)** Overlay of β-Gal and EdU^+. **F)** Overlay of MF20 and EdU^+. Arrowheads identifying to EdU^+ CMs. Arrows identifying EdU^+ CPCs. Scale Bar: 25μM for all panels. Note: Click-iT EdU panels were pseudocoloured.

3.7 Blockade of α1-ARs with carvedilol does not affect cell proliferation of embryonic ventricular cells

E11.5 NCRL ventricular cell cultures were treated with Carv [10μM] in the presence or absence of ISO [1μM] for 20 hrs. Since Carv was dissolved in DMSO, control cultures were treated with DMSO at a final concentration of 0.03%. In addition, cell cultures treated with ISO also received DMSO at a final concentration of 0.03%. As described in an earlier section, (**Section 2.12**) immunostaining methods were used to differentiate between CMs and CPCs in the embryonic ventricular cell cultures. The total number of cells was determined by counting the number of Hoechst stained nuclei in each field. The total number of nuclei in combination with β-Gal and MF20 staining was used to determine the percentage of CMs, CPCs, and non-CMs in reference to the total number of nuclei present. Based on results from one-way ANOVA and Tukey's multiple comparisons test, cells treated with ISO [1μM], Carv [10μM], and a combination of ISO+Carv [1μM+10μM], revealed no significant difference between control and treatment groups in total cell numbers or percentages of CMs and CPCs per field (**Figure 3.11A, 3.11C, 3.11E**).

Click-iT EdU cell proliferation assays were used to determine differences in cell cycle activity of CMs and CPCs treated with Carv [10μM] in the presence or absence of ISO [1μM]. Total numbers of cells determined by Hoechst stained nuclei/field were used to determine the percentage of EdU^+ nuclei, CMs, and CPCs. Based on results from one-way ANOVA and Tukey's multiple comparisons test, there was no significant difference in the cell cycle activity of CMs and CPCs between control and treatment groups (**Figure 3.11B, 3.11D, 3.11F**). These results suggest

that carvedilol blockade of α1-ARs does not affect cell proliferation of embryonic ventricular cells.

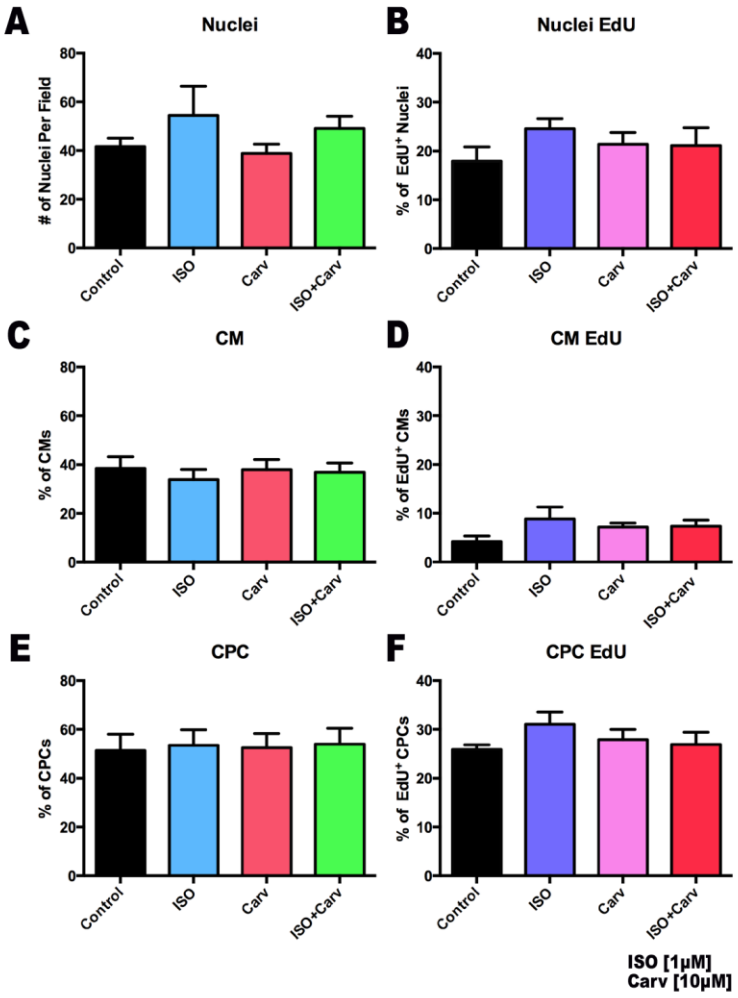

Figure 3.11: Quantification of cell counts, percentage of CMs, CPCs and EdU⁺ cells in E11.5 ventricular cells treated with drugs acting on adrenergic receptors. E11.5 ventricular cells from Nkx-cre and Rosa-lacZ mice were plated at 250,000 cells/well. Cell treatments include Control, ISO [1μM], Carv [10μM], and ISO+Carv [1μM+10μM]. Immunostaining was performed with MF20 and β-Gal antibodies to detect CM and CPC respectively. Hoechst and Click-iT EdU staining was performed to detect nuclei and cells undergoing DNA synthesis respectively. Cell counts used to determine differences in cell proliferation of CMs and CPCs were expressed as the average number of nuclei per field. **A)** Total number of nuclei per field. **B)** Percentage (%) of EdU⁺ nuclei compared to the total number of nuclei per field. **C)** Percentage of cardiomyocytes (CM) per field. **D)** Percentage of EdU⁺ CMs compared to the total number of CMs per field. **E)** Percentage of cardiac progenitor cells (CPC) per field. **F)** Percentage of EdU⁺ CPCs compared to the total number of CPCs per field. No significant difference between control and treatment groups. N=4-6 experiments. Eight 40X magnification fields were counted per treatment in each experiment. Total number of nuclei counted: 245-872 per experiment. One-way ANOVA and Tukey's multiple comparison test.

3.8 ISO significantly decreases cell proliferation when no DMSO is added

Carvedilol stock was prepared by diluting carvedilol in DMSO. As a result, DMSO was also added to ISO and control groups before treating embryonic E11.5 ventricular cells. Final concentration of DMSO in cell culture media for control and treatment groups was kept at 0.03% **(Figure 3.12).** However, 1μM ISO dissolved in aqueous medium without any DMSO was shown to elicit an inhibitory effect on cell cycle activity of embryonic ventricular cells using a tritiated thymidine labeling assay in a previous study (Feridooni et al., 2017). Therefore, cell proliferation experiments were also conducted on cells treated with ISO in the absence of DMSO to determine if there was a significant difference in cell proliferation of CMs and CPCs. Cell counts were determined along with the percentages of EdU^+ nuclei, CMs, and CPCs. Results from one-way ANOVA and Tukey's multiple comparisons test revealed that cells treated with ISO resulted in a significant decrease (1.8–fold decrease) in the total number of nuclei present (**Figure 3.12A**). There was also a significant decrease in the percentage of CPCs per field as cells treated with ISO resulted in a 1-fold decrease compared to control groups (**Figure 3.12E**). Cell counts for CMs revealed no significant difference between ISO and control groups (**Figure 3.12C**).

Results based on EdU labeling revealed that the percentage of cells undergoing DNA synthesis was significantly reduced in ISO treated cells. Total cell proliferation as determined by EdU^+ nuclei decreased by 1.4–fold in ISO treated groups compared to the control group (**Figure 3.12B**). CPC proliferation in cultures treated with ISO also resulted in a 1.4–fold decrease compared to control groups (**Figure 3.12F**). There was no significant difference between ISO and control groups for EdU^+ CMs. These

results suggest that ISO has a significant negative effect on cell proliferation of CPCs when no DMSO is added.

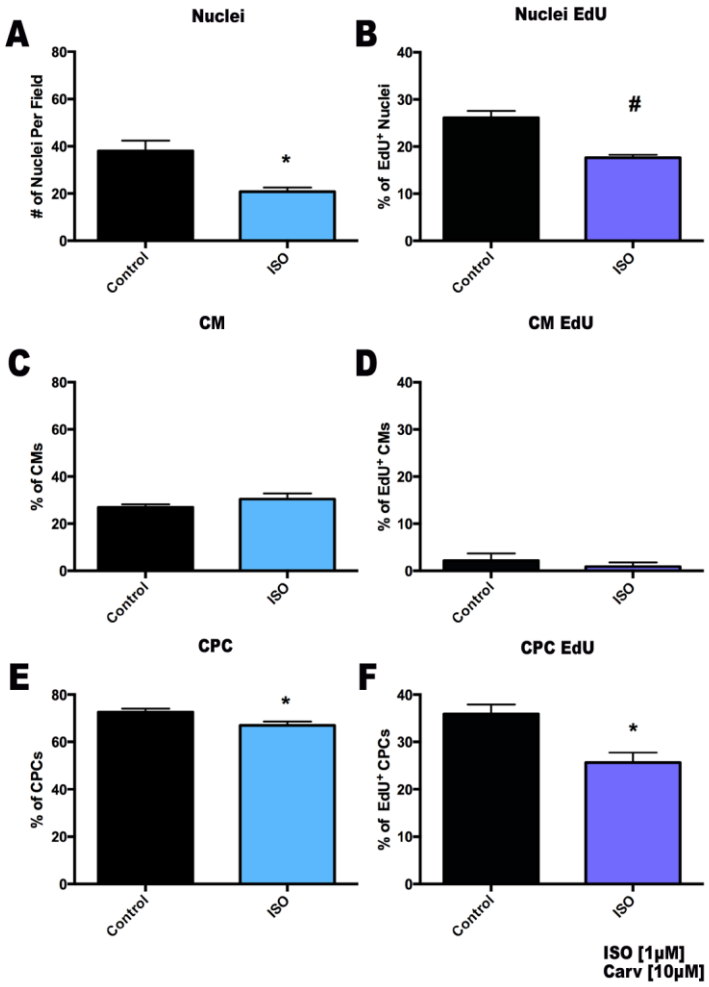

Figure 3.12: Quantification of cell counts, percentage of CMs, CPCs and EdU⁺ cells in E11.5 ventricular cells treated with isoproterenol (ISO) in the absence of DMSO. E11.5 ventricular cells from Nkx-cre and Rosa-lacZ mice were plated at 250,000 cells/well. Cell treatments include Control and ISO [1μM]. Immunostaining was performed with MF20 and β-Gal antibodies to detect CM and CPC respectively. Hoechst and Click-iT EdU stainings were performed to detect nuclei and cells undergoing DNA synthesis respectively. Cell counts used to determine differences in cell proliferation of CM and CPCs were expressed as the average number of nuclei per field. **A)** Total number of nuclei per field. **B)** Percentage (%) of EdU⁺ nuclei compared to the total number of nuclei per field. **C)** Percentage of cardiomyocytes (CM) per field. **D)** Percentage of EdU⁺ CMs compared to the total number of CMs per field. **E)** Percentage of cardiac progenitor cells (CPC) per field. **F)** Percentage of EdU⁺ CPCs compared to the total number of CPCs per field. N=4 experiments. Eight 40X magnification fields were counted per treatment in each experiment. * $P < 0.05$. # $P < 0.005$. Total number of nuclei counted: 143-390 per experiment. Two tailed T test.

3.9 α1-AR acting drugs phenylephrine and prazosin do not affect cell proliferation in embryonic ventricular cells

Primary NCRL embryonic E11.5 ventricular cell cultures were treated with PE [50μM], prazosin [1μM], and a combination of PE+PZ [50μM+1μM] to determine the effects on cell proliferation. As described in earlier sections, total number of cells was determined by counting the number of Hoechst stained nuclei in each field. The percentage of CMs and CPCs was then determined based on the total number of nuclei present. Cell count results from one-way ANOVA and Tukey's multiple comparisons test revealed that cells treated with PZ [1μM], PE [50μM], and a combination of PE+PZ [1μM+50μM], revealed no significant difference between control and treatment groups (**Figure 3.13A, 3.13C, 3.13E**).

Click-it EdU proliferation assays were used to determine the effect that PE and PZ have on cell proliferation of embryonic ventricular cells. The percentage of EdU^+ nuclei, CMs, and CPCs was determined based on the total number of cells present in each field. Results from one-way ANOVA and Tukey's multiple comparisons test revealed that treatment with PE and PZ did not significantly affect cell proliferation of CMs and CPCs (**Figure 3.13B, 3.13D, 3.13E**). These results suggest that α1-AR stimulation (PE) and antagonism (PZ) does not negatively affect cell proliferation of embryonic ventricular cells.

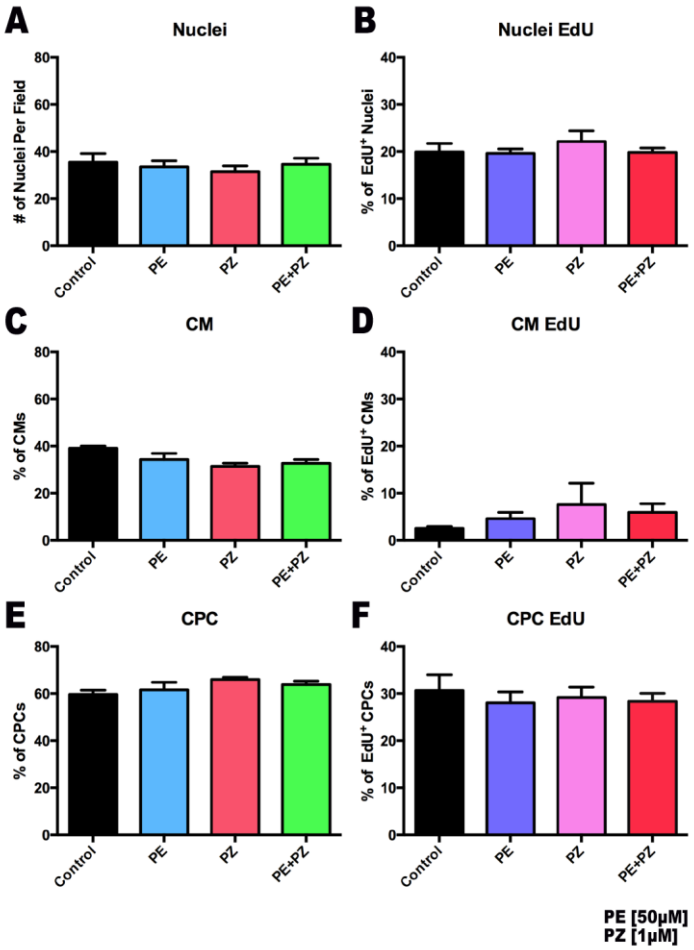

Figure 3.13: Quantification of cell counts, percentage of CMs, CPCs and EdU⁺ cells in E11.5 ventricular cells treated with phenylephrine (PE) and prazosin (PZ). E11.5 ventricular cells from Nkx-cre and Rosa-lacZ mice were plated at 250,000 cells/well. Cell treatments include PE [50µM], PZ [1µM], and PE+PZ [50µM+1µM]. Immunostaining was performed with MF20 and β-Gal antibodies to detect CM and CPC respectively. Hoechst and Click-iT EdU staining was performed to detect nuclei and cells undergoing DNA synthesis respectively. Cell counts used to determine differences in cell proliferation of CM and CPCs were expressed as the average number of nuclei per field. **A)** Total number of nuclei per field. **B)** Percentage (%) of EdU⁺ nuclei compared to the total number of nuclei per field. **C)** Percentage of cardiomyocytes (CM) per field. **D)** Percentage of EdU⁺ CMs compared to the total number of CMs per field. **E)** Percentage of cardiac progenitor cells (CPC) per field. **F)** Percentage of EdU⁺ CPCs compared to the total number of CPCs per field. No significant difference between control and treatment groups. N=5 for experiments. Eight 40X magnification fields were counted per treatment in each experiment. Total number of nuclei counted: 188-389 per experiment. One-way ANOVA and Tukey's multiple comparison test.

3.10 ISO and carvedilol treatment does not affect cell size in embryonic ventricular cell cultures

Primary embryonic E11.5 ventricular cell cultures were treated with different agonists and antagonists to determine the effect on cell differentiation. Cells were treated with ISO [1μM], Carv [10μM], and a combination of ISO+Carv [1μM+10μM]. As described earlier, immunostaining methods were used to differentiate between CMs and CPCs. CM cell sizes were measured using a colour subtractive image analysis method previously described by (Gaspard and Pasumarthi, 2008). Based on results from one-way ANOVA and Tukey's multiple comparisons test, there was no significant difference in cell sizes between control and treatment groups with or without DMSO (**Figure 3.14**). This result suggests that carvedilol blockade of α1- and β-ARs does not affect embryonic ventricular cell size.

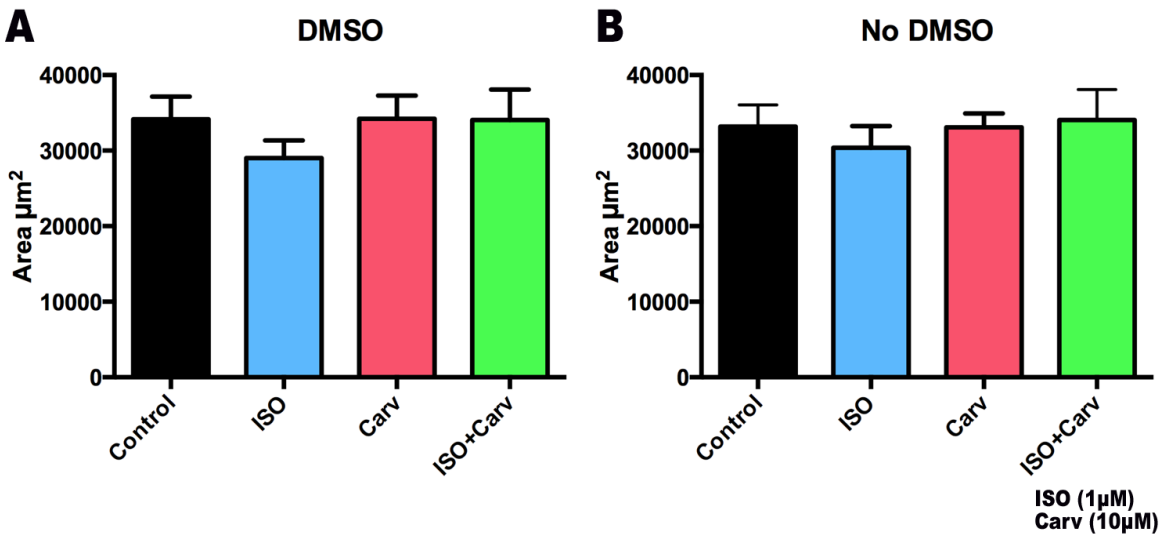

Figure 3.14: Cell size measurements of E11.5 ventricular cells treated with ISO and Carv in the presence or absence of DMSO. E11.5 ventricular cells from Nkx-cre and Rosa-lacZ mice were plated at 250,000 cells/well. Cell treatments include Control, ISO [1µM], Carv [10µM], and ISO+Carv [1µM+10µM]. Immunostaining was performed with MF20 and β-Gal antibodies to detect CM and CPC respectively. Cell size measurements (μm^2) were based on average cell size of CMs. No significant difference between control and treatment groups. N=4-5 experiments. 20 cells were measured per treatment for each experiment. One-way ANOVA and Tukey's multiple comparison test.

3.11 ISO and Carvedilol treatments alter gene expression of some differentiation markers in embryonic ventricular cell cultures

Primary embryonic E11.5 ventricular cell cultures were treated with agonists and antagonists to determine the effects on cell differentiation. Cells were treated with ISO [1μM], Carv [10μM], and a combination of ISO+Carv [1μM+10μM] and RT-qPCR analysis was performed to determine the effects on cell differentiation markers including CATA4, Hand2, Mef2c, TBX5. These are genes coding for transcription factors, which are known to be associated with cardiac development and are known to play a role in CM differentiation. Final concentration of DMSO in cell culture media for control and treatment groups was kept at 0.03%. Based on the results, cells treated with ISO and carvedilol revealed no significant changes in the relative expression of GATA4, Mef2c, and TBX5 **(Figure 3.15A, 3.15C, 3.15D).** The relative expression of Hand2 resulted in a significant decrease when cells were treated with ISO, carvedilol, and a combination of ISO+Carv in comparison to the untreated group **(Figure 3.15B).**

RT-qPCR analysis was also performed to determine the effects of ISO and carvedilol on cell differentiation markers including ANP, Cx40, and HCN4, which are known to be associated with development of the cardiac conduction system (Govindapillai et al., 2018). Based on the results, cells treated with ISO and carvedilol revealed no significant changes in the relative expression of ANP and HCN4 **(Figure 3.16A and 3.16C).** The relative expression of Cx40 resulted in a significant increase when cells were treated with ISO compared to untreated control cultures **(Figure 3.16B).**

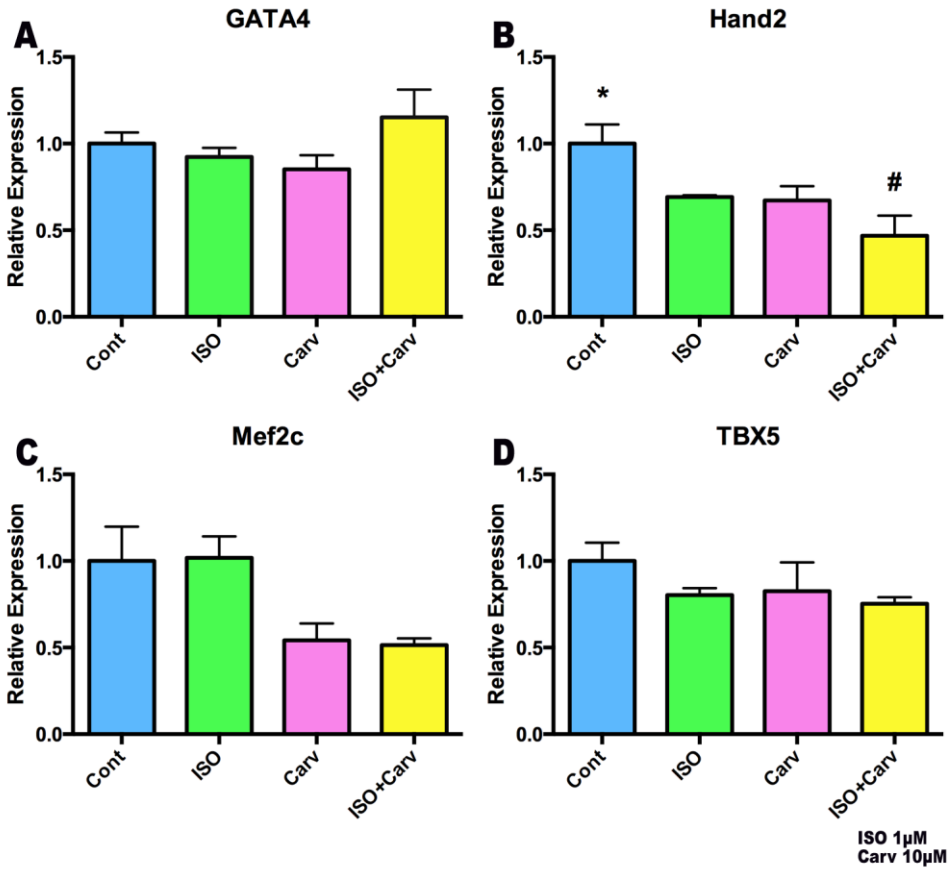

Figure 3.15: RT-qPCR analysis of gene expression of cell differentiation markers in E11.5 mouse ventricular cells treated with Isoproterenol (ISO) and carvedilol (Carv). E11.5 ventricular cells were treated with ISO [1μM], Carv [10μM], and ISO+Carv [1μM+10μM] and RNA was extracted. RT-qPCR was performed using primers for various cell differentiation markers. Levels of control were set as 1.0 in all panels. GAPDH was used as the house keeping gene for normalization of gene expression. **A, C, D)** No significant difference between control and treatment groups. **B)** * $P < 0.05$ Cont Vs. ISO; Cont Vs. Carv. * < P 0.005 Cont Vs. ISO+Carv. Each bar represents mean ± SEM, N=3 independent RNA extractions/treatment, analyzed in duplicates for each extraction. One-way ANOVA with Tukey's multiple comparison test.

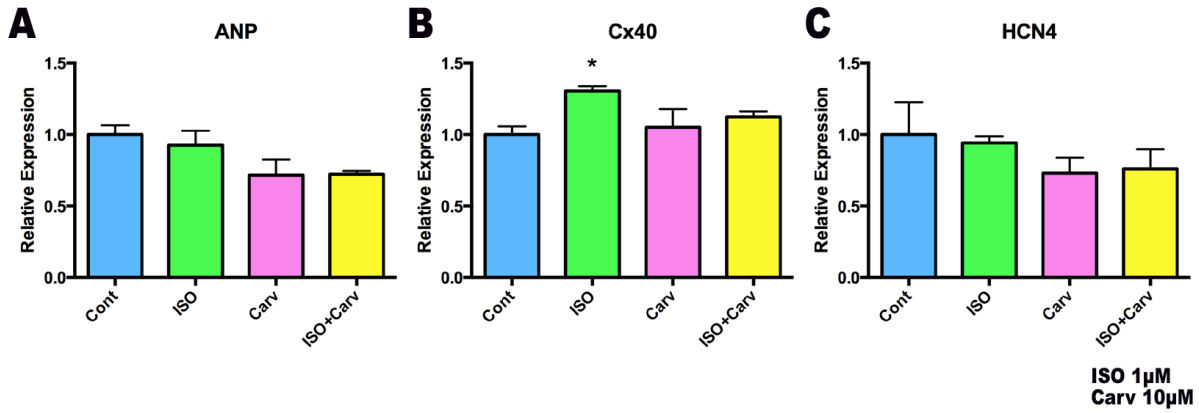

Figure 3.16: RT-qPCR analysis of gene expression of cell differentiation markers in E11.5 mouse ventricular cells treated with Isoproterenol (ISO) and carvedilol (Carv). E11.5 ventricular cells were treated with ISO [1µM], Carv [10µM], and ISO+Carv [1µM+10µM] and RNA was extracted. RT-qPCR was performed using primers for various cell differentiation markers. Levels of control were set as 1.0 in all panels. GAPDH was used as the house keeping gene for normalization of gene expression. **A, C)** No significant difference between control and treatment groups. **B)** * $P < 0.05$ Cont Vs. ISO. Each bar represents mean ± SEM, N=3 independent RNA extractions/treatment, analyzed in duplicates for each extraction. One-way ANOVA with Tukey's multiple comparison test.

Chapter 4: Discussion

4.1 Summary of Results

The expression profiles α1-AR subtypes during cardiac ontogeny are unknown and there is scant information on whether these receptors play any role in the regulation of cell proliferation and differentiation. Thus, the overall aim of this study was to determine the role of adrenergic receptor signaling in embryonic ventricular cell proliferation and differentiation. Additionally, it is unknown whether these receptors play any role in cell size regulation of embryonic ventricular cells.

In the present study, the mRNA and protein expression profiles of α1-AR subtypes (α1A, α1B, α1D) were characterized along with the relative expression of the three subtypes during ventricular development across several embryonic through neonatal and adult stages. Subsequent experiments focused on the subcellular localization of α1-AR subtypes in embryonic E11.5 ventricular cells using extracellular domain specific antibodies. Second messenger responses in embryonic ventricular cells were examined in the presence or absence of adrenergic agonists and antagonists. Additionally, the effect of adrenergic agonists and antagonists on embryonic ventricular cell proliferation and differentiation were examined.

It is unknown whether certain α1-AR targeted medications used for the treatment of heart failure (e.g. carvedilol), hypertension (e.g. prazosin) or common cold (e.g. phenylephrine) have an effect on embryonic cell proliferation and differentiation and donor cell transplantation. This area of study is of interest as new research is focused on the use of pluripotent stem cell derived CPCs and CMs for

regenerative therapies in cardiovascular patients (Menasche et al., 2015; Shiba et al., 2012). Recent studies revealed that a calcium channel blocking drug, nifedipine can inhibit proliferation and differentiation of CPCs and CMs in vitro and significantly decrease graft size post intracardiac cell transplantation (Hotchkiss et al., 2014). In another study, metoprolol (β1-AR blocker) was shown to rescue the inhibitory effects of ISO on embryonic ventricular cell proliferation and intracardiac graft formation (Feridooni et al., 2017). Therefore, it is also important to characterize whether drugs targeting α1-ARs or both α- and β-ARs will have any effect on these cells, as some of these medications are typically prescribed to patients with heart failure and other diseases as well as during pregnancy.

The embryonic E11.5 developmental stage was used in this study for experiments, as CPCs have not committed to a cardiac lineage. Approximately 40% of ventricular cells contain undifferentiated CPCs at this stage, which can differentiate into cardiomyocytes (McMullen et al., 2009; Zhang et al., 2015). Taken together, the information from this study could provide additional insight into the safe usage of non-selective adrenergic receptor blockers during pregnancy and cell transplantation studies.

4.2 Examination of gene expression profiles of α1-AR subtypes (α1A, α1B, α1D) during cardiac development

The heart contains two main ARs, β1-ARs, which account for 90% of ARs in the heart, and α1-ARs, accounting for 10% of ARs (O'Connell et al., 2014), however there is limited information regarding the expression profiles of α1-AR subtypes during

cardiac ontogeny. In this study, we found that the mRNA levels of α1-AR subtypes generally increase during cardiac development. The α1A subtype gene expression levels remained low through most of development with a significant increase during the adult stage. The α1B and α1D subtype gene expression levels also increased through development, with levels spiking at the neonatal stage, followed by a decrease in the adult stage. Changes in the relative expression of α1-ARs suggest that the receptors are required for postnatal development.

Postnatal cardiac development is a time of physiologic heart growth where cardiac hypertrophy is occurring. Following the early postnatal period, normal physiological myocyte hypertrophy occurs, which is intended to increase heart size in order to maintain cardiac output. Subtype α1A and α1B knock out studies conducted by O'Connell et al. resulted in smaller hearts suggesting that α1-AR are required for cardiac hypertrophy during postnatal development (O'Connell et al., 2003).

The mRNA expression profiles of α1-AR subtypes may vary with regards to the actual levels of proteins present in the heart. It is suggested that α1A and α1B subtype receptor proteins are expressed in adult CMs, and that the α1B subtype is predominant. Additionally it is suggested that the α1D subtype may only be expressed in coronary vasculature (O'Connell et al., 2014). This notion may explain the resulting lower levels of α1D mRNA expression compared to other subtypes observed in this study. Both α1A and α1B expressed higher levels of mRNA in the adult stage compared to the α1D subtype, which might correspond with the levels of receptor proteins in the heart as suggested by the literature. Our gene expression results also revealed that the α1B subtype was predominant among the three

subtypes in the heart throughout development, which is also in line with the literature for the postnatal gene expression of these receptor subtypes (O'Connell et al., 2014).

4.3 Western Blot Analysis

Western blot analysis was conducted using ventricular tissue extracts from multiple developmental stages (E11.5 – adult) to detect the presence of α1-AR subtype proteins. Based on the results, α1-AR subtype proteins were present in large quantities in the cytosol. Multiple protein isoforms observed with α1A specific antibodies may represent products of alternate splice variants as previously reported for human α1A receptor subtype (Chang et al., 1998). The α1A and α1B subtype proteins were also present in the membrane fractions of E16.5, neo and adult stages whereas α1D was not detected in the membrane fractions. Although sufficient membrane proteins could not be derived from E11.5 ventricular samples, the western blotting results from other developmental stages are consistent with immunostaining results from primary cultures of E11.5 ventricular cells. The α1A, α1B, and α1D subtypes were localized in the cytoplasm as well as the membrane compartments of E11.5 ventricular cells. These findings are consistent with the literature, which suggests that the α1-ARs are localized to the inner nuclear membrane, where second messenger responses are initiated and carry on downstream signaling in the cytoplasm (Wu et al., 2014).

Western blot analysis results suggested a progressive increase in the α1B protein levels from E11.5 to adult stage, while the levels of α1D remained relatively

constant in all stages of ventricular development. However, these results need to be confirmed by increasing the number of experiments and performing quantitative densitometric analysis. Nonetheless, these results are consistent with a previous report which revealed no developmental differences in the overall binding affinities of a radiolabeled non-selective α1-AR ligand in the rat ventricular myocardium from fetal to adult stages (Schaffer & Williams, 1986). However, this study found a higher number of α1-ARs in the membrane fraction of fetal rat hearts compared to the adult heart and suggested that α1-ARs play a critical role in the promotion of growth during early developmental stages of the heart (Schaffer & Williams, 1986).

There is evidence that the concentrations of α1-ARs and β-ARs shift with age. It has been shown that in canine cardiac membranes, the density of α1-ARs decreases during maturation from fetal and neonatal stages to adult. Buchthal, Bilezikian, and Danilo conducted radioligand binding experiments with [^{125}I]-IBE 2254 in canine cardiac membranes (Buchthal et al., 1987). They determined that the density of α1-ARs decreases during maturation from fetal and neonatal stages to adult (Buchthal et al., 1987).

4.4 Examination of the subcellular localization of α1-AR subtypes in embryonic ventricular cells

α1-AR subtype specific antibodies were used to determine the subcellular localization of adrenergic receptors in embryonic ventricular cells. All three receptor subtypes were predominantly localized in the cytoplasm and nuclear compartments when compared to the plasma membrane localization in E11.5 ventricular cells. The prevalent view is that α1-AR GPCRs are localized to the plasma membrane however

novel models now suggest that some receptors may be localized to the nucleus, exhibiting a novel signaling mechanism. This model suggests that the α1-ARs are localized to the inner nuclear membrane, where second messenger responses are initiated and carry on downstream signaling in the cytoplasm (Dahl et al., 2018; O'Connell et al., 2014; Wright et al., 2008).

It is suggested that α1A, α1B, and α1D subtypes are present in adult hearts however only α1A and α1B are present in adult cardiomyocytes (O'Connell et al., 2003). Studies conducted by Wright and colleagues confirmed that α1A and α1B subtypes were localized to the nucleus in adult cardiomyocytes (Huang et al., 2007; Wright et al., 2008). When these studies were conducted, there was a lack of α1-AR subtype specific antibodies. These researchers developed adenoviral vectors expressing α1-AR–green fluorescent protein (GFP) fusion proteins and confirmed the nuclear localization of these receptor subtypes by transducing myocytes from α1A and α1B double knockout (ABKO) mice. However, these studies do not exclude the possibility that inactive α1-ARs also reside unoccupied at the plasma membrane (Huang et al., 2007). The prevalent view still remains that α1-ARs are localized to the plasma membrane in the heart and of adult CMs based on binding assays, radioligand binding to membrane fractions, and α1-AR antibody studies (O'Connell et al., 2014).

Results from our study suggest that α1A, α1B, and α1D subtypes are localized to the nucleus and the cytoplasm in embryonic ventricular cells. This corresponds with literature, which also suggested that α1-AR subtypes α1A and α1B are localized to the nucleus, although the literature does not support our finding of the nuclear localization of the α1D subtype. The literature suggests that the α1D subtype is

present and functional in coronary artery smooth muscle cells (O'Connell et al., 2014). Our results suggest that the α1D subtype is also present in CMs and CPCs. However, this difference could be attributed to studies in adult cardiac cells versus our studies, which used embryonic ventricular cells.

One interesting result from examining the subcellular localization of α1-ARs was that the receptors also co-localized with sarcomeric myosin. Both α1A and α1D subtypes were clearly present along CM sarcomeres. Filamin is an actin cross-linking cytoskeletal protein known to interact with GPCRs. Tirupula et al. (2015) suggested that GPCRs involved in cardiac physiology may contain a filamin A binding motif, which binds and activates filamin A. Binding of the α1D specific filamin binding motif by a filamin A surrogate (filamin A Ig16-24) was shown to trigger the phosphorylation of filamin by cellular protein kinases (Tirupula et al., 2015). Filamin is also found on the sarcomere borders and in the intercalated disks between cardiomyocytes (Koteliansky et al., 1986). Filamin A null mice die in the early embryonic or perinatal stages due to severe cardiovascular abnormalities (Feng et al., 2006). The suggested interaction of filamin A with α1D receptors may provide an explanation for the co-localization of α1A and α1D receptors with sarcomeric myosin and further work is needed to confirm the significance of these interactions in CMs.

Zhang et al. also suggested an interaction between α1-ARs and filamin (Zhang et al., 2004). Their experiments were conducted using yeast-two hybrid assays to screen for proteins that interact with α1-ARs. Screening identified filamin C as a binding partner with the C terminus of α1-ARs. Filamin C is known to interact only with myocardiac muscles and the cytoskeleton of skeletal muscles, a characteristic

different from filamin A and filamin B. The interaction between α1-ARs and filamin C suggests that filamin C plays an important role in cellular signaling and localization of α1-ARs. However, functional significance of these interactions has not been explored in mammalian cells (Zhang et al., 2004).

4.5 Characterizing the effects of second messenger responses in embryonic ventricular cells

cAMP assays were conducted to determine second messenger responses following treatment with carvedilol and isoproterenol. β-AR GPCRs bind to G_s stimulatory proteins when activated, which leads to increased levels of cAMP following stimulation. Since carvedilol has α1-AR and β-AR blocking activity, we first examined the effects of carvedilol and ISO on cAMP levels. Results from this assay revealed significant increases in cAMP levels induced by ISO. Additionally, when ISO was combined with 10μM of carvedilol, cAMP levels were similar to the basal untreated group. This suggests that carvedilol is capable of blocking β1-ARs at a dose of 10μM. Cells treated with different concentrations of carvedilol (0.1μM, 1μM and 10μM) in the absence of ISO did not significantly alter the levels of cAMP compared to control. This suggests that when administered alone, carvedilol has no affect on cAMP levels within cells.

A study conducted by Feridooni et al. observed that E11.5 ventricular cells treated with 1μM ISO resulted in significant increases in cAMP concentrations compared to basal untreated groups (Feridooni et al., 2017). Another study conducted by Andreka et al. observed that ISO increased levels of cAMP following

treatment of rat myocardial tissue (Andreka et al., 2002). This suggests that the β-ARs are coupled to adenylyl cyclase. Additionally, carvedilol had no affect on cAMP levels in myocardial tissue (Andreka et al., 2002). These findings are in accordance with our findings that when administered alone, carvedilol did not affect levels of cAMP.

A study conducted by Maack et al. explored the effects of carvedilol on subsarcolemmal cAMP (Maack C. et al., 2013). They found that when carvedilol was incubated with human atrial trabeculae (muscular columns) prior to exposure of NE, carvedilol did not prevent the force of contraction induced by NE, however it did prevent the decay in the force of contraction. Phosphodiesterase 4 (PDE4) is an enzyme that degrades the phosphodiester bond in cAMP in order to regulate signal transduction. PDE4 is known to be associated with β1-ARs at high concentrations to control levels of subsarcolemmal cAMP, and dissociates in the presence of NE. Additionally, researchers found that treatment with carvedilol facilitated the dissociation of PDE4 from β1-ARs. Contrary to our findings, these results suggest that carvedilol potentiated subsarcolemmal cAMP while maintaining contractility following administration of NE. This mechanism may provide an explanation for how carvedilol maintains NE contractility, without upregulating the density of β1-ARs (Maack C. et al., 2013).

Our study also explored the effect of phenylephrine (α1-AR agonist) on inositol monophosphate (IP1) levels within embryonic ventricular cells. IP3 is a second messenger released following the activation of α1-AR Gq-coupled GPCRs. IP3 induces the release of calcium from intracellular stores and is then rapidly degraded

to IP2, and then IP1 (Garbison et al., 2004). As a result, it is easier to measure levels of IP1 within cells.

We tested the effect of PE on IP1 levels in various cell densities ranging from 40,000 to 80,000 cells. Cells treated with 10μM PE resulted in increased levels of IP1 compared to untreated controls, although the fold increase was minimal. PE only had a significant affect on IP1 levels at cell densities of 50,000, 60,000, and 80,000 cells suggesting that the effect of PE on IP1 levels is dependent on cell density.

In comparison, our results from cAMP assays revealed that ISO was capable of inducing a significant response with as little as 5000 cells, which resulted in a large fold increase in cAMP levels. These results suggest that there is a significant difference in response between α1-ARs and β1-ARs within embryonic ventricular cells. This difference could be attributed to the difference in relative abundance of the receptors. In the postnatal heart, it is known that β1-ARs account for 90% of adrenergic receptors while α1-ARs only account for 10% (O'Connell et al., 2014). Our experiments suggest that β1-ARs are also predominant at the embryonic stage.

4.6 Examination of the effects of adrenergic receptor agonists and antagonists on embryonic ventricular cell proliferation

Adrenergic receptor agonists and antagonists were used to determine the effect on NCRL embryonic E11.5 ventricular cell proliferation. It is unknown whether different adrenergic receptor blockers negatively affect cell proliferation of embryonic ventricular cells. Carvedilol and ISO were used to determine the role of β1-ARs on cell proliferation of CMs and CPCs. Cells were treated with carvedilol in the

presence or absence of ISO and cell counts were conducted to determine the percentage of CMs and CPCs present. Additionally, Click-iT EdU was used to identify cell proliferation of CMs and CPCs determined by the presence of EdU^+ labeled cells.

Cells treated with ISO, carvedilol, and a combination of ISO and carvedilol resulted in no significant difference in the percentage of CMs and CPCs compared to untreated cells. Additionally, results from Click-iT EdU cell proliferation assay revealed that carvedilol and ISO did not affect cell proliferation of CMs and CPCs. These results also suggest that carvedilol blockade of α1-ARs does not affect cell proliferation of embryonic ventricular cells.

A study conducted by Feridooni et al. found that there was a significant decrease in the number of E11.5 ventricular cells treated with ISO. Feridooni et al. also showed that cotreatment with metoprolol (selective β1-AR antagonist) abrogated the antiproliferative effect of ISO. Additionally, it was determined that catecholamine stimulation of β-ARs arrests cells in the G_1/S phase transition, resulting in decreased cell proliferation (Feridooni et al., 2017).

The present study resulted in a lower percentage of proliferating CPCs compared to E11.5 ventricular cell proliferation results from Feridooni et al. Our results showed that the average percentage of proliferating CPCs in the untreated group was 25% compared to approximately 55% (proliferating CPCs) in the study conducted by Feridooni et al. The differences in results between the studies could be attributed to methodology. Our studies utilized the Click-iT EdU proliferation assay, which had not been used in the lab prior to this study. Feridooni and colleagues conducted proliferation studies using tritiated [^{3}H]thymidine labeling. Perhaps

differing results could be attributed to cells having a reduced sensitivity to the Click-iT EdU assay.

Another notable difference in results could be attributed to the presence of DMSO. Carvedilol stock was prepared in DMSO, therefore DMSO was added to ISO and control groups. Subsequently, additional experiments were conducted with ISO and control groups without the addition of DMSO.

Results revealed that ISO significantly decreased EdU^+ CPCs compared to untreated groups. These results are in accordance with results from Feridooni et al. (2017). Additionally, our results showed that the average percentage of EdU^+ CPCs (approximately 35%) from control groups (no DMSO) was lower than the percentage of $[^3H]^+$ CPCs (approximately 55%) reported by Feridooni et al. (2017). Again, differing results could be attributed to the methodology used for identifying cell proliferation (Click-iT EdU Vs. $[^3H]$ thymidine).

α1-AR agonist, phenylephrine and α1-AR antagonist, prazosin were used to determine the effect of α1-ARs on CM and CPC cell proliferation in NCRL embryonic E11.5 ventricular cells. Results suggested that there was no significant difference between control and treatment groups. Contrary to these findings, Li et al. found that PE stimulation of day 7 (post-differentiation) $Nkx2.5^+$ CPCs in murine induced pluripotent stem cell (miPSC) cultures led to a significant increase in BrdU incorporation compared to control cultures (Li et al., 2017). BrdU incorporation is measured to determine cell proliferation, therefore this result suggests that PE treatment may lead to an increase in CPC proliferation (Li et al., 2017).

Li et al. also found that PE stimulation of day 15 CMs did not have any effect on cell proliferation, which is in accordance with our results (Li et al., 2017). Interestingly, their study found that PE stimulation of α1-AR in undifferentiated miPSC cultures resulted in a significant decrease in the proportion of cells undergoing S-phase compared to the controls. Based on these findings, it appears that the effects of α1-AR signaling on cell proliferation may vary depending on the differentiation status of miPSC cultures (Li et al., 2017).

There are some differences to acknowledge between this study and the study conducted by Li et al. The study conducted by Li and colleagues used $Nkx2.5^{+}$ miPSC whereas this study used $Nkx2.5^{+}$ ventricular cells. Additionally, results from Li et al. were from day 7 $Nkx2.5^{+}$ CPCs, however this does not guarantee that all cells in the population are CPCs. Zhang and Pasumarthi conducted a study to identify the different cell populations in embryonic E11.5 mouse ventricular myocardial cells. Results from the study identified three different cell populations including undifferentiated cells, moderately differentiated cells, and mature cardiomyocytes (Zhang & Pasumarthi, 2007). To account for the presence of different cell populations, our study used MF20 immunostaining to distinguish between CMs and $Nkx2.5^{+}$ CPC cells, whereas the study conducted by Li et al. did not confirm the differentiation status of CPCs. However, it would be important to examine the effects of PE and prazosin on cell proliferation using early or later stages of embryonic ventricular cell cultures.

4.7 Examination of the effects of adrenergic receptor agonists and antagonists on embryonic ventricular cell differentiation

It is unknown whether different adrenergic receptor blockers negatively affect cell differentiation of embryonic ventricular cells. It is suggested that α1-ARs are required for hypertrophic growth. Studies have shown that double knockouts for α1A and α1B subtypes resulted in reduced heart and cardiomyocyte size during postnatal development (O'Connell et al. 2014). Additionally, results from α1-AR knockout studies conducted by O'Connell et al. suggest that the α1B subtype is required during postnatal cardiac development for hypertrophic growth (O'Connell et al. 2014).

Primary NCRL embryonic E11.5 ventricular cell cultures were treated with agonists and antagonists to determine the affect on cell differentiation. Cells were treated with carvedilol in the presence or absence of ISO and CM cell sizes were measured using a colour subtractive image analysis method previously described by (Gaspard & Pasumarthi, 2008). Results from this study suggested that carvedilol and ISO had no affect on CM size. Notably, RT-qPCR data for candidate differentiation markers revealed that ISO treatment could significantly increase Cx40 gene expression whereas both ISO and Carv treatments can significantly decrease Hand2 gene expression in E11.5 ventricular cultures. Cx40 is expressed in conduction system cells and vascular endothelial cells (Govindapillai et al., 2018; Miquerol et al., 2004).

Our second messenger analysis results in this study as well as previous studies (Feridooni et al., 2017) showed that ISO could increase cAMP levels in embryonic ventricular cells. Thus, the effect of ISO on Cx40 gene expression is in

agreement with a recent report which showed that activation of cAMP signaling can promote generation of conduction system cells in ESC cultures (Tsai et al., 2015). Hand2 is a transcription factor, which is required for the development of the right ventricle as well as for successful reprogramming of fibroblasts into cardiomyocytes (McFadden et al., 2005; Song et al., 2012). Given the inhibitory effects on Hand2 expression in this study, additional studies are required to validate the functional status of embryonic ventricular cells treated with drugs acting on adrenergic receptors. However, it is important to note that drugs acting on α1-ARs (carvedilol, PE and prazosin) did not reveal any significant effects on the cell numbers, EdU labeling or relative proportion of CPCs and CMs when compared to those parameters in control cultures.

Li et al. treated miPSC with epinephrine (Epi) to determine if activation of adrenergic receptors affects CM differentiation (Li et al., 2017). Their findings suggested that Epi enhances CM differentiation through α1-AR signaling. Contrary to our findings, Li et al. demonstrated that PE also stimulated differentiation of miPSC by performing western blot analysis for the expression levels of cardiac-specific markers such as cTnT, α-actinin, Nkx2.5 and GATA4 (Li et al., 2017).

A study conducted by Lehmann and colleagues (2013) used embryonic stem cell cultures and demonstrated that pharmacological blockade of α-ARs and β-ARs resulted in delayed differentiation of embryonic stem cells toward CMs. Although our study showed differences in gene expression of differentiation markers, there were no significant differences in the relative percentages of CPCs and CMs in cultures treated with or without AR blockers. Differences in results between this study and the

studies conducted by Li et al. and Lehmann et al. could be attributed to methodological differences. The α1-AR antagonist used in our study was carvedilol whereas Lehmann et al. applied phentolamine (a non-selective α1- and α2-AR blocker). Additionally, their experiments were conducted using embryonic stem cell cultures whereas our study conducted experiments on embryonic ventricular cells (Lehmann et al., 2013).

4.8 Limitations and Future Directions

The findings in this thesis indicate that all three α1-AR subtypes are expressed in embryonic ventricular cells and remain present throughout cardiac ontogeny. It was also determined that carvedilol and prazosin had no affect on embryonic ventricular cell proliferation. Both ISO and Carv had inhibitory effects on Hand2 gene expression. Results from this study suggested that α1-ARs co-localize with sarcomeric myosin, however significance of this observation needs to be further examined in detail. Future work needs to be done to characterize the interaction of these receptors with sarcomeric myosin. Additional research is required to determine the functional attributes of embryonic CMs and CPCs treated with AR blockers in vivo. This can be accomplished through monitoring intracellular calcium transients using Fura-2 and a RatioMaster fluorescence microscopy. Contractile properties of CMs after treatment with different adrenergic drugs can also be determined using a microelectrode array system. Furthermore, the effects of carvedilol on intracardiac cell transplantation remain to be determined.

4.9 Conclusion

Results from this thesis provide some insights into treatment options for patients with HF for combining drugs acting on ARs with cell therapies. New research suggests that CPCs can give rise to three different cell types within the heart, including cardiomyocytes, smooth muscle cells, and endothelial cells, making CPCs ideal for cell transplantation for patients with HF. However, it remains unknown whether different non-selective adrenergic blocking drugs affect these cells. Therefore, results from this study may provide additional information on the potential safe usage of non-selective adrenergic receptor blockers with cell transplantation studies. Additionally, results from this thesis demonstrated that carvedilol and prazosin had no effects on embryonic ventricular cell proliferation, however, inhibitory effects of carvedilol on Hand2 gene expression needs further investigation. These results are also relevant for usage of carvedilol in women who are pregnant.

References

Allen, L. F., Lefkowitz, R. J., Caron, M. G., & Cotecchia, S. (1991). G-protein-coupled receptor genes as protooncogenes: constitutively activating mutation of the alpha 1B-adrenergic receptor enhances mitogenesis and tumorigenicity. *Proc Natl Acad Sci U S A, 88*(24), 11354-11358.

Alonso-Llamazares, A., Zamanillo, D., Casanova, E., Ovalle, S., Calvo, P., & Chinchetru, M. A. (1995). Molecular cloning of alpha 1d-adrenergic receptor and tissue distribution of three alpha 1-adrenergic receptor subtypes in mouse. *J Neurochem, 65*(6), 2387-2392.

Andreka, P., Aiyar, N., Olson, L. C., Wei, J. Q., Turner, M. S., Webster, K. A., . . . Bishopric, N. H. (2002). Bucindolol displays intrinsic sympathomimetic activity in human myocardium. *Circulation, 105*(20), 2429-2434.

Arkin, M. R., Connor, P. R., Emkey, R., Garbison, K. E., Heinz, B. A., Wiernicki, T. R., . . . Sittampalam, S. (2004). FLIPR Assays for GPCR and Ion Channel Targets. In G. S. Sittampalam, N. P. Coussens, K. Brimacombe, A. Grossman, M. Arkin, D. Auld, C. Austin, J. Baell, B. Bejcek, T. D. Y. Chung, J. L. Dahlin, V. Devanaryan, T. L. Foley, M. Glicksman, M. D. Hall, J. V. Hass, J. Inglese, P. W. Iversen, S. D. Kahl, S. C. Kales, M. Lal-Nag, Z. Li, J. McGee, O. McManus, T. Riss, O. J. Trask, Jr., J. R. Weidner, M. Xia, & X. Xu (Eds.), *Assay Guidance Manual*. Bethesda (MD).

Boehm, S., & Huck, S. (1995). alpha 2-Adrenoreceptor-mediated inhibition of acetylcholine-induced noradrenaline release from rat sympathetic neurons: an action at voltage-gated Ca2+ channels. *Neuroscience, 69*(1), 221-231.

Buchthal, S. D., Bilezikian, J. P., & Danilo, P., Jr. (1987). Alpha 1-adrenergic receptors in the adult, neonatal, and fetal canine heart. *Dev Pharmacol Ther, 10*(2), 90-99.

Cannesson, M., Jian, Z., Chen, G., Vu, T. Q., & Hatib, F. (2012). Effects of phenylephrine on cardiac output and venous return depend on the position of the heart on the Frank-Starling relationship. *J Appl Physiol (1985), 113*(2), 281-289. doi:10.1152/japplphysiol.00126.2012

Capote, L., Nyakundi, R., Martinez, B., & Lumperopoulos, A. (2015). *Pathophysiology of Heart Failure* P. B. Gowraganahalli Jagadeesh, Khin Maung-U (Ed.) *Pathophysiology and Pharmacotherapy of Cardiovascular Disease* doi: 10.1007/978-3-319-15961-4

Chang, D. J., Chang, T. K., Yamanishi, S. S., Salazar, F. H., Kosaka, A. H., Khare, R., . . . Chan, H. W. (1998). Molecular cloning, genomic characterization and expression of novel human alpha1A-adrenoceptor isoforms. *FEBS Lett, 422*(2), 279-283.

Cotecchia, S., Del Vescovo, C. D., Colella, M., Caso, S., & Diviani, D. (2015). The alpha1-adrenergic receptors in cardiac hypertrophy: signaling mechanisms and functional implications. *Cell Signal, 27*(10), 1984-1993. doi:10.1016/j.cellsig.2015.06.009

Crespo, M. J. (2000). Interaction between AT1 and alpha1-adrenergic receptors in cardiomyopathic hamsters. *J Card Fail, 6*(3), 257-263. doi:10.1054/jcaf.2000.9672

Cui, W., Taub, D. D., & Gardner, K. (2007). qPrimerDepot: a primer database for quantitative real time PCR. *Nucleic Acids Res, 35*(Database issue), D805-809. doi:10.1093/nar/gkl767

Dahl, E. F., Wu, S. C., Healy, C. L., Harsch, B. A., Shearer, G. C., & O'Connell, T. D. (2018). Subcellular Compartmentalization of proximal Galphaq-receptor signaling produces unique hypertrophic phenotypes in adult cardiac myocytes. *J Biol Chem*. doi:10.1074/jbc.RA118.002283

Delorme, B., Dahl, E., Jarry-Guichard, T., Marics, I., Briand, J. P., Willecke, K., . . . Theveniau-Ruissy, M. (1995). Developmental regulation of connexin 40 gene expression in mouse heart correlates with the differentiation of the conduction system. *Dev Dyn, 204*(4), 358-371. doi:10.1002/aja.1002040403

Desjardins, C. A., & Naya, F. J. (2016). The Function of the MEF2 Family of Transcription Factors in Cardiac Development, Cardiogenomics, and Direct Reprogramming. *J Cardiovasc Dev Dis, 3*(3). doi:10.3390/jcdd3030026

FDA. (2005). Carvedilol. Retrieved from https://www.accessdata.fda.gov/drugsatfda_docs/label/2005/020297s013lbl.pdf

FDA. (2006). Metoprolol Succinate. Retrieved from https://www.accessdata.fda.gov/drugsatfda_docs/label/2006/019962s032lbl.pdf

Felder, R. A., Calcagno, P. L., Eisner, G. M., & Jose, P. A. (1982). Ontogeny of myocardial adrenoceptors II. Alpha adrenoceptors. *Pediatr Res, 16*(5), 340-342.

Feng, Y., Chen, M. H., Moskowitz, I. P., Mendonza, A. M., Vidali, L., Nakamura, F., . . . Walsh, C. A. (2006). Filamin A (FLNA) is required for cell-cell contact in vascular development and cardiac morphogenesis. *Proc Natl Acad Sci U S A, 103*(52), 19836-19841. doi:10.1073/pnas.0609628104

Feridooni, T., Hotchkiss, A., Baguma-Nibasheka, M., Zhang, F., Allen, B., Chinni, S., & Pasumarthi, K. B. S. (2017). Effects of beta-adrenergic receptor drugs on embryonic ventricular cell proliferation and differentiation and their impact on donor cell transplantation. *Am J Physiol Heart Circ Physiol, 312*(5), H919-H931. doi:10.1152/ajpheart.00425.2016

Florea, V. G., & Cohn, J. N. (2014). The autonomic nervous system and heart failure. *Circ Res, 114*(11), 1815-1826. doi:10.1161/CIRCRESAHA.114.302589

Fu, S., Zhuo, R., Yao, M., Zhang, J., Zhou, H., & Xiao, J. (2013). MicroRNA basis of physiological hypertrophy. *Front Genet, 4*, 253. doi:10.3389/fgene.2013.00253

Garbison, K. E., Heinz, B. A., & Lajiness, M. E. (2004). IP-3/IP-1 Assays. In G. S. Sittampalam, N. P. Coussens, K. Brimacombe, A. Grossman, M. Arkin, D. Auld, C. Austin, J. Baell, B. Bejcek, T. D. Y. Chung, J. L. Dahlin, V. Devanaryan, T. L. Foley, M. Glicksman, M. D. Hall, J. V. Hass, J. Inglese, P. W. Iversen, S. D. Kahl, S. C. Kales, M. Lal-Nag, Z. Li, J. McGee, O. McManus, T. Riss, O. J. Trask, Jr., J. R. Weidner, M. Xia, & X. Xu (Eds.), *Assay Guidance Manual*. Bethesda (MD).

Garcia-Frigola, C., Shi, Y., & Evans, S. M. (2003). Expression of the hyperpolarization-activated cyclic nucleotide-gated cation channel HCN4 during mouse heart development. *Gene Expr Patterns, 3*(6), 777-783.

Gaspard, G. J., & Pasumarthi, K. B. (2008). Quantification of cardiac fibrosis by colour-subtractive computer-assisted image analysis. *Clin Exp Pharmacol Physiol, 35*(5-6), 679-686. doi:10.1111/j.1440-1681.2008.04930.x

Giovannitti, J. A., Jr., Thoms, S. M., & Crawford, J. J. (2015). Alpha-2 adrenergic receptor agonists: a review of current clinical applications. *Anesth Prog, 62*(1), 31-39. doi:10.2344/0003-3006-62.1.31

Gonzalez-Cabrera, P. J., Shi, T., Yun, J., McCune, D. F., Rorabaugh, B. R., & Perez, D. M. (2004). Differential regulation of the cell cycle by alpha1-adrenergic receptor subtypes. *Endocrinology, 145*(11), 5157-5167. doi:10.1210/en.2004-0728

Govindapillai, A., Hotchkiss, A., Baguma-Nibasheka, M., Rose, R. A., Miquerol, L., Smithies, O., . . . Pasumarthi, K. B. S. (2018). Characterizing the role of atrial natriuretic peptide signaling in the development of embryonic ventricular conduction system. *Sci Rep, 8*(1), 6939. doi:10.1038/s41598-018-25292-0

Hawrylyshyn, K. A., Michelotti, G. A., Coge, F., Guenin, S. P., & Schwinn, D. A. (2004). Update on human alpha1-adrenoceptor subtype signaling and genomic organization. *Trends Pharmacol Sci, 25*(9), 449-455.

Hotchkiss, A., Feridooni, T., Zhang, F., & Pasumarthi, K. B. (2014). The effects of calcium channel blockade on proliferation and differentiation of cardiac progenitor cells. *Cell Calcium, 55*(5), 238-251. doi:10.1016/j.ceca.2014.02.018

Huang, Y., Wright, C. D., Merkwan, C. L., Baye, N. L., Liang, Q., Simpson, P. C., & O'Connell, T. D. (2007). An alpha1A-adrenergic-extracellular signal-regulated kinase survival signaling pathway in cardiac myocytes. *Circulation, 115*(6), 763-772. doi:10.1161/CIRCULATIONAHA.106.664862

Ieda, M., Fu, J. D., Delgado-Olguin, P., Vedantham, V., Hayashi, Y., Bruneau, B. G., & Srivastava, D. (2010). Direct reprogramming of fibroblasts into functional cardiomyocytes by defined factors. *Cell, 142*(3), 375-386. doi:10.1016/j.cell.2010.07.002

Kim, E. K., & Choi, E. J. (2010). Pathological roles of MAPK signaling pathways in human diseases. *Biochim Biophys Acta, 1802*(4), 396-405. doi:10.1016/j.bbadis.2009.12.009

Koch-Weser, J., Graham, R. M., & Pettinger, W. A. (1979). Drug therapy. Prazosin. *N Engl J Med, 300*(5), 232-236. doi:10.1056/NEJM197902013000505

Koteliansky, V. E., Glukhova, M. A., Gneushev, G. N., Samuel, J. L., & Rappaport, L. (1986). Isolation and localization of filamin in heart muscle. *Eur J Biochem, 156*(3), 619-623.

Lehmann, M., Nguemo, F., Wagh, V., Pfannkuche, K., Hescheler, J., & Reppel, M. (2013). Evidence for a critical role of catecholamines for cardiomyocyte lineage commitment in murine embryonic stem cells. *PLoS One, 8*(8), e70913. doi:10.1371/journal.pone.0070913

Lei, B., Schwinn, D. A., & Morris, D. P. (2013). Stimulation of alpha1a adrenergic receptors induces cellular proliferation or antiproliferative hypertrophy dependent solely on agonist concentration. *PLoS One, 8*(8), e72430. doi:10.1371/journal.pone.0072430

Li, X. L., Zeng, D., Chen, Y., Ding, L., Li, W. J., Wei, T., . . . Zheng, Q. S. (2017). Role of alpha- and beta-adrenergic receptors in cardiomyocyte differentiation from murine-induced pluripotent stem cells. *Cell Prolif, 50*(1). doi:10.1111/cpr.12310

Lin, Q., Schwarz, J., Bucana, C., & Olson, E. N. (1997). Control of mouse cardiac morphogenesis and myogenesis by transcription factor MEF2C. *Science, 276*(5317), 1404-1407.

Liu, T. T., Ding, T. L., Ma, Y., & Wei, W. (2014). Selective alpha1B- and alpha1D-adrenoceptor antagonists suppress noradrenaline-induced activation, proliferation and ECM secretion of rat hepatic stellate cells in vitro. *Acta Pharmacol Sin, 35*(11), 1385-1392. doi:10.1038/aps.2014.84

Livak, K. J., & Schmittgen, T. D. (2001). Analysis of relative gene expression data using real-time quantitative PCR and the 2(-Delta Delta C(T)) Method. *Methods, 25*(4), 402-408. doi:10.1006/meth.2001.1262

Lymperopoulos, A., Rengo, G., & Koch, W. J. (2013). Adrenergic nervous system in heart failure: pathophysiology and therapy. *Circ Res, 113*(6), 739-753. doi:10.1161/CIRCRESAHA.113.300308

Maack C., Lee I., Molina C., Richter W., Wannenmacher N., Zimmer A., . . . Bohm M. (2013). Carvedilol sensitizes cardiac beta1-adrenergic receptors by increasing subsarcolemmal cAMP levels through ligand-induced dissociation of PDE4 from beta1-adrenergic receptors. *European Heart Journal,, 34*(1), 11. doi:10.1093/eurheartj/eht307.65

Madamanchi, A. (2007). Beta-adrenergic receptor signaling in cardiac function and heart failure. *Mcgill J Med, 10*(2), 99-104.

McFadden, D. G., Barbosa, A. C., Richardson, J. A., Schneider, M. D., Srivastava, D., & Olson, E. N. (2005). The Hand1 and Hand2 transcription factors regulate expansion of the embryonic cardiac ventricles in a gene dosage-dependent manner. *Development, 132*(1), 189-201. doi:10.1242/dev.01562

McMullen, N. M., Zhang, F., Hotchkiss, A., Bretzner, F., Wilson, J. M., Ma, H., . . . Pasumarthi, K. B. (2009). Functional characterization of cardiac progenitor cells and their derivatives in the embryonic heart post-chamber formation. *Dev Dyn, 238*(11), 2787-2799. doi:10.1002/dvdy.22112

Meidahl Petersen, K., Jimenez-Solem, E., Andersen, J. T., Petersen, M., Brodbaek, K., Kober, L., . . . Poulsen, H. E. (2012). beta-Blocker treatment during pregnancy and adverse pregnancy outcomes: a nationwide population-based cohort study. *BMJ Open, 2*(4). doi:10.1136/bmjopen-2012-001185

Meins, M., Henderson, D. J., Bhattacharya, S. S., & Sowden, J. C. (2000). Characterization of the human TBX20 gene, a new member of the T-Box gene family closely related to the Drosophila H15 gene. *Genomics, 67*(3), 317-332. doi:10.1006/geno.2000.6249

Menasche, P., Vanneaux, V., Hagege, A., Bel, A., Cholley, B., Cacciapuoti, I., . . . Larghero, J. (2015). Human embryonic stem cell-derived cardiac progenitors for severe heart failure treatment: first clinical case report. *Eur Heart J, 36*(30), 2011-2017. doi:10.1093/eurheartj/ehv189

Miquerol, L., Meysen, S., Mangoni, M., Bois, P., van Rijen, H. V., Abran, P., . . . Gros, D. (2004). Architectural and functional asymmetry of the His-Purkinje system of the murine heart. *Cardiovasc Res, 63*(1), 77-86. doi:10.1016/j.cardiores.2004.03.007

Molenaar, P., Christ, T., Berk, E., Engel, A., Gillette, K. T., Galindo-Tovar, A., . . . Kaumann, A. J. (2014). Carvedilol induces greater control of beta2- than beta 1-adrenoceptor-mediated inotropic and lusitropic effects by PDE3, while PDE4 has no effect in human failing myocardium. *Naunyn Schmiedebergs Arch Pharmacol, 387*(7), 629-640. doi:10.1007/s00210-014-0974-4

Molkentin, J. D. (2000). The zinc finger-containing transcription factors GATA-4, -5, and -6. Ubiquitously expressed regulators of tissue-specific gene expression. *J Biol Chem, 275*(50), 38949-38952. doi:10.1074/jbc.R000029200

Moorthy, B. S., Gao, Y., & Anand, G. S. (2011). Phosphodiesterases catalyze hydrolysis of cAMP-bound to regulatory subunit of protein kinase A and mediate signal termination. *Mol Cell Proteomics, 10*(2), M110 002295. doi:10.1074/mcp.M110.002295

Myagmar, B. E., Flynn, J. M., Cowley, P. M., Swigart, P. M., Montgomery, M. D., Thai, K., . . . Simpson, P. C. (2017). Adrenergic Receptors in Individual Ventricular Myocytes: The Beta-1 and Alpha-1B Are in All Cells, the Alpha-1A Is in a Subpopulation, and the Beta-2 and Beta-3 Are Mostly Absent. *Circ Res, 120*(7), 1103-1115. doi:10.1161/CIRCRESAHA.117.310520

Noguchi, A., Whitsett, J. A., & Dickman, L. (1981). Ontogeny of myocardial alpha 1-adrenergic receptor in the rat. *Dev Pharmacol Ther, 3*(3), 179-188.

O'Connell, T. D., Ishizaka, S., Nakamura, A., Swigart, P. M., Rodrigo, M. C., Simpson, G. L., . . . Simpson, P. C. (2003). The alpha(1A/C)- and alpha(1B)-adrenergic receptors are required for physiological cardiac hypertrophy in the double-knockout mouse. *J Clin Invest, 111*(11), 1783-1791. doi:10.1172/JCI16100

O'Connell, T. D., Jensen, B. C., Baker, A. J., & Simpson, P. C. (2014). Cardiac alpha1-adrenergic receptors: novel aspects of expression, signaling mechanisms, physiologic function, and clinical importance. *Pharmacol Rev, 66*(1), 308-333. doi:10.1124/pr.112.007203

Prazeres, D. M., & Martins, S. A. (2015). G protein-coupled receptors: an overview of signaling mechanisms and screening assays. *Methods Mol Biol, 1272*, 3-19. doi:10.1007/978-1-4939-2336-6_1

Price, D. T., Lefkowitz, R. J., Caron, M. G., Berkowitz, D., & Schwinn, D. A. (1994). Localization of mRNA for three distinct alpha 1-adrenergic receptor subtypes in human tissues: implications for human alpha-adrenergic physiology. *Mol Pharmacol, 45*(2), 171-175.

Ruffolo, R. R., Jr., & Feuerstein, G. Z. (1997). Pharmacology of carvedilol: rationale for use in hypertension, coronary artery disease, and congestive heart failure. *Cardiovasc Drugs Ther, 11 Suppl 1*, 247-256.

Ruffolo, R. R., Jr., Gellai, M., Hieble, J. P., Willette, R. N., & Nichols, A. J. (1990). The pharmacology of carvedilol. *Eur J Clin Pharmacol, 38 Suppl 2*, S82-88.

Ruuskanen, J. O., Laurila, J., Xhaard, H., Rantanen, V. V., Vuoriluoto, K., Wurster, S., . . . Scheinin, M. (2005). Conserved structural, pharmacological and functional properties among the three human and five zebrafish alpha 2-adrenoceptors. *Br J Pharmacol, 144*(2), 165-177. doi:10.1038/sj.bjp.0706057

Santulli, G. (2015). Sympathetic Nervous System Signaling in Heart Failure and Cardiac Aging *Pathophysiology and Pharmacotherapy of Cardiovascular Disease* (pp. 83-105). Switzerland: Springer International Publishing.

Santulli, G., & Iaccarino, G. (2016). Adrenergic signaling in heart failure and cardiovascular aging. *Maturitas, 93*, 65-72. doi:10.1016/j.maturitas.2016.03.022

Saunders, C., & Limbird, L. E. (1999). Localization and trafficking of alpha2-adrenergic receptor subtypes in cells and tissues. *Pharmacol Ther, 84*(2), 193-205.

Schaffer, W., & Williams, R. S. (1986). Age-dependent changes in expression of alpha 1-adrenergic receptors in rat myocardium. *Biochem Biophys Res Commun, 138*(1), 387-391.

Schirger, A., & Sheps, S. G. (1977). Prazosin-new hypertensive agent. A double-blind crossover study in the treatment of hypertension. *JAMA, 237*(10), 989-991.

Scofield, M. A., Liu, F., Abel, P. W., & Jeffries, W. B. (1995). Quantification of steady state expression of mRNA for alpha-1 adrenergic receptor subtypes using reverse transcription and a competitive polymerase chain reaction. *J Pharmacol Exp Ther, 275*(2), 1035-1042.

Shi, T., Duan, Z. H., Papay, R., Pluskota, E., Gaivin, R. J., de la Motte, C. A., . . . Perez, D. M. (2006). Novel alpha1-adrenergic receptor signaling pathways: secreted factors and interactions with the extracellular matrix. *Mol Pharmacol, 70*(1), 129-142. doi:10.1124/mol.105.020735

Shiba, Y., Fernandes, S., Zhu, W. Z., Filice, D., Muskheli, V., Kim, J., . . . Laflamme, M. A. (2012). Human ES-cell-derived cardiomyocytes electrically couple and suppress arrhythmias in injured hearts. *Nature, 489*(7415), 322-325. doi:10.1038/nature11317

Shibata, K., Katsuma, S., Koshimizu, T., Shinoura, H., Hirasawa, A., Tanoue, A., & Tsujimoto, G. (2003). alpha 1-Adrenergic receptor subtypes differentially control the cell cycle of transfected CHO cells through a cAMP-dependent mechanism involving p27Kip1. *J Biol Chem, 278*(1), 672-678. doi:10.1074/jbc.M201375200

Shore, S. A., & Drazen, J. M. (2003). Beta-agonists and asthma: too much of a good thing? *J Clin Invest, 112*(4), 495-497. doi:10.1172/JCI19642

Shukla AC, Steven JM, & FX., M. (2009). Copyright *A Practice of Anesthesia for Infants and Children* (4th ed., pp. 361-395): Natasha Andjelkovic.

Siehler, S. (2009). Regulation of RhoGEF proteins by G12/13-coupled receptors. *Br J Pharmacol, 158*(1), 41-49. doi:10.1111/j.1476-5381.2009.00121.x

Skeberdis, V. A. (2004). Structure and function of beta3-adrenergic receptors. *Medicina (Kaunas), 40*(5), 407-413.

Song, K., Nam, Y. J., Luo, X., Qi, X., Tan, W., Huang, G. N., . . . Olson, E. N. (2012). Heart repair by reprogramming non-myocytes with cardiac transcription factors. *Nature, 485*(7400), 599-604. doi:10.1038/nature11139

Srivastava, D., Cserjesi, P., & Olson, E. N. (1995). A subclass of bHLH proteins required for cardiac morphogenesis. *Science, 270*(5244), 1995-1999.

Srivastava, D., Thomas, T., Lin, Q., Kirby, M. L., Brown, D., & Olson, E. N. (1997). Regulation of cardiac mesodermal and neural crest development by the bHLH transcription factor, dHAND. *Nat Genet, 16*(2), 154-160. doi:10.1038/ng0697-154

Stanley, E. G., Biben, C., Elefanty, A., Barnett, L., Koentgen, F., Robb, L., & Harvey, R. P. (2002). Efficient Cre-mediated deletion in cardiac progenitor cells conferred by a 3'UTR-ires-Cre allele of the homeobox gene Nkx2-5. *Int J Dev Biol, 46*(4), 431-439.

Thomas C. Malig, M. R. A., Austin L. Burman, Manuel Barday, Belinda J. M. Heyne and Thomas G. Back. (2017). Comparison of free-radical inhibiting antioxidant properties of carvedilol and its phenolic metabolites. *Medicinal Chemistry Communication, 8*(3), 606-615. doi:10.1039/C7MD00014F

Tina Shah, N. P., and Biykem Bozkurt. (2015). Heart Failure, Introduction. In G. J. e. al. (Ed.), *Pathophysiology and Pharmacotherapy of Cardiovascular Disease* (pp. 3-20). Switzerland: Springer International Publishing

Tirupula, K. C., Ithychanda, S. S., Mohan, M. L., Naga Prasad, S. V., Qin, J., & Karnik, S. S. (2015). G protein-coupled receptors directly bind filamin A with high affinity and promote filamin phosphorylation. *Biochemistry, 54*(44), 6673-6683. doi:10.1021/acs.biochem.5b00975

Tsai, S. Y., Maass, K., Lu, J., Fishman, G. I., Chen, S., & Evans, T. (2015). Efficient Generation of Cardiac Purkinje Cells from ESCs by Activating cAMP Signaling. *Stem Cell Reports, 4*(6), 1089-1102. doi:10.1016/j.stemcr.2015.04.015

UniProt. (1995a). UniProtKB - P25100 (ADA1D_HUMAN).

UniProt. (1995b). UniProtKB - P35348 (ADA1A_HUMAN).

UniProt. (2006). UniProtKB - P35368 (ADA1B_HUMAN).

Weber, K., Bohmeke, T., van der Does, R., & Taylor, S. H. (1998). Hemodynamic differences between metoprolol and carvedilol in hypertensive patients. *Am J Hypertens, 11*(5), 614-617.

WHO. (2017, May 2017). Cardiovascular diseases (CVDs). Retrieved from http://www.who.int/mediacentre/factsheets/fs317/en/

Williams, N. G., Zhong, H., & Minneman, K. P. (1998). Differential coupling of alpha1-, alpha2-, and beta-adrenergic receptors to mitogen-activated protein kinase pathways and differentiation in transfected PC12 cells. *J Biol Chem, 273*(38), 24624-24632.

Wisler, J. W., DeWire, S. M., Whalen, E. J., Violin, J. D., Drake, M. T., Ahn, S., . . . Lefkowitz, R. J. (2007). A unique mechanism of beta-blocker action: carvedilol stimulates beta-arrestin signaling. *Proc Natl Acad Sci U S A, 104*(42), 16657-16662. doi:10.1073/pnas.0707936104

Wright, C. D., Chen, Q., Baye, N. L., Huang, Y., Healy, C. L., Kasinathan, S., & O'Connell, T. D. (2008). Nuclear alpha1-adrenergic receptors signal activated ERK localization to caveolae in adult cardiac myocytes. *Circ Res, 103*(9), 992-1000. doi:10.1161/CIRCRESAHA.108.176024

Wright, C. D., Wu, S. C., Dahl, E. F., Sazama, A. J., & O'Connell, T. D. (2012). Nuclear localization drives alpha1-adrenergic receptor oligomerization and signaling in cardiac myocytes. *Cell Signal, 24*(3), 794-802. doi:10.1016/j.cellsig.2011.11.014

Wu, S. C., Dahl, E. F., Wright, C. D., Cypher, A. L., Healy, C. L., & O'Connell, T. D. (2014). Nuclear localization of a1A-adrenergic receptors is required for signaling in cardiac myocytes: an "inside-out" a1-AR signaling pathway. *J Am Heart Assoc, 3*(2), e000145.

Xiao, R. P. (2001). Beta-adrenergic signaling in the heart: dual coupling of the beta2-adrenergic receptor to G(s) and G(i) proteins. *Sci STKE, 2001*(104), re15. doi:10.1126/stke.2001.104.re15

Yue, T. L., Cheng, H. Y., Lysko, P. G., McKenna, P. J., Feuerstein, R., Gu, J. L., . . . Feuerstein, G. (1992). Carvedilol, a new vasodilator and beta adrenoceptor antagonist, is an antioxidant and free radical scavenger. *J Pharmacol Exp Ther, 263*(1), 92-98.

Zhang, F., Feridooni, T., Hotchkiss, A., & Pasumarthi, K. B. (2015). Divergent cell cycle kinetics of midgestation ventricular cells entail a higher engraftment efficiency after cell transplantation. *Am J Physiol Cell Physiol, 308*(3), C220-228. doi:10.1152/ajpcell.00319.2014

Zhang, F., & Pasumarthi, K. B. (2007). Ultrastructural and immunocharacterization of undifferentiated myocardial cells in the developing mouse heart. *J Cell Mol Med, 11*(3), 552-560. doi:10.1111/j.1582-4934.2007.00044.x

Zhang, L., Taniguchi, T., Tanaka, T., Shinozuka, K., Kunitomo, M., Nishiyama, M., . . . Muramatsu, I. (2002). Alpha-1 adrenoceptor up-regulation induced by prazosin but not KMD-3213 or reserpine in rats. *Br J Pharmacol, 135*(7), 1757-1764. doi:10.1038/sj.bjp.0704639

Zhang, T., Xu, Q., Chen, F. R., Han, Q. D., & Zhang, Y. Y. (2004). Yeast two-hybrid screening for proteins that interact with alpha1-adrenergic receptors. *Acta Pharmacol Sin, 25*(11), 1471-1478.

Zhong, H., & Minneman, K. P. (1999). Alpha1-adrenoceptor subtypes. *Eur J Pharmacol, 375*(1-3), 261-276.